Adv. Chem. Phys. **92**, 1–159, (1996).

Electrolytes and the Electric Double Layer

Phil Attard

Department of Physics, Faculty of Science,
Australian National University,
Canberra, ACT, 0200, Australia.

Contents

Introduction

Background

Particles in polar solvents usually develop surface charges, due either to dissociation of chemical groups on the surface, or to chemical binding or physical adsorption of ions from the electrolyte. This surface charge is balanced by an equal and opposite net charge of ions in the electrolyte. These counterions are those that have either dissociated from the surface, or they are the ex-partners of the adsorbed ions, since the electrolyte was originally electroneutral. Although definitely attracted to the oppositely charged surface, due to entropy these counterions remain dispersed and mobile in the solvent in the vicinity of the surface. This spatial separation of charge is termed the electric double layer.

The electric double layer affects the properties of individual particles, and also the interactions between them. Usually two similarly charged particles in a solvent will experience a mutual repulsion, as one might expect, but the repulsion is not given simply by Coulomb's law because of the presence of the counterions in the double layer. At large separations there is no interaction because the 'bare' charge on the particles is screened by the neutralising counterions that surround them; at small separations their diffuse double layers begin to overlap and the ions in them must rearrange, which gives rise to a force. This electric double layer repulsion is opposed by the van der Waals attraction that exists between all particles, and it is the precise balance between these two that is important. The dominance of one or the other, for example, primarily determines whether colloidal particles remain dispersed and mobile in the solvent, or whether they coagulate and float or precipitate out of solution. Similarly, the properties of individual particles or aggregates can depend upon the nature of the surrounding double layer. For instance, membranes such as those forming biological cells, or those stabilising bubbles or foams, are often comprised of amphiphilic molecules that have a solvophilic head and a solvophobic tail, and these molecules typically spontaneously assemble to form a bilayer film with the tails in the interior away from the solvent, and with the heads wet by the solvent. For polar solvents such as water, the head-groups often have a net charge that is balanced by an electric double layer, and it is the properties of the latter that determines whether the membrane forms in the first place, and if so, the geometry and curvature of the resultant structure.

These two examples –the stability of colloidal dispersions and the formation of bilayer membranes– are indicative of the widespread occurrence of the electric double layer. The approach and fusion of biological cells, (conception, infection, recognition), the tertiary conformation of proteins, and the transport of ions and other molecules across cell membranes, are all fundamental life processes involving the electric double layer at surfaces in an aqueous environment. The swelling of clays affects the drainage of soils in agriculture, the stability of building foundations, and the consistency of drilling muds, and is directly determined by the double layer repulsion between the clay platelets. Technological applications include the adhesion of glues, inks, and paints, the formation and cohesion of ceramics, the propagation of cracks in metals and glasses, and the lubrication of surfaces in proximal motion. The ability to

predict these phenomena, and to control and to use these systems, relies upon a quantitative understanding of the electric double layer.

Several experimental techniques have been developed that enable the double layer to be characterised in various systems. An essential requirement is that the method by surface-specific, since one has to discriminate between the properties of the double layer and those of the bulk electrolyte; for most properties the former are swamped by the latter. Voltage and capacitance measurements give information about the double layer in the vicinity of the electrode and its dependence upon the electrolyte. Electrophoresis measures the mobility of particles in an applied electric field, and this is related to the double layer potential near the surface. Electrolysis and electro-deposition experiments quantify ion transport in the double layer. Various spectroscopic, x-ray, and optical techniques can be surface-specific, probing the state of the surface and the adjacent electrolyte. Neutron and x-ray scattering measures the correlations between sub-microscopic particles, which is related to the interaction free energy due to the overlap of double layers between their surfaces. The interaction free energy can also be measured directly between macroscopic surfaces using force balance techniques, including the atomic force microscope, or by applying osmotic stress. Less directly it can be inferred from colloid sedimentation or flotation rates.

The task of theory is to provide a framework within which these measurements can be quantitatively interpreted, and to rationalise double layer phenomena more generally. Clearly if one is to describe so many diverse systems one must simplify the problem to its essential ingredients. One hopes first to deduce principles that hold in general, and thence to address exceptional or specific behaviour by including more complicated effects as the need arises. The abstract representation of the electric double layer fundamentally consists of uniformly charged surfaces, either planar or with constant curvature, immersed in an electrolyte comprised of simple ions in a dielectric continuum. More sophisticated models of the particles include the effects of discrete surface charges, (fixed or mobile), non-uniformly curved, flexible, or rough surfaces, and image charges due to the dielectric boundaries necessarily present. In dense suspensions the double layer interactions between the particles are not simply pair-wise additive, as is assumed in the usual treatments. For the electrolyte, ion size and shape may become involved, as well as their polarizability. It may also become necessary to go beyond the continuum picture and to include the solvent as a distinct molecular species. These possibilities notwithstanding, the essence of the double layer consists of charged surfaces and mobile ions, and it will be seen that this already provides a challenge for theory, and that a rich and varied behaviour is encompassed by the minimal model.

The theoretical techniques that are applied to the electric double layer are those of classical statistical mechanics, which describes the sub-microscopic behaviour of atoms and molecules. The traditional approach is the Poisson-Boltzmann theory, which is a mean-field method that takes the density of ions in the diffuse layer near the charged surface to be proportional to the Boltzmann factor of the average electrostatic potential; the latter is related to the ion density by Poisson's equation. With the advent of computers more sophisticated numerical treatments have prevailed. These are primarily Monte Carlo and molecular dynamics simulations, whose exactitude is limited only by the computer time and size, and integral equation theories, which though fundamentally approximate are very efficient. Whereas the simulations follow the motion of individual ions in the double layer, integral equations are based on mathematical relationships between the ion density profiles and the ion pair correlation functions, either those of the bulk electrolyte or those in the double layer. Density functional techniques are variational procedures that minimise the double layer free energy with respect to the ion density profiles; the free energy is approximated by an integral involving the bulk direct correlation function. The Ornstein-Zernike equation is the fundamental integral equation of statistical mechanics, and it provides a relation between the direct and total correlation functions. It is solved by iteration, invoking some closure relation such as the hypernetted chain approximation. The pair correlation functions that appear in it are either those between ions in the presence of the particle (inhomogeneous integral equations), or they are between the particle and the ions (singlet integral equations). In the latter case the ion density profile of the double layer corresponds to the particle-ion distribution function. These rather sophisticated numerical treatments have revealed not only quantitative deficiencies in the classic Poisson-Boltzmann approximation for the double layer, but even qualitatively different behaviour, particularly at higher ionic strengths and/or higher surface charges.

As an example of a quantitative deficiency, the Poisson-Boltzmann theory can be fit to the numerical data for the potential drop across the double layer provided that one used an *effective* surface charge rather than the actual surface charge. A rather surprising qualitative difference was the prediction, obtained by several different methods, that the force between two similarly charged surfaces can be *attractive*. There are two distinct regimes for this non-classical behaviour. At small separations the force changes from repulsive to attractive as the surface charge and electrolyte concentration is increased. This is the van der Waals regime, and the attractions are due to the electrostatic correlations between the ions confined between the surfaces; the effect is most pronounced for high ion couplings, which for aqueous electrolytes at room temperature means multivalent ions. Second, there is the large separation regime, where asymptotic analysis reveals an intimate connection between the interaction due to overlapping double layers, the double layer density profiles at an isolated surface, and the ion-ion correlation functions in the bulk electrolyte. At low

concentrations the asymptotic interaction is monotone repulsive, as predicted by Poisson-Boltzmann approximation; it has the same functional form as in the classical theory but with effective parameters, (e.g. decay length, surface charge), which can be expressed as integrals of bulk and particle correlation functions. At higher electrolyte couplings, the bulk radial distribution function becomes oscillatory, and so does the asymptotic force between two similarly charged surfaces; it is alternately attractive and repulsive with the same period and decay length of the bulk ion-ion correlation functions. These asymptotic and other analyses have rationalised the discrepancies between the classic Poisson-Boltzmann prediction and the recent rather sophisticated numerical treatments, and have made it possible to interpret a number of novel and unusual experimental measurements. It is these newer theoretical approaches and analyses that are the subject of this review of the electric double layer.

Review of reviews

The original book of Verwey and Overbeek[1] remains the classic text on the electric double layer as the fundamental basis of colloid stability, and on its description by the Poisson-Boltzmann approximation (Gouy-Chapman theory). Two recent reviews in this series[2,3] have focussed on the isolated planar double layer. Carnie and Torrie[2] give a comprehensive coverage of theories for the primitive model electrolyte, including the modified Poisson-Boltzmann theory, the singlet Ornstein-Zernike approach, and comparison with simulations. Blum[3] extended the coverage to the inhomogeneous Ornstein-Zernike equation.

More specific reviews include that of Lozada-Cassou[4] who gives singlet hypernetted chain results for the primitive model electric double layer, and that of Patey and Torrie[5] who cover discrete solvent effects at a similar level of approximation. Reviews of the bulk Coulomb fluid include the mathematical treatments of sum rules by Martin[6], and of the soluble two-dimensional plasma by Alastuey[7]. The structure and dynamics of ionic liquids have been reviewed by Parrinello and Tosi[8].

Scope

This review concentrates on the theory of the equilibrium electric double layer, using the simplest model for the charged surfaces and the primitive model for the electrolyte. Regrettably, solvent effects and the application to experiment are discussed only superficially. The modern integral equation methods of statistical mechanics are emphasised, and the related analytic techniques. The double layer interactions between particles receive the most attention, although one theme concerns the relationship of these with the double layer of an isolated particle, and with the properties of the bulk electrolyte. This review is composed of several sections: a formally exact analysis of bulk electrolytes (§I), analysis and asymptotics of the double layer (§II), modern computational methods (§III) and numerical results (§IV), and elaborations of the basic model (§V). Sections I and II are somewhat mathematical, whereas in the remainder a more discursive approach is taken. The review concludes with a discussion of the relevance and application of these modern theories to experiment.

The primitive model electrolyte is defined in §IA, and the behaviour of the ion correlation functions in the homogeneous electrolyte is analysed in the remainder of the first section. The fact that these decay exponentially is established in §IB, along with the electroneutrality and moment conditions. In §IC it is shown that the classic Debye screening length has to be changed in order for the modified Debye-Hückel theory for finite sized ions to satisfy the Stillinger-Lovett second moment condition. This forshadows the formally exact asymptotic analysis of §ID, where the actual screening length is determined by equations involving the short range part of the correlation functions. Here it is shown that the Yukawa form for the ion pair correlation function, as given by Debye-Hückel theory, is formally exact asymptotically but with effective parameters. As the electrolyte coupling is increased three asymptotic regimes are identified: monotonic, charge oscillations, and density oscillations.

The connection with the electric double layer is made in §II where the intimate relation between the properties of the bulk electrolyte and those of the double layer is described. For example, it is shown that the decay length of the ion profiles in the diffuse layer next to the charged surface is the same as the screening length of the bulk electrolyte (i.e. not the Debye length). Spherical solutes are treated in §IIA and an isolated planar wall in §IIB, where it is shown that asymptotically the double layer has linear Poisson-Boltzmann form but with an effective surface charge. The algebraic correlations between ions along a wall are also derived. In §IIC the properties of interacting planar electric double layers are determined, and again the asymptote has a linear Poisson-Boltzmann form that involves the effective surface charge for the isolated surface. Section III concludes with a summary of methods to treat the double layer in various geometries, including cylinders, pores, and dumb-bells; the latter regards two interacting particles as a single solute.

The discussion of computational methods in §III focusses mainly on singlet integral equations, since arguably their combination of accuracy and computational efficiency makes feasible a reliable analysis of experimental data. The singlet hypernetted chain approximation is treated in §IIIA, and methods for including bridge diagrams are discussed. Expressions for the solvation free energy are derived for this approximation, and this provides an alternative pathway to the contact theorem for the pressure. Inhomogeneous integral equations are mentioned in §IIIB, a brief description of density functional methods can be found in §IIIC, and simulations are covered in §IIID.

Section IV provides some numerical results and comparisons for the planar double layer. The effective surface charge, which converts a fit made with the linear Poisson-Boltzmann approximation to the actual surface charge, is calculated in §IVA, and the hypernetted chain approximation is compared with the analytic effective Poisson-Boltzmann approximation. In §IVB the interaction pressure due to two walls is calculated in the wall-wall and dumb-bell hypernetted chain approximations and tested against simulation and inhomogeneous integral equation results.

Section V summarises extensions of the basic model of the double layer that include different physical effects. Concentrated dispersions, discrete, variable, and rough surface charges, dielectric images, and molecular solvents, are all briefly discussed. The article concludes with a discussion of the relevance and implications for experiment. The focus is on the use of the simplest model of the double layer, and on the utility of the Poisson-Boltzmann theory in the light of the non-classical behaviour revealed by more advanced theories.

I. CORRELATION FUNCTIONS OF THE BULK ELECTROLYTE

The electric double layer is an inhomogeneous fluid in the sense that the ion densities vary in space in the vicinity of the charged particle or wall. This is in contrast to the bulk electrolyte where the ion densities are uniform and constant. Similarly, in the bulk the ion pair correlation functions are isotropic, and depend only upon the separation of the ions, whereas in the double layer they are not only anisotropic but also inhomogeneous. They depend upon from three (for a spherical macroion, or for one or two planar walls, which have the highest symmetry) to six coordinates of the two ions.

Despite these qualitative differences, it turns out that the techniques used to analyse the electric double layer are virtually the same as those used for a bulk electrolyte, since what is common and essential to both is the long-ranged Coulomb potential. Moreover, it will be seen that the bulk electrolyte determines in a quantitative fashion many of the properties of the electric double layer, in particular the asymptotic decay of the density profiles and the interaction between overlapping double layers. Hence this section is concerned with the analysis of the correlation functions of bulk electrolytes, and it is in the later sections that the methods and results are applied to the electric double layer. In §IB the moment conditions are given, and it is proven that the pair correlation functions in the bulk electrolyte decay exponentially, §IC treats Debye-Hückel theory with a modification for the Debye screening length, and §ID is concerned with a formal analysis of the asymptotic behaviour of the pair correlation functions, again in the bulk.

A. The primitive model

The minimal model of the double layer (uniformly curved and charged surfaces, and ions in a continuum solvent) requires first the specification of the electrolyte. In this article classical statistical mechanics will be used. In general quantum mechanics affects small particles, such as photons and electrons, but the dynamics of atoms, molecules, and ions are governed by Newton's equations of motion. Thus classical statistical mechanics in general suffices to describe the behaviour of most fluids; argon, which is one of the smaller atoms, in the liquid state has a quantum correction of the order of 1% for the internal energy and of the order of 10% for the pressure[9]. In classical statistical mechanics, the kinetic energy or momentum integrals are independent Gaussians, and hence their contribution to the free energy is trivial; it is the potential energy, which depends upon the configurations of the particles, whose contribution is highly non-trivial.

An electrolyte, in general, consists of ions and solvent molecules. In most of this review the primitive model will be used. This ignores the solvent molecules explicitly, and subsumes their effect into a continuum dielectric constant, ϵ. Accordingly the ions interact via Coulomb's law *in media*

$$u_{\alpha\gamma}^{\mathrm{Coul}}(r) = \frac{q_\alpha q_\gamma}{\epsilon r}. \tag{1}$$

Here q_α is the charge on ions of species α, $\epsilon = 4\pi\epsilon_0\epsilon_r$ is the total permittivity, (ϵ_0 is the permittivity of free space, and ϵ_r is the relative dielectric constant of the medium), and r is the separation between the ions. This Coulomb potential is strictly an interaction free energy (c.f. the temperature dependence of the dielectric constant), and corresponds to

first the Born-Oppenheimer procedure for averaging out the electron contribution, and second the McMillan-Mayer representation, where the solvent coordinates have been integrated out of the problem. The 'dielectric screening' of the ionic interaction by the solvent is valid in the limit of large separations; incorporating the solvent contributions via the dielectric constant is exact asymptotically. At intermediate separations one begins to see departures from Coulomb's law *in media*. For example, there is a repulsive cavity term due to exclusion of polarizable solvent by the ion that decays as r^{-4}[10]. There are also many-body contributions due to ionic polarizability that decay as r^{-6}, and hence the assumption of pair-wise additivity is an approximation. And at still closer separations one expects oscillatory behaviour as the molecular size of the solvent becomes important[5], as well as solvent-induced many-body interactions. In the primitive model all of these effects are ignored, and the exact asymptote that is Coulomb's law *in media* is applied at all separations.

In addition to their charge, the primitive model recognizes that ions have size, which prevents them from overlapping. This excluded volume effect is incorporated into the model by adding to Coulomb's law a short-range repulsion, the most common choice being the hard-sphere potential,

$$u_{\alpha\gamma}^{\rm hs}(r) = \begin{cases} \infty & r < d_{\alpha\gamma} \\ 0 & r > d_{\alpha\gamma}, \end{cases} \tag{2}$$

where additive hard-sphere diameters are used, $d_{\alpha\gamma} = (d_\alpha + d_\gamma)/2$, d_α being the hard-sphere diameter of ions of type α. Again the hard-sphere repulsion is an approximation that roughly models the Pauli exclusion of electrons, which is what in reality prevents molecular overlap. It is true of course that $u(r) \to \infty$, $r \to 0$, but in fact the repulsion is softer than that used in the hard-sphere model, (sometimes a r^{-12} form is used), and again there are three-body contributions[11]. The ion diameter that is used in the primitive model includes approximately the first solvation shell, since it is larger than the bare ion diameter of ionic crystals. A particularly simple version of the model is the so-called restricted primitive model, which is a binary symmetric electrolyte with all ions being the same size and the two species having equal but opposite charge.

B. Electroneutrality, moments, and screening

This section is concerned with establishing electroneutrality and the exponential screening of the correlation functions in the electrolyte. Most would take these facts to be self-evident, and, while Debye shielding has been rigorously established at vanishing concentration[12–16], there does not appear to be a more general proof of exponential behaviour. Of course one person's rigor is another's mortis, and hopefully the analysis below will convince rather than convict.

For a multi-component fluid, the Ornstein-Zernike equation is[17]

$$h_{\alpha\gamma}(r) = c_{\alpha\gamma}(r) + \sum_\lambda \rho_\lambda \int h_{\alpha\lambda}(s) c_{\lambda\gamma}(|\mathbf{r}-\mathbf{s}|)\, d\mathbf{s}, \tag{3}$$

where h and c are the total and the direct correlation functions, ρ is the number density, and the Greek subscripts index the species. The total correlation function is directly related to the more familiar radial distribution function, $h_{\alpha\gamma}(r) = g_{\alpha\gamma}(r) - 1$; $g_{\alpha\gamma}(r)$ is proportional to the probability of finding ions of type α and γ at a separation r. This can be written in matrix form

$$\underline{\underline{H}}(r) = \underline{\underline{C}}(r) + \int \underline{\underline{H}}(s)\underline{\underline{C}}(|\mathbf{r}-\mathbf{s}|)\, d\mathbf{s}, \tag{4}$$

which factors in Fourier space

$$\hat{\underline{\underline{H}}}(k) = \hat{\underline{\underline{C}}}(k) + \hat{\underline{\underline{H}}}(k)\hat{\underline{\underline{C}}}(k). \tag{5}$$

The symmetric matrices have components

$$\{\underline{\underline{H}}(r)\}_{\alpha\gamma} = \rho_\alpha^{1/2}\rho_\gamma^{1/2} h_{\alpha\gamma}(r), \tag{6}$$

and

$$\{\underline{\underline{C}}(r)\}_{\alpha\gamma} = \rho_\alpha^{1/2}\rho_\gamma^{1/2} c_{\alpha\gamma}(r). \tag{7}$$

As mentioned above, the long-range part of the pair potential in the primitive model electrolyte follows Coulomb's law *in media*, $u_{\alpha\gamma}^{\rm Coul}(r) = q_\alpha q_\gamma/\epsilon r$. In view of this, one defines the dyadic matrix[18]

$$\underline{\underline{Q}} = \frac{4\pi\beta}{\epsilon}\underline{q}\,\underline{q}^T, \tag{8}$$

where $\beta = 1/k_B T$ is the inverse of the thermal energy, and where $\underline{q}^T$ is the row vector corresponding to the transpose of the column vector $\underline{q}$, which has components

$$\{\underline{q}\}_\alpha = \rho_\alpha^{1/2} q_\alpha. \tag{9}$$

The matrix $\underline{\underline{Q}}$ has a number of convenient properties. Its trace is related to the Debye length,

$$\mathrm{Tr}\{\underline{\underline{Q}}\} = \frac{4\pi\beta}{\epsilon} \underline{q}^T \, \underline{q} = \frac{4\pi\beta}{\epsilon} \sum_\alpha \rho_\alpha q_\alpha^2 = \kappa_D^2, \tag{10}$$

it is essentially idempotent,

$$\underline{\underline{Q}}^{n+1} = \kappa_D^{2n} \underline{\underline{Q}}, \tag{11}$$

and, although $\underline{\underline{Q}}$ itself is singular, $\mathrm{Det}\{\underline{\underline{Q}}\} = 0$, one has

$$(\underline{\underline{I}} + \alpha \underline{\underline{Q}})^{-1} = \underline{\underline{I}} - \frac{\alpha}{1 + \alpha \kappa_D^2} \underline{\underline{Q}}. \tag{12}$$

1. Moment Conditions

All of the analysis below is based upon the fundamental assumption that the total correlation function is integrable,

$$\int h_{\alpha\gamma}(r) \, d\mathbf{r} \equiv \hat{h}_{\alpha\gamma}(0) < \infty, \tag{13}$$

where the circumflex denotes the three-dimensional radial Fourier transform. With the exception of the spinodal, it is axiomatic that this always holds. It will be shown below that the direct correlation function goes like $c_{\alpha\gamma}(r) \sim -\beta u_{\alpha\gamma}^{\mathrm{Coul}}(r), \; r \to \infty$. Hence one defines

$$\chi_{\alpha\gamma}(r) \equiv c_{\alpha\gamma}(r) + \beta u_{\alpha\gamma}^{\mathrm{Coul}}(r), \tag{14}$$

where for the present $\chi_{\alpha\gamma}(r)$ is assumed to be of shorter range than the Coulomb potential. (Later it will be shown to be exponentially decaying.)

The Fourier transform of the Ornstein-Zernike equation, Eq. (5), may be written

$$\hat{\underline{\underline{H}}}(k) = \hat{\underline{\underline{\chi}}}(k) - \underline{\underline{Q}} k^{-2} + \hat{\underline{\underline{H}}}(k) \hat{\underline{\underline{\chi}}}(k) - \hat{\underline{\underline{H}}}(k) \underline{\underline{Q}} k^{-2}, \tag{15}$$

where the k^{-2} term is the transform of the Coloumb potential. Now in the limit $k \to 0$, $k^2 \hat{\underline{\underline{\chi}}}(k) \to 0$, since $\chi(r)$ decays faster than the Coulomb potential. Hence multiplying both sides by k^2 and taking the limit, in view of the integrability of the total correlation function, one must have

$$0 = -\underline{\underline{Q}} - \hat{\underline{\underline{H}}}(0) \underline{\underline{Q}}. \tag{16}$$

Explicitly, this is the electroneutrality condition

$$q_\alpha = -\sum_\gamma \rho_\gamma q_\gamma \int h_{\alpha\gamma}(r) \, d\mathbf{r}, \tag{17}$$

which expresses the fact that each ion is surrounded by a cloud of ions bearing a net equal and opposite charge. Note that although $\underline{\underline{H}}$ and $\underline{\underline{C}}$ commute, the three matrices $\underline{\underline{H}}$, $\underline{\underline{\chi}}$, and $\underline{\underline{Q}}$ in general don't commute, except at $k = 0$.

The electroneutrality condition is also called the zeroth moment condition, and it is here appropriate to define the moments. In general the transform of an integrable function possesses a small-k Taylor series expansion; in the case of radial functions only even powers of k appear. One has

$$\hat{\underline{\underline{H}}}(k) \sim \underline{\underline{H}}^{(0)} + \underline{\underline{H}}^{(2)} k^2 + \underline{\underline{H}}^{(4)} k^4 + \ldots, \quad k \to 0, \tag{18}$$

and similarly for $\underline{\underline{\hat{\chi}}}(k)$. This expression may be obtained by expanding the integrand of the Fourier transform, and the moments are defined as

$$\underline{\underline{H}}^{(2n)} = \frac{4\pi(-1)^n}{(2n+1)!}\int_0^\infty \underline{\underline{H}}(r)\, r^{2n+2}\, dr. \tag{19}$$

In general only a finite number of moments exist; if $h(r) \sim r^{-\eta}$, $r \to \infty$, then the moment integral is divergent for $2n + 2 - \eta > -1$. All moments exist for an exponentially short-ranged function, and the task is to show that this is indeed the case for the correlation functions of the electrolyte.

The electroneutrality condition provides constraints on the sums of the zeroth moments of the total correlation functions; for an m-component electrolyte in the most general case there are $m(m+1)/2$ total correlation functions and m constraints. For the case of a binary electrolyte, the $\hat{h}_{\alpha\gamma}(0)$ can in fact be expressed in terms of the isothermal compressibility[8,19–22],

$$\rho_+^{-1} + \hat{h}_{++}(0) = \rho_-^{-1} + \hat{h}_{--}(0) = \hat{h}_{+-}(0) = \frac{k_B T}{\rho}\left(\frac{\partial\rho}{\partial p}\right)_T, \tag{20}$$

where $\rho = \rho_+ + \rho_-$ and p is the pressure. This result holds only for the binary electrolyte; more generally the individual $\hat{h}_{\alpha\gamma}(0)$ are given as linear combinations of the molecular chemical potential derivatives of the molecular densities, since the individual ion chemical potentials are undetermined. The chemical potential derivative of ion distribution functions of a binary electrolyte have been given[23]. Suttorp and van Wonderen give results for an ionic mixture in the presence of a neutralising background (multicomponent jellium)[24,25]. According to Kirkwood-Buff theory[26], the isothermal compressibility can also be expressed in terms of the direct correlation function

$$\beta\chi_T^{-1} \equiv \rho\left(\frac{\partial\beta p}{\partial\rho}\right)_T = \underline{\rho}^T\left[\underline{\underline{I}} - \underline{\underline{\hat{C}}}(0)\right]\underline{\rho}, \tag{21}$$

where $\{\underline{\rho}\}_\alpha = \rho_\alpha^{1/2}$. Here the direct correlation function may be replaced by its short-ranged part because $\underline{\rho}^T\underline{q} = 0$. In the case of the binary electrolyte one has

$$\beta\chi_T^{-1} = \rho - \rho_+^2\hat{\chi}_{++}(0) - 2\rho_+\rho_-\hat{\chi}_{+-}(0) - \rho_-^2\hat{\chi}_{--}(0), \tag{22}$$

and it does not appear possible to express the individual $\hat{\chi}_{\alpha\gamma}(0)$ in terms of measurable thermodynamic parameters.

The zeroth moment condition arose from the equality of the coefficients of k^{-2} in the small-k Taylor expansion of the Fourier transform of the Ornstein-Zernike equation. It depended only upon the long-range nature of the Coulomb potential, the assumption that the total correlation function is integrable, and the assumption that the direct correlation function decayed no slower than the Coulomb potential. The second moment condition uses the coefficients of k^0, and it is necessary to establish the integrability of $\chi(r)$, (i.e. the existence of its zeroth moment). At this stage this will simply be assumed; in the next section a much stronger result will emerge, namely that $\chi(r)$ is exponentially short-ranged.

Using the (assumed) integrability of $\chi(r)$ and equating the coefficients of k^0 in the small k Taylor expansion of the Ornstein-Zernike equation one obtains,

$$\underline{\underline{H}}^{(0)} = \underline{\underline{\chi}}^{(0)} + \underline{\underline{H}}^{(0)}\underline{\underline{\chi}}^{(0)} - \underline{\underline{H}}^{(2)}\underline{\underline{Q}}. \tag{23}$$

Pre-multiplying by $\underline{\underline{Q}}$, this gives

$$\underline{\underline{Q}}\,\underline{\underline{H}}^{(0)} = \underline{\underline{Q}}\,\underline{\underline{\chi}}^{(0)} + \underline{\underline{Q}}\,\underline{\underline{H}}^{(0)}\underline{\underline{\chi}}^{(0)} - \underline{\underline{Q}}\,\underline{\underline{H}}^{(2)}\underline{\underline{Q}}, \tag{24}$$

or, using Eq. (16),

$$-\underline{\underline{Q}} = -\underline{\underline{Q}}\,\underline{\underline{H}}^{(2)}\underline{\underline{Q}}. \tag{25}$$

Explicitly this is,

$$1 = \frac{-4\pi\beta}{6\epsilon}\sum_{\gamma\lambda} q_\gamma q_\lambda \rho_\gamma \rho_\lambda \int h_{\gamma\lambda}(r) r^2\, d\mathbf{r}. \tag{26}$$

This is the second moment condition, which was first given by Stillinger and Lovett[27,28]. The current derivation that equates Fourier coefficients is due to Mitchell et al.[29].

Outhwaite[30] showed that the second moment condition can be written as a condition on the zeroth moment of the mean electrostatic potential about an ion. The latter is also called the fluctuation potential and is

$$\psi_\alpha(r) = \frac{q_\alpha}{\epsilon r} + \sum_\gamma \rho_\gamma \int h_{\alpha\gamma}(s) \frac{q_\gamma}{\epsilon|\mathbf{r}-\mathbf{s}|}\, d\mathbf{s}, \tag{27}$$

in terms of which the Ornstein-Zernike equation may be rewritten

$$\underline{\underline{H}}(r) = -\beta \underline{\psi}(r)\underline{q}^T + \underline{\underline{\chi}}(r) + \int \underline{\underline{H}}(s)\underline{\underline{\chi}}(|\mathbf{r}-\mathbf{s}|)\, d\mathbf{s}, \tag{28}$$

where $\{\underline{\psi}(r)\}_\alpha = \rho_\alpha^{1/2}\psi_\alpha(r)$. Pre-multiplying both sides by $\underline{\underline{Q}}$, integrating over $\mathbf{r}$, and using the electroneutrality condition, one obtains

$$1 = \beta \underline{q}^T \hat{\underline{\psi}}(0), \tag{29}$$

or

$$1 = \beta \sum_\alpha \rho_\alpha q_\alpha \int \psi_\alpha(r)\, d\mathbf{r}. \tag{30}$$

This may be shown to be equivalent to the second moment condition, Eq. (26), by using Poisson's equation (integrate twice by parts, and sum appropriate multiples of the two integrands to give the Laplacian in spherical coordinates[30]). This form of the condition, as a constraint on the total ion fluctuation potential, is in some ways more fundamental than the form involving the second moments of the total correlation functions; the simple form of the latter is peculiar to a uniform electrolyte, whereas the former holds in the electric double layer for arbitrary charge inhomogeneities[31].

For an m-component electrolyte there are m zeroth moment conditions but only one second moment condition; the latter provides a constraint on the total sum of the second moments of the ion pair correlation functions but does not determine the individual second moments. Like the electroneutrality condition, summing the second moments with weights equal to the ionic charges results in the cancellation of the terms involving the $\hat{\chi}_{\alpha\gamma}(0)$, which accounts for the universal nature of the result; it is independent of any short range interactions between the ions. Simply adding the correlation functions (i. e. without the ionic charge weights) results in various sum rules and fluctuation formulae that involve thermodynamic derivatives; these have been explicitly analysed for a multicomponent ionic mixture in the presence of a neutralising background[24,25].

The fourth moment of the total correlation function is important because it is related to the decay length of the electrolyte. In contrast to the zeroth and second moments, all the sum rules for the fourth moment are of a non-universal character. This can be illustrated by equating the coefficients of k^2 in the Ornstein-Zernike equation,

$$\underline{\underline{H}}^{(2)} = \underline{\underline{\chi}}^{(2)} + \underline{\underline{H}}^{(2)}\underline{\underline{\chi}}^{(0)} + \underline{\underline{H}}^{(0)}\underline{\underline{\chi}}^{(2)} - \underline{\underline{H}}^{(4)}\underline{\underline{Q}}. \tag{31}$$

The second moment of the shortened direct correlation function, (whose existence at this stage is assumed), can be eliminated by pre-multiplying by $\underline{\underline{Q}}$ and using the zeroth moment condition,

$$\underline{\underline{Q}}\,\underline{\underline{H}}^{(2)} = \underline{\underline{Q}}\,\underline{\underline{H}}^{(2)}\underline{\underline{\chi}}^{(0)} - \underline{\underline{Q}}\,\underline{\underline{H}}^{(4)}\underline{\underline{Q}}. \tag{32}$$

Finally, the second moment equation can be used to relate the fourth moment of the total correlation function to the two zeroth moments,

$$\underline{\underline{Q}}\,\underline{\underline{H}}^{(4)}\underline{\underline{Q}} = (\underline{\underline{H}}^{(0)} - \underline{\underline{\chi}}^{(0)} - \underline{\underline{\chi}}^{(0)}\underline{\underline{H}}^{(0)})(\underline{\underline{I}} - \underline{\underline{\chi}}^{(0)}). \tag{33}$$

Hence summing the fourth moments with ionic charge weights gives a result dependent upon the non-Coulombic interactions between the ions, and which in general cannot be simply expressed as thermodynamic properties of the electrolyte. In the case of the one component plasma, where fluctuations in charge are equivalent to fluctuations in number density, the fourth moment of the total correlation function is proportional to the isothermal compressibility, which to the same order equals the screening length of the plasma[32–35]; results for the multicomponent jellium have also been established[24,25]. For the restricted primitive model, (symmetric binary electrolyte), the above equation reduces to

$$\kappa_D^4(h_{++}^{(4)} - h_{+-}^{(4)}) = \chi_{++}^{(0)} - \chi_{+-}^{(0)} - 1/(\rho_+ + \rho_-). \tag{34}$$

As mentioned above, although the sum of the $\chi^{(0)}$ equals the isothermal compressibility, their difference has no physical interpretation, and hence it is not possible to give the fourth moment of the total correlation function in terms of a measurable thermodynamic property. Within a linearised hydrodynamic approximation, retaining only terms to order k^4, the fourth moment of the charge-charge correlation function of the restricted primitive model has been identified with the decay length[8,20,21].

2. Exponential screening

The above moment conditions relied upon the assumptions that the direct correlation function went like the negative of the Coulomb potential, and that the remainder was integrable. These assumptions will now be justified by establishing a stronger condition, namely that either the short-range part of the direct correlation function decays as the square of the total correlation function, or it decays exponentially. This will be sufficient to show that the total correlation function decays exponentially. Rigorous mathematical bounds have established the Debye-Hückel theory as the zero coupling limit of the electrolyte, including the exponential Debye shielding of the total correlation function[12–16]. These works and the present analysis seek to establish exponential behaviour from deeper principles, which is in contrast to most other studies where the exponential behaviour is assumed from the outset, (the clustering hypothesis, e.g. Refs[6,18,36,37]).

The argument is based upon the exact closure to the Ornstein-Zernike equation[17],

$$\begin{aligned} h_{\alpha\gamma}(r) &= -1 + \exp\left[-\beta u_{\alpha\gamma}^{\mathrm{Coul}}(r) - c_{\alpha\gamma}(r) + h_{\alpha\gamma}(r) + d_{\alpha\gamma}(r)\right] \\ &= -1 + \exp\left[h_{\alpha\gamma}(r) - \chi_{\alpha\gamma}(r) + d_{\alpha\gamma}(r)\right], \end{aligned} \tag{35}$$

where $d(r)$ is the bridge function. Now since the left hand side decays to zero for large r, ($h(r)$ is integrable by fiat), then so must the exponent, and in the asymptotic limit one linearises the exponential to obtain

$$h_{\alpha\gamma}(r) \sim -\chi_{\alpha\gamma}(r) + h_{\alpha\gamma}(r) + d_{\alpha\gamma}(r),\ r \to \infty, \tag{36}$$

where the neglected terms decay as the square of the pair correlation functions.

If the total correlation function is exponentially decaying, which is to be proved, then it can be shown that both the direct correlation function and the bridge function are also exponentially decaying (see below). At this stage the contrary will be assumed, namely that the total correlation function decays as an integrable power law, $h(r) \sim r^{-\eta},\ \eta > 3$.

The bridge function consists of diagrams comprised of h-bonds, and there are no nodal points between the root points[17]. This means that at least two h-bonds must bridge between the root points, and the individual diagrams of $d(r)$ decay at least as fast as the square of $h(r)$[38,39]. This result is certainly true if $h(r)$ decays as an integrable power law because then the convolution integrals are dominated by regions with the field point close to one or other of the root points, (because $(r/2)^{-2\eta} \ll r^{-\eta}$). In order to apply this result to the bridge function itself, which contains an infinite sum of such binodal diagrams, it is sufficient to observe that the range of the individual binodal diagrams does not change as the number of field points increases, and that the trinodal and higher order diagrams decay faster than this. (This is in contrast to, for example, the Gaussian fluid, where one can show for the series diagrams that the range of each diagram is proportional to the square root of the number of nodal points; the individual diagrams decay as Gaussians, but the infinite sum of them is renormalised to give exponential decay.) One concludes that the bridge function goes like

$$d_{\alpha\gamma}(r) \sim \mathcal{O}h_{\alpha\gamma}(r)^2,\ r \to \infty, \tag{37}$$

at least when $h(r) \sim r^{-\eta},\ \eta > 3$. Strictly speaking what appears on the right hand side should be the most long-ranged of the various $h(r)$. It will later be shown that in fact the total correlation functions between different pairs of ions all have the same range; for the present the analysis may be interpreted as applying to the longest ranged of the correlation functions.

There then remains from the linearisation of the closure only the short range part of the direct correlation function, (the $h_{\alpha\gamma}(r)$ being subtracted from both sides). Evidently this can decay no slower than the square of the total correlation function, (because there is nothing left to cancel any more slowly decaying parts). One concludes that

$$\chi_{\alpha\gamma}(r) \sim \mathcal{O}h_{\alpha\gamma}(r)^2,\ r \to \infty, \tag{38}$$

which is sufficient to ensure that the zeroth and second moments of $\chi(r)$ exist, as was assumed above in the proof of the second and fourth moment conditions. For fluids that interact with integrable power-law potentials, the coefficient of this term is just the second density derivative of the chemical potential[39]. This also completes the proof of the earlier assumption that

$$c_{\alpha\gamma}(r) \sim -\beta u_{\alpha\gamma}^{\mathrm{Coul}}(r),\ r \to \infty. \tag{39}$$

This last result is rather well-known and well-used; the present derivation represents a detailed attempt at a proof (see also Ref.[39]). It is only in exceptional circumstances that the result is known not to hold. In fluids near the spinodal line or the critical point it may possibly be dominated by the square of the total correlation function[40]. In the case

of what may be called infinitely short-ranged fluids (e.g. the hard-sphere fluid, or the Gaussian fluid), both the total and the direct correlation functions exhibit exponential decay, which dominates this direct contribution from the pair potential.

The above shows that if $h(r)$ decays as an integrable power law, then $\chi(r) \sim \mathcal{O}h(r)^2$, $r \to \infty$. It is now shown that if $h(r)$ is exponentially decaying, then all of the moments of $\chi(r)$ exist and hence it is also exponentially decaying. The proof is by induction. Assume that all of the $\underline{\underline{\chi}}^{(n)}$, exist for $n \leq 2m-2$, where $m \geq 1$ is an integer. Since $h(r)$ is exponential (by present assumption) all of the $\underline{\underline{H}}^{(l)}$ exist. Now equate the coefficients of k^{2m} in the small-k Taylor expansion of the Ornstein-Zernike equation,

$$\underline{\underline{H}}^{(2m)} = \underline{\underline{\chi}}^{(2m)} + \left[\underline{\underline{H}}^{(2m)}\underline{\underline{\chi}}^{(0)} + \underline{\underline{H}}^{(2m-2)}\underline{\underline{\chi}}^{(2)} + \ldots + \underline{\underline{H}}^{(0)}\underline{\underline{\chi}}^{(2m)}\right] + \underline{\underline{H}}^{(2m+2)}\underline{\underline{Q}}, \tag{40}$$

which gives $\underline{\underline{\chi}}^{(2m)}$ as the sum of a finite number of moments, which by assumption are themselves finite. Hence if all the moments $\leq 2m-2$ exist, then $|\underline{\underline{\chi}}^{(2m)}| < \infty$. (Note that the compressibility must be positive, $\underline{\underline{I}} + \underline{\underline{\hat{H}}}(0) > 0$.) The zeroth moment exists (by inspection), and hence by induction all moments of $\chi(r)$ exist. Thus if $h(r)$ decays exponentially, then so does $\chi(r)$. Hence either all moments of $\chi(r)$ exist, or, if $h(r)$ decays as an integrable power law, then $\chi(r)$ has at least as many moments as $h(r)$, (since it decays as the square of the latter).

The existence of $\hat{h}(0)$ and the fact that $\chi(r)$ is either exponentially decaying or of no longer range than $h(r)$ are all that are required to establish the exponential decay of the total correlation function. The proof is again by induction on the moments. Assume that all moments, $\underline{\underline{H}}^{(n)}$, exist for $n \leq 2m$, where $m \geq 1$ is an integer. Since $\chi(r)$ is either exponential or at least as short ranged as $h(r)$, all of the $\underline{\underline{\chi}}^{(n)}$, $n \leq 2m$ also exist. Equation (40) gives $\underline{\underline{H}}^{(2m+2)}$ as the sum of a finite number of moments, which by assumption are themselves finite. Hence if all the moments $\leq 2m$ exist, then $|\underline{\underline{H}}^{(2m+2)}| < \infty$. Since the zeroth moment exists by fundamental assumption, then, by induction, all moments of the total correlation function exist. This proves that the total correlation function must be at least exponentially decaying.

From the above the short range part of the direct correlation function is also at least exponentially decaying, and, from Eq. (36), so is the bridge function. For the case of a simple fluid when $h(r)$ decays as an integrable power law, both $\chi(r)$ and $d(r)$ decay as its square (see above). For the present electrolyte with an exponentially decaying $h(r)$, $\chi(r) - d(r) \sim h(r)^2/2$, $r \to \infty$, but the two functions do not necessarily individually decay as the square of the total correlation function; Kjellander and Mitchell[37] assumed that $h(r)$ decayed exponentially and showed that at high electrolyte concentrations the decay lengths of $\chi(r)$ and of $d(r)$ may be larger than $\kappa^{-1}/2$, (but not as large as κ^{-1}), where κ^{-1} is the decay length of $h(r)$. In what follows it will be assumed that $\chi(r)$ and $d(r)$ have a decay length strictly less than that of $h(r)$. The mathematical justification of this requires some detailed diagrammatic analysis, but the basic idea is that $\chi(r)$ is the multiply-connected subset of diagrams of $h(r)$ and hence cannot be of longer range. This is perhaps clearest for the bridge function where there are always two or more h-bonds connected in parallel between the root points, and hence $d(r)$ is more short-ranged than $h(r)$, and consequently so is $\chi(r)$.

This completes the proof that the total correlation function is exponentially decaying in a bulk electrolyte, where 'exponential' covers both monotonic and damped sinusoidal behaviour. Obviously undamped sinusoidal behaviour is precluded in a disordered fluid, and there is no evidence that the total correlation function decays faster than exponential. The fact that the total correlation function for an electrolyte is more short-ranged than the pair potential is in marked contrast to fluids with integrable power-law potentials; for these the total correlation function decays at the same rate as the pair potential, with a coefficient proportional to the isothermal compressibility[38,39,41]. (Hence the total correlation function is of exactly the same range as the full direct correlation function.) An analogous result holds in the case of the conditionally convergent dipolar fluid[42,43]. For the case of fluids with infinitely short-ranged pair potentials (e.g. the Gaussian fluid or the hard-sphere fluid), the total correlation function is of longer range than the pair potential.

The preceding discussion considered only the effect of the long range Coulomb potential, since one does not expect the short range interactions between the ions to qualitatively change the behaviour deduced above. (These additional interactions cannot be too ill-behaved because of the fundamental assumption of a finite compressibility.) Such short-ranged potentials are present in any realistic model of an electrolyte, and include the soft or hard core repulsion that prevents ion overlap, and also perhaps an r^{-6} dispersion attraction. One's expectation is that the charge-charge correlations will remain exponentially screened, and that the density-density correlations will decay in proportion to any power-law potentials that are present[21,41]. (In the context of the present proof, only a finite number of moments exist for these power law potentials.) For the case of an infinitely short-ranged potential such as the hard-sphere, one expects there to be exponential decay of the density-density correlation function; at low density that decay length will be shorter than the electrostatic decay length, but at high packing it should be longer, and both types of correlations will be oscillatory. (The individual ion-ion correlation functions will all decay with the same decay length, namely the longer one of the two.)

In addition to modifying the interactions between the ions, one can envisage adding solvent as a specific molecular species. The civilised model electrolyte includes a multipolar solvent, and, since the multipoles can be represented as a sum of discrete charges each of which is screened, then the solvent multipolar interactions themselves are screened. Hence the ion-ion, ion-solvent, and solvent-solvent correlation functions should all decay exponentially[44–46]. However if the ions themselves carry multipole moments, only the charge-charge correlations are exponentially screened; the non-spherical projections of the ion pair correlation functions (such as the dipole-dipole) decay as power laws[6]. In summary then, irrespective of the specific short range interactions between ions, or the presence of solvent or other additives, in an electrolyte the long range Coulomb potential can be expected to cause the charge-charge correlations to decay exponentially.

3. n-ions

The result for the pair correlation function is now extended to the many-body correlation functions, where it is shown that these are also exponentially screened, which implies that the charge and multipole moments of an ion cluster are compensated by the surrounding electrolyte[47,48]. There is nothing unexpected in these results; an electrolyte that screens the charge on a single ion will obviously screen the individual charges on a cluster, and at large distances neither the net charge nor the multipole moments are visible.

Define $h^{(n)}_{\underline{\alpha}^n}(\mathbf{r}^n)$ to be the n-body total correlation function for ions of type $\alpha_1, \alpha_2, \ldots, \alpha_n$ at $\mathbf{r}_1, \mathbf{r}_2, \ldots, \mathbf{r}_n$. Consider its behaviour as $\mathbf{r}_n \to \infty$, (by this is meant $r_i/r_n \to 0,\ 1 \le i < n$). $h^{(n)}$ comprises the connected diagrams with n root points, and it may be split into those diagrams in which the root point at $\mathbf{r}_n$ hangs from a node (nodal diagrams) and those in which it doesn't (binodal and higher diagrams). By topological reduction, the bond between the root point and the node of the nodal diagrams is the pair total correlation function. Those nodal diagrams in which the node is also a root point go like $h(r)$. Denote by $\mathbf{r}_0$ the position of the field point node in the remaining nodal diagrams. In the asymptotic limit the dominant contribution to the integral is when the nodal field point is around the remaining ions at the origin, $r_0/r_n \to 0$. This is because the nodal point must be connected to the $n-1$ remaining ions by at least binodal points due to the topological reduction, and stretching them is like stretching the bridge function. Hence any diagrams with $r_0/r_n = \mathcal{O}(1)$ are of order $h(r)^2$, (more precisely, they have the same range as the pair bridge function, which as argued above is shorter than that of $h(r)$), whereas the diagrams with $r_0/r_n \to 0$ go like $h(r)$. In the multinodal diagrams h-bonds also link the multinodal points to the root points, and one concludes that the binodal and higher diagrams decay at least as fast as $h(r)^2$ as $\mathbf{r}_n \to \infty$. Hence asymptotically the many-ion total correlation function is dominated by the mononodal diagrams, which decay like the pair total correlation function, $h^{(n)}_{\underline{\alpha}^n}(\mathbf{r}^n) \sim \mathcal{O}h(r_n),\ r_n \to \infty$, which from the above is exponentially decaying.

The many-ion total correlation function $h^{(n+1)}$ is the connected subset of the many-ion distribution function, $g^{(n+1)}_{\underline{\alpha}^{n+1}}(\mathbf{r}^{n+1})$, which represents the probability of finding the $n+1$ ions in that particular configuration in the electrolyte. One may single out the ion α_{n+1}, and the function $\rho_{\alpha_{n+1}} g^{(n+1)}/g^{(n)}$ may be interpreted as the density profile of ions of type α_{n+1} in the presence of an n-ion. This consists of a uniform bulk electrolyte contribution, which arises from the diagrams in which the ion α_{n+1} is disconnected from the rest, and a distance-dependent contribution, which includes $h^{(n+1)}_{\underline{\alpha}^{n+1}}(\mathbf{r}^{n+1})$, that consists of diagrams in which α_{n+1} is connected to one or more of the remaining n ions. By the same arguments as above this latter contribution is exponentially decaying. Now in general the n-ion has a net charge and multipole moments, which give rise to power-law interaction potentials. If these charges or moments were not screened (i.e. neutralised, or compensated) by the surrounding electrolyte, then the density would decay to its bulk value as a power law. Since the the rate of decay is exponential, one concludes that the charge and the multipole moments of an ion cluster are perfectly screened by the surrounding electrolyte.

Martin[6] has reviewed sum rules in electrolytes, using a somewhat more mathematical approach than here. These sum rules show that if the n-ion distribution function decays faster than r^{-l}, then the n-ion plus the surrounding electrolyte has no multipole moments of order l or less[6,47,48]. If the correlations are exponentially screened, as was shown above, then this gives rise to an infinite number of sum rules on the n-ion distribution function. The (l,m)-sum rule on the $(n+1)$-ion distribution function is[6]

$$\sum_{\alpha_{n+1}} q_{\alpha_{n+1}} \int \left[\rho_{\alpha_{n+1}}(\mathbf{r}_{n+1}) \frac{g^{(n+1)}_{\underline{\alpha}^{n+1}}(\mathbf{r}^{n+1})}{g^{(n)}_{\underline{\alpha}^{n}}(\mathbf{r}^{n})} \right] |\mathbf{r}_{n+1}|^l \, Y_{lm}(\hat{\mathbf{r}}_{n+1}) \, d\mathbf{r}_{n+1}$$
$$= \ -Q^{\text{ext}}_{lm} - \sum_{j=1}^{n} q_{\alpha_j} |\mathbf{r}_j|^l Y_{lm}(\hat{\mathbf{r}}_j). \tag{41}$$

The bracketed part of the integrand represents the density of ions of type α_{n+1} in the presence of an n-ion and an external field. ($Q^{\rm ext} = 0$ corresponds to the bulk electrolyte with uniform density, $\rho_\alpha(\mathbf{r}) = \rho_\alpha$.) Since Y_{lm} is the spherical harmonic, the left side represents the (l,m)-multipole moment of this inhomogeneous electrolyte, and the right side is the negative of the multipole moment of the n-ion and of the external charge distribution. The case $l = m = 0$ yields the electroneutrality condition.

For the homogeneous electrolyte, $Q^{\rm ext} = 0$, the $n = 0$ case gives the bulk electroneutrality condition,

$$\sum_{\alpha=1}^{m} q_\alpha \rho_\alpha \int_V d\mathbf{r} = V \sum_{\alpha=1}^{m} q_\alpha \rho_\alpha = 0, \tag{42}$$

which restricts the concentrations of the species in the electrolyte. The $n = 1$ case yields the zeroth moment condition given above

$$\sum_{\alpha=1}^{m} q_\alpha \rho_\alpha \int g_{\alpha\gamma}(r_{\alpha\gamma})\, d\mathbf{r}_\alpha = \sum_{\alpha=1}^{m} q_\alpha \rho_\alpha \int h_{\alpha\gamma}(r_{\alpha\gamma})\, d\mathbf{r}_\alpha = -q_\gamma, \tag{43}$$

since $h_{\alpha\gamma}(r) = g_{\alpha\gamma}(r) - 1$.

For the electric double layer for $n = 0,\ l = m = 0$ one has

$$\sum_{\alpha=1}^{m} q_\alpha \int_V \rho_\alpha(\mathbf{r})\, d\mathbf{r} = -Q^{\rm ext}, \tag{44}$$

and, for $n = 1,\ l = m = 0$,

$$\sum_{\alpha=1}^{m} q_\alpha \int \rho_\alpha(\mathbf{r}) g_{\alpha\gamma}(\mathbf{r}_\alpha, \mathbf{r}_\gamma)\, d\mathbf{r}_\alpha = -Q^{\rm ext} - q_\gamma, \tag{45}$$

or, in terms of the inhomogeneous total correlation function, $h_{\alpha\gamma}(\mathbf{r}_\alpha, \mathbf{r}_\gamma) = g_{\alpha\gamma}(\mathbf{r}_\alpha, \mathbf{r}_\gamma) - 1$,

$$\sum_{\alpha=1}^{m} q_\alpha \int \rho_\alpha(\mathbf{r}) h_{\alpha\gamma}(\mathbf{r}_\alpha, \mathbf{r}_\gamma)\, d\mathbf{r}_\alpha = -q_\gamma. \tag{46}$$

This shows the local screening of each ion in the double layer.

C. Debye-Hückel theory

The exponential screening of ion correlations in electrolytes is well known. And nearly as wide-spread is the use of the Debye length as the decay length, both in the electrolyte and in the double layer. In this section a simple demonstration is given that even at the level of Debye-Hückel theory the screening length of the electrolyte is different from the Debye length.

The linearised Debye-Hückel theory, originally derived on the basis of the Poisson-Boltzmann approximation[49], may also be obtained by neglecting the short-ranged part of the direct correlation function,

$$\underline{\underline{\hat{\chi}}}(k) = 0. \tag{47}$$

Note that this is an approximation even for point ions. It is expected to become an increasingly better approximation as the coupling between the ions is reduced, for example in monovalent electrolyte at low concentrations. The Ornstein-Zernike equation (5) becomes

$$\begin{aligned} \underline{\underline{\hat{H}}}(k) &= -\left(\underline{\underline{I}} + \underline{\underline{Q}} k^{-2}\right)^{-1} \underline{\underline{Q}} k^{-2} \\ &= -\left(\underline{\underline{I}} - \frac{1}{k^2 + \kappa_D^2} \underline{\underline{Q}}\right) \underline{\underline{Q}} k^{-2} \\ &= \frac{-1}{k^2 + \kappa_D^2} \underline{\underline{Q}}, \end{aligned} \tag{48}$$

where Eqs (11) and (12) have been used. This has inverse transform

$$\underline{\underline{H}}(r) = \frac{-e^{-\kappa_D r}}{4\pi r}\underline{\underline{Q}}, \tag{49}$$

or, in component form,

$$h_{\alpha\gamma}(r) = \frac{-\beta q_\alpha q_\gamma}{\epsilon r} e^{-\kappa_D r}. \tag{50}$$

Hence the Debye-Hückel theory predicts that the ion correlation functions are exponentially decaying, with the decay length being the Debye length, and with the amplitude proportional to the product of the charges on the ions.

The Debye-Hückel approximation only satisfies the electroneutrality condition if this exponential form holds for all of r, not just asymptotically. For ions all with a hard-core of diameter d, $h_{\alpha\gamma}(r) = -1,\ r < d$. This means that the electroneutrality condition is no longer satisfied by applying Eq. (50) beyond the core. Retaining the Yukawa form, Eq. (50), but scaling the prefactor to satisfy electroneutrality, one obtains the modified linearised Debye-Hückel approximation,

$$h_{\alpha\gamma}(r) = \begin{cases} -1, & r < d \\ \dfrac{-\beta q_\alpha q_\gamma e^{\kappa_D d}}{\epsilon[1+\kappa_D d]} \dfrac{e^{-\kappa_D r}}{r}, & r > d. \end{cases} \tag{51}$$

A problem with this linearised theory is that it allows the coion radial distribution function to become negative. For this reason the Yukawa form is often applied instead to the potential of mean force,

$$w_{\alpha\gamma}(r) = \frac{q_\alpha q_\gamma}{\epsilon} \frac{e^{-\kappa_D r}}{r}, r > d, \tag{52}$$

When exponentiated this gives the radial distribution function, $g_{\alpha\gamma}(r) = \exp -\beta w_{\alpha\gamma}(r)$. The justification for this lies in the traditional derivation of Debye-Hückel theory, which sets the potential of mean force equal to the charge times the mean electrostatic potential, and solves Poisson's equation for the latter by linearising the radial distribution function. When the non-linear terms are negligible, the linear and the non-linear total correlation functions will be approximately equal and the theory could be said to be internally consistent. But when the non-linear terms make a contribution, it is arguably better to use the exponential of the potential of mean force even though this is not fully consistent with the linearisation that was assumed to solve Poisson's equation. This non-linear version has the same asymptotic form as the modified Debye-Hückel approximation, but experience shows that overall it tends to be a better approximation, in part because it always remains physical at small separations.

For the case when α is a macroion, the Debye-Hückel result is called the linear Poisson-Boltzmann approximation for an isolated spherical macroion, and $\rho_\gamma g_{\alpha\gamma}(r)$ represents the density profile for ions of type γ in the double layer about the macroion. It is not possible to obtain an analytic solution for the non-linear Poisson-Boltzmann approximation in spherical geometry. If both α and γ are taken to be macroions, then the Debye-Hückel $w_{\alpha\gamma}(r)$ represents an approximation for their interaction. This however is not the same as solving the linear Poisson-Boltzmann equation for two interacting macroions, since the solution of the latter involves two-center Bessel function expansion[50–52]. The 'linear' in linear Poisson-Boltzmann refers only to the local proportionality between the electrostatic potential and the density; the potential itself is clearly a non-linear function of distance. The presence of a second macroion changes the boundary conditions such that the potential between two macroions is not strictly the pair-wise sum of the potentials due to the isolated macroions (except as an approximation when one can ignore the presence of the second sphere in the boundary condition, possibly at asymptotic separations). This is an example of how the level of approximation depends upon whether one regards both solutes as fixed and the source of a single external field, or whether one treats the second solute the same as the electrolyte and allows it to respond to the field due to the first solute. A similar situation has already arisen in the discussion of n-ions, and will occur again in the treatment of interacting planar walls. Numerical solutions of the non-linear Poisson-Boltzmann equation for two spheres have been given[53–55].

1. Self-consistent screening length

The other problem with the (linear) modified Debye-Hückel result is that it does not obey the second moment condition. This was noted by Stillinger and Lovett[28], who pointed out that for finite-sized ions the modified Debye-Hückel result could only satisfy their condition by allowing for an effective screening length rather than the Debye

length. That is,

$$h_{\alpha\gamma}(r) = \begin{cases} -1, & r < d \\ \dfrac{-\beta q_\alpha q_\gamma e^{\kappa d}}{\epsilon[1+\kappa d]} \dfrac{\kappa^2}{\kappa_D^2} \dfrac{e^{-\kappa r}}{r}, & r > d. \end{cases} \tag{53}$$

This satisfies the electroneutrality condition, and κ is determined by the second moment condition[18],

$$\begin{aligned} 1 &= \frac{-4\pi\beta}{6\epsilon} \sum_{\alpha\gamma} q_\alpha \rho_\alpha q_\gamma \rho_\gamma \int_d^\infty \frac{-\beta q_\alpha q_\gamma e^{\kappa d}}{\epsilon[1+\kappa d]} \frac{\kappa^2}{\kappa_D^2} \frac{e^{-\kappa r}}{r} 4\pi r^4 \, dr \\ &= \frac{\kappa_D^2}{\kappa^2} \frac{1 + \kappa d + (\kappa d)^2/2 + (\kappa d)^3/6}{1+\kappa d}. \end{aligned} \tag{54}$$

The assumption of purely exponential profiles is only expected to be valid for small κd, and one expects this result to correct the Debye-Hückel theory in at least this regime. This expression only yields sensible results for $\kappa_D d \le \sqrt{6}$, which is the upper bound established by Stillinger and Lovett[27] for monotonic ion correlations, $g_{++}(r) \le g_{+-}(r)$, $r > d$, in the restricted primitive model. At higher concentrations than this the correlations *must* be oscillatory, although in practice the oscillations occur before the bound is reached.

For an m-component mixture there are in general $m(m+1)/2$ independent total correlation functions. In the next section it will be shown that in the asymptotic regime the matrix of these is dyadic and that they have Yukawa form, as in the linear Debye-Hückel approximation. The present approximation is to apply the asymptote everywhere beyond the core, which means that one has only $m+1$ unknowns, (essentially the m effective charges and the decay length). By happy coincidence there are m electroneutrality conditions and one second moment condition, and hence in this approximation it is always possible to determine the decay length of a mixture of ions of arbitrary valence and diameter. (The equations given explicitly above only apply to ions of equal size.) It is also possible to implement a non-linear version of this approximation, where it is the potential of mean force that is taken as the dyadic Yukawa beyond the core. One must now solve the $m+1$ equations numerically, and one finds that this exponential approximation is more accurate for multiply charged ions than the analytic linear version given above.

Figure 1 shows the actual screening length of aqueous restricted primitive model electrolytes relative to the Debye length, and compares the self-consistent Debye-Hückel result given here with the results of the more sophisticated hypernetted chain approximation. Equation (54) relates the two dimensionless parameters, κd and $\kappa_D d$, and hypernetted chain results confirm that the latter is an appropriate characteristic for monovalent electrolytes in this regime[18,56]. In the case of divalents at non-vanishing concentrations the results do depend upon the diameter of the ions[18,56], and $\kappa_D d$ is less appropriate. From the figure it may be seen that the actual screening length at low concentrations is initially greater than the Debye length for divalents ($\kappa < \kappa_D$), whereas for monovalents it is mainly less than the Debye length ($\kappa > \kappa_D$). For divalents the linear self-consistent Debye-Hückel approximation, Eq. (54), is inaccurate, but the exponential version lies closer to the hypernetted chain results. Initially the decay length decreases with increasing electrolyte concentration (greater screening), but there comes a point where the hypernetted chain results predict that the decay length increases with increasing concentration. For monovalents this occurs at about $\kappa_D d = 1.3$, which is the transition from monotonic exponential decay to damped sinusoidal behaviour, where the counterion and coion correlation functions oscillate out of phase. This will be discussed in detail in the next section, but beyond this there is another transition to a core-dominated regime where the ion correlation functions oscillate in phase. This can be seen in Fig. 1 at high concentrations where the divalent and monovalent results coincide.

There have been a number of results for the screening length of Coulomb fluids[8,18,20,22,36,37,56–59]. Of particular relevance to the present section are those based upon the linearised Poisson-Boltzmann equation[60,61], and the analytic solution of the mean spherical approximation[62–64]. For the restricted primitive model the latter gives $\kappa d = -1 + \sqrt{(1 + 2\kappa_D d)} = \kappa_D d[1 - \kappa_D d/2 + \ldots]$. On the other hand, the expression given by Stillinger and Kirkwood[65], based upon a charge moment expansion, at low concentrations goes like $\kappa d = \kappa_D d[1 + (\kappa_D d)^2/4 + \ldots]$, which to the exhibited order agrees with Eq. (54). Stell and Lebowitz[36] use a high temperature /low density expansion and obtain corrections to the Debye length in terms of the correlation functions of a reference hard-sphere fluid. For a symmetric electrolyte they give

$$\begin{aligned} \frac{\kappa^2}{\kappa_D^2} &= 1 - \kappa_D^2 \int_0^\infty h^{(0)}(r) r \, dr + \ldots \\ &= 1 + \kappa_D^2 d^2/2 + \ldots, \end{aligned} \tag{55}$$

which again agrees with Eq. (54). Mitchell and co-workers[37,56–59] have also derived low density expansions for the screening length; for a symmetric electrolyte they give[37]

$$\frac{\kappa}{\kappa_D} = 1 + \frac{\beta^2 q^4 \kappa_D^2}{12\epsilon^2} \ln \frac{\beta e^2 \kappa_D}{\epsilon} + \mathcal{O}(\kappa_D^2). \tag{56}$$

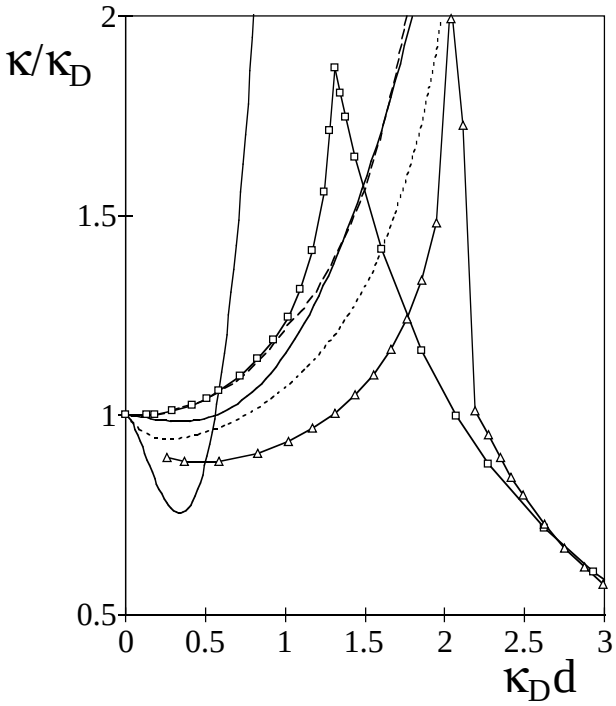

FIG. 1: The actual decay length of the restricted primitive model in terms of the Debye length. The symbols are hypernetted chain calculations (squares are monovalent, $d = 4$Å, triangles are divalent, $d = 4$Å, data from Ref.[18]), the dashed line is the self-consistent linear Debye-Hückel result, Eq. (54), and the dotted line is the exponentiated version for divalents. The solid curves are the low density expansion,[37], Eq. (56), with the divalent having the deeper minimum. Here and in the remaining figures the temperature is $T = 300$K and the relative permittivity is $\epsilon_r = 78.5$, unless otherwise noted.

In contrast to Eq. (54) and to the expansion of Stell and Lebowitz[36], this leading term in the expansion is independent of the ion diameter and it approaches unity from below. In Fig. 1 it is compared to the hypernetted chain data, which is expected to be accurate in the regime shown. For the monovalent electrolyte the expansion is qualitatively correct up to $\kappa_D d \approx 1.5$, although not quite as accurate as the self-consistent Debye-Hückel result, Eq. (54). For the divalent electrolyte the low density expansion is obviously inapplicable at physical electrolyte concentrations. Nevertheless it is in qualitative accordance with the hypernetted chain results in predicting that at lower concentrations the screening length of the divalent electrolyte is greater than the Debye length, (i.e. the ratio κ/κ_D is less than unity). Mitchell and co-workers[37,57,58] find that the primary departure from the Debye length at vanishing concentrations is larger for an asymmetric electrolyte than for a symmetric electrolyte. In particular they find that κ approaches κ_D linearly from above for an asymmetric electrolyte[58]. Stell and Lebowitz, also find an effect due to asymmetry, (their leading order term also vanishes for a symmetric electrolyte); however, they argue for the one component plasma that the screening length should be greater than the Debye length[36]. Whether asymmetry causes a large shift in the screening length, (compared to the symmetric electrolyte), remains to be checked at non-vanishing concentrations by accurate numerical calculations.

D. Asymptotic analysis

This section analyses the asymptotic behaviour of the ion-ion correlation functions for the bulk electrolyte. One of the things to be determined is the transition from monotonic to oscillatory decay of the correlation functions, first discussed for electrolytes by Kirkwood[65–67]; in general fluids this transition is called the Fisher-Widom line[68]. In electrolytes three different asymptotic regimes may be identified, and these are shown rather clearly in Fig. 2. At low concentrations (more precisely low ion coupling) there is monotonic decay of the total correlation function; the counterion density about an ion always exceeds the coion density. This is the exponential behaviour of Debye-Hückel theory. At higher concentrations one finds oscillatory behaviour. In the first place the oscillations are in the charge density, (electrostatic-dominated oscillatory decay), and the counterion and coion densities oscillate out of phase. At the highest couplings it is the number density that oscillates (core-dominated oscillatory decay), and here the

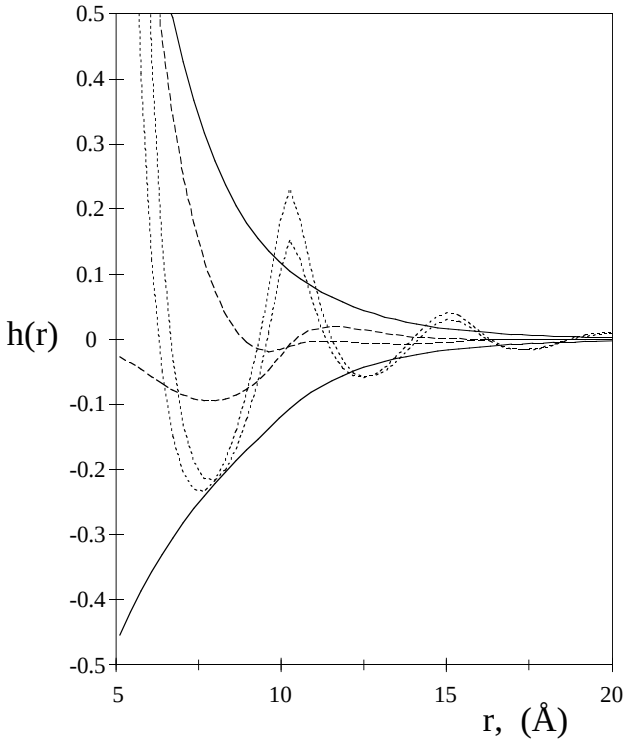

FIG. 2: The hypernetted chain total correlation function for a restricted primitive model monovalent electrolyte with $d = 5$Å. Results are for the monotonic electrostatic regime, (0.5M, solid curves), the oscillatory electrostatic regime, (2M, dashed curves), and the oscillatory core regime, (5M, dotted curves). The counterion curve is greater than the corresponding coion curve near contact. Redrawn from Ref.[18].

counterion and coion densities oscillate in phase. Note the difference in period of these two oscillatory regimes: in the core-dominated regime the period is close to the ionic diameter, whereas in the electrostatic regime it is much larger. Roughly speaking the charge oscillations correspond to alternating shells of positive and negative charge, and hence the period in this case is at least $2d$, and can be considerably larger than this close to the monotonic-oscillatory transition. (It is likely that electrolytes with more than two components have more than two oscillatory asymptotic phases, depending upon their symmetry and the linear combinations that may be formed.)

In the core-dominated regime for the restricted primitive model of Fig. 2, the density-density correlation function has a larger decay length than the charge-charge correlation function, and vice versa in the electrostatic dominated regime. It has to be understood that there is a unique decay length common to all the individual ion-ion pair correlation functions (in this example the larger of the density-density and the charge-charge); it is only particular linear combinations of the individual functions that can decay with different rates. This point, which holds in mixtures generally, has received some recent attention[69–72], although it has probably always been well-known; for example the literature is extensive on *the* decay length of electrolytes. As is discussed in detail below, the asymptotic decay rate is determined by the location in Fourier space of the poles of the pair correlation functions, and the matrix of the latter is, by the Ornstein-Zernike equation, an inverse matrix times the matrix of the direct correlation functions. The poles correspond to the singularities (i.e. the vanishing of the determinant) of this inverse matrix. Hence these singularities are common to all of the pair correlation functions.

The asymptotic behaviour of electrolytes was has been studied in the context of the departure from the Debye length[8,20,22,36,56–64], and it has received more detailed attention recently[18,37,59,73]. The analysis of this section follows that of Ref.[18] rather closely. The results of Section IB are used, namely that the ion correlation functions decay exponentially due to the fact that the direct correlation function goes like the Coulomb potential plus a short-ranged function. By manipulating the Ornstein-Zernike equation in Fourier space expressions are obtained for the amplitude and the decay length of the correlation functions. The asymptote is formally identical to the linear Debye-Hückel total correlation function, but with effective parameters.

1. Monotonic asymptotic decay

The Ornstein-Zernike equation, (15), may be solved for the total correlation function,

$$\begin{aligned}
\underline{\underline{\hat{H}}}(k) &= \left(\underline{\underline{I}} - \underline{\underline{\hat{\chi}}}(k) + \underline{\underline{Q}}k^{-2}\right)^{-1}\left(\underline{\underline{\hat{\chi}}}(k) - \underline{\underline{Q}}k^{-2}\right) \\
&= \left(\underline{\underline{I}} + \left(\underline{\underline{I}} - \underline{\underline{\hat{\chi}}}(k)\right)^{-1}\underline{q}\,\underline{q}^T\frac{4\pi\beta}{\epsilon k^2}\right)^{-1}\left(\underline{\underline{I}} - \underline{\underline{\hat{\chi}}}(k)\right)^{-1}\left(\underline{\underline{\hat{\chi}}}(k) - \underline{q}\,\underline{q}^T\frac{4\pi\beta}{\epsilon k^2}\right) \\
&= \left(\underline{\underline{I}} + \underline{\tilde{q}}(k)\underline{q}^T\frac{4\pi\beta}{\epsilon k^2}\right)^{-1}\left(\underline{\underline{I}} - \underline{\underline{\hat{\chi}}}(k)\right)^{-1}\left(\underline{\underline{\hat{\chi}}}(k) - \underline{q}\,\underline{q}^T\frac{4\pi\beta}{\epsilon k^2}\right). \qquad (57)
\end{aligned}$$

Here an effective charge function has been defined,

$$\underline{\tilde{q}}(k) = \left(\underline{\underline{I}} - \underline{\underline{\hat{\chi}}}(k)\right)^{-1}\underline{q}, \qquad (58)$$

which may be equivalently written

$$\underline{\tilde{q}}(k) = \underline{q} + \underline{\underline{\hat{\chi}}}(k)\underline{\tilde{q}}(k). \qquad (59)$$

Now the first inverse is readily evaluated (c.f. Eq. (12))

$$\left(\underline{\underline{I}} + \underline{\tilde{q}}(k)\underline{q}^T\frac{4\pi\beta}{\epsilon k^2}\right)^{-1} = \underline{\underline{I}} - \frac{4\pi\beta/\epsilon}{k^2+\Lambda(k)^2}\underline{\tilde{q}}(k)\underline{q}^T, \qquad (60)$$

where a function has been defined that will become the screening length, (c.f. Eq. (10)),

$$\Lambda(k)^2 = \frac{4\pi\beta}{\epsilon}\underline{\tilde{q}}^T(k)\underline{q}. \qquad (61)$$

Now if there exists κ such that $\Lambda(i\kappa) = \kappa$, then the total correlation function will have a pole at $k = i\kappa$, which determines its asymptotic behaviour. (This assumes that $\chi(r)$ is more short-ranged than $h(r)$, and hence that any singular behaviour of $\hat{\chi}(k)$ occurs further from the origin than this κ.) This pole corresponds to the vanishing of the denominator, which is a scalar multiplying the remaining matrices. Hence each element of the matrix of total correlation functions has a pole located at $\Lambda(i\kappa)$, and hence each will have the same asymptotic decay. Neglecting the regular part, one has

$$\begin{aligned}
\underline{\underline{\hat{H}}}(k) &\sim \frac{-4\pi\beta/\epsilon}{k^2+\Lambda(k)^2}\underline{\tilde{q}}(k)\underline{q}^T\left(\underline{\underline{I}} - \underline{\underline{\hat{\chi}}}(k)\right)^{-1}\left(\underline{\underline{\hat{\chi}}}(k) - \underline{q}\,\underline{q}^T\frac{4\pi\beta}{\epsilon k^2}\right) \\
&= \frac{-4\pi\beta/\epsilon}{k^2+\Lambda(k)^2}\underline{\tilde{q}}(k)\underline{\tilde{q}}^T(k)\left(\underline{\underline{\hat{\chi}}}(k) - \underline{q}\,\underline{q}^T\frac{4\pi\beta}{\epsilon k^2}\right) \\
&= \frac{-4\pi\beta/\epsilon}{k^2+\Lambda(k)^2}\underline{\tilde{q}}(k)\left(\underline{\tilde{q}}^T(k)\underline{\underline{\hat{\chi}}}(k) - \underline{q}^T\Lambda(k)^2/k^2\right) \\
&\sim \frac{-4\pi\beta/\epsilon}{k^2+\Lambda(k)^2}\underline{\tilde{q}}\,\underline{\tilde{q}}^T, \quad k \to i\kappa \qquad (62)
\end{aligned}$$

Here the second equality follows from Eq. (58) and the final equality from Eq. (59). Also, $\underline{\tilde{q}} \equiv \underline{\tilde{q}}(i\kappa)$. This is in similar form to the Debye-Hückel result, Eq. (48), and in order to cast it in identical form, that is to exhibit the residue explicitly, one needs the Taylor expansion of the denominator about $k = i\kappa$,

$$\begin{aligned}
k^2+\Lambda(k)^2 &\sim (k-i\kappa)\left(2i\kappa + \frac{4\pi\beta}{\epsilon}\underline{q}^T\underline{\tilde{q}}'\right) + \ldots \\
&\sim (k^2+\kappa^2)\left(1 + \frac{4\pi\beta}{2i\kappa\epsilon}\underline{q}^T\underline{\tilde{q}}'\right) + \mathcal{O}(k-i\kappa)^2. \qquad (63)
\end{aligned}$$

Here

$$\begin{aligned}\underline{\tilde{q}}' &= \left.\frac{\partial \underline{\tilde{q}}(k)}{\partial k}\right|_{k=i\kappa} \\ &= \left.\frac{\partial \underline{\underline{\hat{\chi}}}(k)}{\partial k}\right|_{k=i\kappa} \underline{\tilde{q}} + \underline{\underline{\hat{\chi}}}(i\kappa) \left.\frac{\partial \underline{\tilde{q}}(k)}{\partial k}\right|_{k=i\kappa} \\ &= \left(\underline{\underline{I}} - \underline{\underline{\hat{\chi}}}(i\kappa)\right)^{-1} \left.\frac{\partial \underline{\underline{\hat{\chi}}}(k)}{\partial k}\right|_{k=i\kappa} \underline{\tilde{q}} \end{aligned} \tag{64}$$

Hence one defines

$$\begin{aligned}\nu &\equiv 1 + \frac{4\pi\beta}{2i\kappa\epsilon} \underline{q}^T \underline{\tilde{q}}' \\ &= 1 + \frac{4\pi\beta}{2i\kappa\epsilon} \underline{q}^T \left(\underline{\underline{I}} - \underline{\underline{\hat{\chi}}}(i\kappa)\right)^{-1} \underline{\underline{\hat{\chi}}}'(i\kappa) \underline{\tilde{q}} \\ &= 1 + \frac{4\pi\beta}{2i\kappa\epsilon} \underline{\tilde{q}}^T \underline{\underline{\hat{\chi}}}'(i\kappa) \underline{\tilde{q}} \end{aligned} \tag{65}$$

One now has

$$\underline{\underline{\hat{H}}}(k) \sim \frac{-4\pi\beta}{\epsilon\nu} \frac{\underline{\tilde{q}}\,\underline{\tilde{q}}^T}{k^2+\kappa^2}, \quad k \to i\kappa, \tag{66}$$

with inverse

$$h_{\alpha\gamma}(r) \sim \frac{-\beta \tilde{q}_\alpha \tilde{q}_\gamma}{\epsilon\nu} \frac{e^{-\kappa r}}{r}, \quad r \to \infty, \quad \mathrm{Im}\{\kappa\} = 0. \tag{67}$$

Note that if $\underline{\underline{\chi}} = 0$, Eq. (58) implies that $\underline{\tilde{q}} = \underline{q}$, Eq. (61) yields $\kappa = \kappa_D$, and Eq. (65) shows that $\nu = 1$. In other words, the exact asymptote, Eq. (67), reduces to the Debye-Hückel result, Eq. (50).

Recall that $\underline{\tilde{q}}$ is given by Eq. (58) evaluated at $k = i\kappa$. With this definition the actual screening length, Eq. (61), assumes a form similar to the Debye length[18,36,37,59]

$$\kappa^2 = \frac{4\pi\beta}{\epsilon} \underline{\tilde{q}}^T \underline{q} = \frac{4\pi\beta}{\epsilon} \sum_\alpha \rho_\alpha \tilde{q}_\alpha q_\alpha. \tag{68}$$

The quantity $\epsilon\nu$, which appears in the denominator of the asymptote, can be related to the non-local electrostatic susceptibility of the electrolyte[37]; in this connection this dielectric response function was approximated by Lovett and Stillinger and used to find the asymptotic decay length of the electrolyte[61]. Stell and Lebowitz[36] obtained formally the same asymptote and screening length, except that they set $\nu = 1$. To leading order in βq^2, they give an approximation for the effective charges in terms of properties of the reference system (in this case it would be a hard-sphere fluid),

$$\tilde{q}_\alpha \approx q_\alpha + \sum_\gamma q_\gamma \rho_\gamma \int h^0_{\alpha\gamma}(r)\, d\mathbf{r} = \sum_\gamma q_\gamma \frac{\partial \rho_\alpha}{\partial \beta \mu^0_\gamma}, \tag{69}$$

where the superscript denotes the reference system. This first correction to the bare charge vanishes in the symmetric electrolyte and in this case higher order terms are required[36].

The effective charges represent the response of the ions to the mean electrostatic potential[37,59]. This can be seen from the Fourier transform of the Ornstein-Zernike equation written in terms of the latter, Eq. (28),

$$\begin{aligned}\underline{\underline{\hat{H}}}(k) &= -\beta \underline{\hat{\psi}}(k) \underline{q}^T + \underline{\underline{\hat{\chi}}}(k) + \underline{\underline{\hat{H}}}(k) \underline{\underline{\hat{\chi}}}(k) \\ &= -\beta \underline{\hat{\psi}}(k) \underline{q}^T \left(\underline{\underline{I}} - \underline{\underline{\hat{\chi}}}(k)\right)^{-1} + \underline{\underline{\hat{\chi}}}(k) \left(\underline{\underline{I}} - \underline{\underline{\hat{\chi}}}(k)\right)^{-1} \\ &\sim -\beta \underline{\hat{\psi}}(k) \underline{\tilde{q}}^T, \quad k \to i\kappa. \end{aligned} \tag{70}$$

The last line follows since $\chi(r)$ is more short-ranged than $h(r)$, and hence only the first term contributes to the asymptote. In other words, the mean electrostatic potential about an ion has the same range as the total correlation function, and one has

$$h_{\alpha\gamma}(r) \sim -\beta \tilde{q}_\alpha \psi_\gamma(r), \quad r \to \infty. \tag{71}$$

which shows that it is the effective charge on the ion which gives its response to the mean electrostatic potential. Now from symmetry $h_{\alpha\gamma}(r) = h_{\gamma\alpha}(r)$, and one concludes that $\psi_\gamma(r) \propto \tilde{q}_\gamma$. The precise relationship follows from Eq. (67),

$$\psi_\gamma(r) \sim \tilde{q}_\gamma \frac{e^{-\kappa r}}{\epsilon\nu r}, \quad r \to \infty. \tag{72}$$

In the asymptotic regime the potential of mean force has linear Poisson-Boltzmann form, $w_{\alpha\gamma}(r) \sim \tilde{q}_\alpha\psi_\gamma(r) \sim \tilde{q}_\alpha\tilde{q}_\gamma\psi(r)$, which is significant because the full symmetry of the pair correlation functions is preserved. This is not the case for generalisations of Debye-Hückel theory based upon the non-linear Poisson-Boltzmann approximation. Here the mean electrostatic potential about each ion is no longer strictly proportional to the response of that ion (i.e. the charge), and in consequence the pair correlation functions are not symmetric, which is a long-standing criticism of that approximation[74–76].

For an m-component electrolyte, in the most general case there are $m(m+1)/2$ pair total correlation functions, but the dyadic nature of the asymptote given here indicates that in this regime only m of them are independent. A similar situation occurs for fluid mixtures that interact with integrable power law potentials. In general one has

$$h_{\alpha\gamma}(r) \sim -\beta \sum_{\lambda\delta} \frac{\partial \ln \rho_\alpha}{\partial\beta\mu_\lambda}\, u_{\lambda\delta}(r)\, \frac{\partial \ln \rho_\delta}{\partial\beta\mu_\gamma}, \quad r \to \infty. \tag{73}$$

For the case of a dyadic potential, $u_{\alpha\gamma}(r) \sim a_\alpha a_\gamma r^{-n}$, $r \to \infty$, this reduces to

$$h_{\alpha\gamma}(r) \sim -\beta\tilde{a}_\alpha\tilde{a}_\gamma r^{-n}, \quad r \to \infty, \quad n > 3, \tag{74}$$

with

$$\tilde{q}_\alpha = \sum_\lambda q_\lambda \frac{\partial \ln \rho_\alpha}{\partial\beta\mu_\lambda} = \sum_\lambda q_\lambda \frac{\partial \ln \rho_\lambda}{\partial\beta\mu_\alpha}. \tag{75}$$

In the asymptotic regime there are only m-independent quantities, which are linear combinations of the chemical potential derivative of the densities. The assumed dyadic nature of the pair potential is not so specialised as it may at first appear; in the case of a Lennard-Jones mixture the coefficient of the r^{-6} term represents the product of the polarisabilities of the individual atoms.

2. Oscillatory asymptotic decay

One needs to allow for the possibility that κ is complex, which corresponds to oscillatory solutions. In this case one takes twice the real part of the asymptote given above, as may be seen as follows. By definition $h_{\alpha\gamma}(r)$ is a real, even function of r, and hence its Fourier transform is even, $\hat{h}_{\alpha\gamma}(-k) = \hat{h}_{\alpha\gamma}(k)$, and any series expansion in k has real coefficients, $\overline{\hat{h}_{\alpha\gamma}(k)} = \hat{h}_{\alpha\gamma}(\overline{k})$, where the overline denotes the complex conjugate. In other words,

$$\underline{\underline{\hat{H}}}(-k) = \underline{\underline{\hat{H}}}(k) \tag{76}$$

and

$$\overline{\underline{\underline{\hat{H}}}(k)} = \underline{\underline{\hat{H}}}(\overline{k}) \tag{77}$$

These two results imply that there are four poles located at $\pm i\kappa$, and $\pm i\overline{\kappa}$, and the singular part may be written

$$\begin{aligned} \underline{\underline{\hat{H}}}^{\mathrm{s}}(k) &= \frac{\underline{\underline{A}}}{k - i\kappa} + \frac{\underline{\underline{A'}}}{k + i\kappa} + \frac{\underline{\underline{B}}}{k - i\overline{\kappa}} + \frac{\underline{\underline{B'}}}{k + i\overline{\kappa}} \\ &= \frac{\underline{\underline{A}}}{k^2 + \kappa^2} + \frac{\underline{\underline{B}}}{k^2 + \overline{\kappa}^2} \\ &= \frac{\underline{\underline{A}}}{k^2 + \kappa^2} + \frac{\overline{\underline{\underline{A}}}}{k^2 + \overline{\kappa}^2}, \end{aligned} \tag{78}$$

since Eq. (76) implies that $A = -A'$ and $B = -B'$, and Eq. (77) implies that $B = \overline{A}$. Hence when the conventional Fourier inverse is evaluated by closing the contour in the upper half plane, (choosing κ to be in the first quadrant),

one picks up the residue at $k = +i\kappa$, which is $A/(2i\kappa)$, and also its complex conjugate from the residue from the pole at $k = -i\overline{\kappa}$, which is $\overline{A}/(2i\overline{\kappa})$. The sum of these two is twice the real part of either one, and one has

$$h_{\alpha\gamma}(r) \sim 2\mathrm{Re}\left\{\frac{-\beta\tilde{q}_\alpha\tilde{q}_\gamma}{\epsilon\nu}\frac{e^{-\kappa r}}{r}\right\}, \quad r\to\infty, \quad \mathrm{Im}\{\kappa\}\neq 0. \tag{79}$$

The abrupt disappearance of the factor of two as the poles coalesce on the imaginary axis suggests non-analyticity in the amplitude of the correlation functions at the transition from monotonic to oscillatory decay. In fact the amplitude becomes infinite, as will now be shown.

Let the pole just move off the imaginary k-axis, $\kappa = \kappa_r + i\kappa_i$, $\kappa_i \to 0$. Expanding Eq. (61) one obtains

$$\begin{aligned}
\kappa_r + i\kappa_i &= \left(\frac{4\pi\beta}{\epsilon}\underline{q}^T\underline{\tilde{q}}(i\kappa_r - \kappa_i)\right)^{1/2} \\
&\sim \left(\frac{4\pi\beta}{\epsilon}\underline{q}^T\underline{\tilde{q}}(i\kappa_r)\right)^{1/2}\left[1 - \frac{\kappa_i}{2}\frac{\underline{q}^T\underline{\tilde{q}}'(i\kappa_r)}{\underline{q}^T\underline{\tilde{q}}(i\kappa_r)} + \mathcal{O}(\kappa_i^2)\right] \\
&= \kappa_r - \frac{\kappa_i}{2\kappa_r}\frac{4\pi\beta}{\epsilon}\underline{q}^T\underline{\tilde{q}}'.
\end{aligned} \tag{80}$$

Equating the coefficients of κ_i, one obtains

$$\frac{4\pi\beta}{2\kappa_r\epsilon}\underline{q}^T\underline{\tilde{q}}' = -i, \quad \kappa_i \to 0, \tag{81}$$

or from the first equality of Eq. (65),

$$\nu \to 0, \quad \kappa_i \to 0. \tag{82}$$

That is, the amplitude of the total correlation function becomes infinite at the oscillatory to monotonic transition.

One has to be careful in interpreting this result. The vanishing of ν means that the next term in the Taylor expansion (63) is non-negligible. Hence the denominator corresponds to a double pole, and the residue comes from the linear term in the numerator, which ensures that the asymptotic behaviour remains exponential. For infinitesimal but non-zero ν, the present formulae give the strict asymptote, but the regime of applicability moves to ever larger separations. For fixed r, as $\nu \to 0$ the $h(r)$ have a large contribution from the (finite) second term. (This limit has been discussed in the context of a dominant and a sub-dominant pole coalescing on, and then parting off, the imaginary axis[37,73].) For fixed non-zero ν, as $r \to \infty$ the $h(r)$ are given by the strict asymptote. So even though the amplitude diverges, so do the relevant separations, and consequently thermodynamic properties such as the internal energy remain finite at the monotonic-oscillatory transition.

3. Core domination

The analysis of the previous section is formally exact, and the Fourier transforms of the total correlation functions are guaranteed to have a pole at $k = i\kappa$, for κ satisfying Eqs (58) and (61). Nevertheless this pole does not necessarily determine the asymptotic behaviour of the correlations, because there could be another pole, $k = i\xi$, with $\mathrm{Re}\{\xi\} < \mathrm{Re}\{\kappa\}$, even assuming that κ represents the solution of the preceding equations with smallest real part. Such a qualitatively different pole would correspond to the matrix $\underline{\underline{I}} - \underline{\underline{\hat{\chi}}}(i\xi)$ being singular.

The implicit reason for splitting the matrix $\underline{\underline{I}} - \underline{\underline{\hat{C}}}(k)$ in the fashion of the preceding section was the assumption that the matrix $\underline{\underline{Q}}$ was the most important in the asymptotic regime. This would be the case when electrostatics determined the asymptotic behaviour, hence the title of the section. However at high densities one might expect the short-range interactions to become important asymptotically, and this regime might be termed the 'core-dominated asymptote', and is the subject of this section.

This regime will not be treated in full generality, but instead the following restriction will be observed. Denote the amplitude of the total correlation functions in the asymptotic regime by $a_{\alpha\gamma}$. Then because electrostatic effects are of shorter range, locally the asymptotic charge density about an ion must vanish, and one has

$$\sum_\alpha q_\alpha\rho_\alpha a_{\alpha\gamma} = 0. \tag{83}$$

It is emphasised that this is an exact result that holds in the core-dominated asymptotic regime. One way of satisfying this equation is if

$$a_{\alpha\gamma} = a, \text{ all species.} \tag{84}$$

What follows is predicated on this restriction. Two cases can be mentioned where this equation will hold exactly with no approximation. First, there is the general binary electrolyte, in which case this is the only possible solution. Second, there is a multi-component electrolyte with the short-range interactions between the ions being identical; since it is the latter that determine the asymptote, then the total correlation functions between all the species must be asymptotically equal.

The condition Eq. (84) means that the short range part of the direct correlation function goes like

$$\underline{\underline{\hat{\chi}}}(k) \sim \underline{\rho}\,\underline{\rho}^T x(k), \quad k \to i\xi, \tag{85}$$

where $\{\underline{\rho}\}_\alpha = \rho_\alpha^{1/2}$. (This follows from the Ornstein-Zernike equation solved for the direct correlation function near the pole.) Note that $\underline{\rho}^T \underline{q} = 0$, and hence near the pole

$$\begin{aligned}\left(\underline{\underline{I}} - \underline{\underline{\hat{C}}}(k)\right)^{-1} &\sim \left(\underline{\underline{I}} - \underline{\rho}\,\underline{\rho}^T x(k) + \underline{q}\,\underline{q}^T 4\pi\beta/\epsilon k^2\right)^{-1} \\ &= \underline{\underline{I}} + \frac{\underline{\rho}\,\underline{\rho}^T x(k)}{1 - \underline{\rho}^T \underline{\rho}\, x(k)} - \frac{\underline{q}\,\underline{q}^T 4\pi\beta/\epsilon k^2}{1 + \underline{q}^T \underline{q} 4\pi\beta/\epsilon k^2}.\end{aligned} \tag{86}$$

Now it is the middle term which has the pole at $k = i\xi$, and neglecting the remaining regular parts one obtains

$$\begin{aligned}\underline{\underline{\hat{H}}}(k) &\sim \frac{\underline{\rho}\,\underline{\rho}^T x(k)}{1 - \underline{\rho}^T \underline{\rho}\, x(k)} \left(\underline{\rho}\,\underline{\rho}^T x(k) - \underline{q}\,\underline{q}^T 4\pi\beta/\epsilon k^2\right) \\ &= \frac{\underline{\rho}^T \underline{\rho}\, x(k)^2}{1 - \underline{\rho}^T \underline{\rho}\, x(k)} \underline{\rho}\,\underline{\rho}^T \\ &\sim \frac{-2i\xi x(i\xi)}{\underline{\rho}^T \underline{\rho}\, x'(i\xi)(k^2 + \xi^2)} \underline{\rho}\,\underline{\rho}^T, \quad k \to i\xi.\end{aligned} \tag{87}$$

Here a Taylor expansion of the denominator has been used, together with the fact that ξ satisfies

$$\underline{\rho}^T \underline{\rho} x(i\xi) = \rho x(i\xi) = 1, \tag{88}$$

where the total number density is $\rho = \sum_\alpha \rho_\alpha = \underline{\rho}^T \underline{\rho}$. One concludes that

$$h_{\alpha\gamma}(r) \sim 2\mathrm{Re}' \left\{ \frac{-2i\xi}{4\pi\rho^2 x'(i\xi)} \frac{e^{-\xi r}}{r} \right\}, \quad r \to \infty. \tag{89}$$

The notation $\mathrm{Re}'\{z\}$ means to take the real part of z if z is complex, and to take half of z if z is real. (In this regime ξ will always be complex because the analysis only makes sense when the correlation functions are oscillatory.) In contrast to the preceding section, this analysis holds for uncharged particles, subject to the restriction (84). In the core dominated regime the ion-ion total correlation functions decay like damped sinusoids, with a prefactor that corresponds to the unique amplitude that they have in common. The charge on an ion is very rapidly neutralised by the surrounding counterions, and the correlations that persist are due to packing of the ions in the dense electrolyte or molten salt. One anticipates that the period of the oscillations will correspond to the size of the ions, whereas in the case of charge oscillations the period was greater than about

II. ANALYSIS OF THE DOUBLE LAYER

There are two approaches to analysing the electric double layer: one can regard the charged macro-particles as solutes in the electrolyte and take the infinite dilution limit of this species of the multicomponent mixture (singlet method), or one can regard these particles as fixed and as the source of an external field causing a non-uniform distribution of ions in their vicinity (inhomogeneous method). These are but alternative viewpoints of the same phenomena, and both can be used to obtain formally exact results. In many ways the distinction between them is

not so much conceptual as practical and historical, and the relative numerical merits of the two approaches will be discussed in more detail under approximate methods, (§III), and under results (§IV). For asymptotic analysis, which forms a large part of this section, the singlet approach is the most useful, and here it is used to formulate the electric double layer in various geometries.

The charged particles that are the source of the electric double layer are here taken to be solutes at infinite dilution. Section IIA treats spherical macroions, and establishes their charge neutralisation by the excess of counterions in the double layer, the exponential decay of the latter with the decay length of the bulk electrolyte, and the fact that the asymptotic interaction between two macroions scales with the square of the effective charge of an isolated macroion. Isolated and interacting planar solutes are treated in §§IIB and IIC, both with a view to establishing the wall-ion and the wall-wall Ornstein-Zernike equations, and to determining the asymptotic behaviour of the planar double layer. The Derjaguin approximation is derived in §IIC2, and its domain of applicability delineated. The section concludes with the application of the singlet approach to other solute geometries, specifically cylinders, pores, and dumb-bells.

A. Spherical solutes

1. Double layer moments

The analysis of §IB is here extended to the double layer about a charged solute, following Ref.[18]. For the multi-component electrolyte, one of the components is taken to be a spherical solute, species $\alpha = 0$ with charge q_0. One is interested in the double layer about this solute, which is treated in isolation by taking the infinite dilution limit, $\rho_0 = 0$. One then focusses on the solute-ion contributions to the multi-component Ornstein-Zernike equation (3) by defining a vector of solute-ion total correlation functions

$$\{\underline{H}(r)\}_\gamma = \rho_\gamma^{1/2} h_{0\gamma}(r), \quad \gamma > 0, \tag{90}$$

and similarly for the direct correlation functions. The density of ions in the double layer about the solute is $\rho_\gamma(r) = \rho_\gamma[h_{0\gamma}(r) + 1]$. Since $\rho_0 = 0$, there is no solute-solute contribution to the convolution integral, and the solute-ion Ornstein-Zernike equation becomes

$$\underline{H}(r) = \underline{C}(r) + \int \underline{\underline{C}}(s)\underline{H}(|\mathbf{r} - \mathbf{s}|)\, d\mathbf{s}, \tag{91}$$

with Fourier transform

$$\begin{aligned} \hat{\underline{H}}(k) &= \hat{\underline{C}}(k) + \hat{\underline{\underline{C}}}(k)\hat{\underline{H}}(k) \\ &= \hat{\underline{\chi}}(k) - \frac{4\pi\beta q_0}{\epsilon k^2}\underline{q} + \hat{\underline{\underline{\chi}}}(k)\hat{\underline{H}}(k) - \underline{\underline{Q}}\hat{\underline{H}}(k)k^{-2}. \end{aligned} \tag{92}$$

The proof by induction that the ion-solute correlation functions are exponentially decaying is almost unchanged from the ion-ion case treated in §IB2. Since the exact solute-ion closure is identical to the ion-ion closure, it can be concluded that the short range part of solute-ion direct correlation function, $\underline{\chi}(r)$, is either exponentially decaying or more short ranged than $\underline{H}(r)$. Then by equating the various powers of k in the Fourier transform of the Ornstein-Zernike equation, and using the established fact that the necessary moments of $\underline{\underline{\chi}}(r)$ exist, it is found that both solute-ion correlation functions are exponentially short-ranged. That is to say that the ion densities in the double layer around a charged solute decay to their bulk electrolyte concentrations at an exponential rate. $\chi_{0\gamma}(r)$ is also exponentially decaying, and one has $\chi_{0\gamma}(r) - d_{0\gamma}(r) \sim h_{0\gamma}(r)^2/2,\ r \to \infty$. For the asymptotic analysis below, one assumes that the short range part of solute-ion direct correlation function is more short ranged than the solute-ion total correlation function, $\chi_{0\gamma}(r)/h_{0\gamma}(r) \to 0,\ r \to \infty$.

Since the moments exist, one may equate the coefficients of k^{-2} to obtain the solute electroneutrality condition

$$-q_0 = \underline{q}^T \underline{H}^{(0)} = \sum_\gamma q_\gamma \rho_\gamma \int h_{0\gamma}(r)\, d\mathbf{r}, \tag{93}$$

which confirms the result given above, Eq. (44). This shows that the charge on the solute is exactly cancelled by the net charge in the double layer. This counter-charge must have either dissociated from the originally neutral surface, or ions from the originally neutral bulk electrolyte must have adsorbed to the solute giving it its charge. The only way that the charge on the solute is not neutralised by the double layer is if the ion density profile about the solute were to be so long-ranged as to be non-integrable, (and vice versa).

Turning now to the second moment, by equating the coefficients of k^0 in the Fourier transform of the Ornstein-Zernike equation one obtains

$$\underline{H}^{(0)} = \underline{\chi}^{(0)} + \underline{\underline{\chi}}^{(0)}\underline{H}^{(0)} - \underline{\underline{Q}}\underline{H}^{(2)}, \tag{94}$$

or, using the electroneutrality condition,

$$-q_0 = \underline{q}^T\underline{\chi}^{(0)} + \underline{q}^T\underline{\underline{\chi}}^{(0)}\underline{H}^{(0)} - \kappa_D^2\underline{q}^T\underline{H}^{(2)}. \tag{95}$$

In this case the second moment of the ion-solute total correlation function depends upon the zeroth moment of the short range part of the ion-solute direct correlation function. The former is analogous to one of the individual second moments of the ion-ion total correlation functions of the bulk electrolyte, and it will be recalled that these were not individually constrained by the second moment condition. It was only their sum that was constrained, and because the solute is at infinite dilution, this last result can be added to the bulk second moment condition, Eq. (26), without effect. As in the case of the bulk electrolyte, one can rewrite Eq. (95) in terms of the zeroth moment of the mean electrostatic potential about the solute since the latter is related to the second moment of the ion-solute total correlation function by Poisson's equation. (Note that no new information is obtained by reversing the Ornstein-Zernike integrand, (i.e. replacing $c * h$ by $h * c$); all that results are identities corresponding to the two moment conditions of the bulk electrolyte.)

The pairwise interaction between the solutes is given by the singlet approach when $\alpha = \gamma = 0$ in Eq. (3). The solute-solute Ornstein-Zernike equation for identical solutes is

$$h_{00}(r) = c_{00}(r) + \int \underline{C}(s)^T\underline{H}(|\mathbf{r}-\mathbf{s}|)\,d\mathbf{s}, \tag{96}$$

with Fourier transform

$$\begin{aligned}\hat{h}_{00}(k) &= \hat{c}_{00}(k) + \underline{\hat{C}}(k)^T\underline{\hat{H}}(k)\\ &= \hat{\chi}_{00}(k) - \frac{4\pi\beta q_0^2}{\epsilon k^2} + \underline{\hat{\chi}}(k)^T\underline{\hat{H}}(k) - \frac{4\pi\beta q_0}{\epsilon k^2}\underline{q}^T\underline{\hat{H}}(k).\end{aligned} \tag{97}$$

Since the bulk closure remains the same, the exponential decay of the solute-solute interaction follows immediately. However, the coefficient of k^{-2} yields

$$-q_0 = \underline{q}^T\underline{H}^{(0)}, \tag{98}$$

which contains nothing new, and the coefficient of k^0 yields

$$h_{00}^{(0)} = \chi_{00}^{(0)} + \underline{\chi}^{(0)\,T}\underline{H}^{(0)} - \frac{4\pi\beta q_0}{\epsilon}\underline{q}^T\underline{H}^{(2)}. \tag{99}$$

Using the result given above, the second moment could be eliminated and this could be re-expressed in terms of the zeroth moments of the various correlation functions. There is no electroneutrality condition for the solute-solute total correlation function; in this case the zeroth moment is non-universal and depends upon the zeroth moments of various solute correlation functions.

2. Asymptotic analysis

In the context of the singlet approach, the formal asymptotic analysis for the behaviour of the double layer about a spherical solute is virtually unchanged from that for the bulk electrolyte, §ID. The solute is at infinite dilution, (species 0, $\rho_0 \to 0$), and does not contribute to the solvent correlation functions because the Ornstein-Zernike convolution integral, Eq. (3), is multiplied by ρ_0 whenever the solute correlation functions appear in the integrand. That is, the properties of the bulk solvent are not affected by the addition of the infinitely dilute solute, and all of the preceding analysis for the ionic correlations remains. Hence the decay length κ^{-1}, the effective charge on the ions $\tilde{q}_\gamma$, $\gamma > 0$, and the scale factor ν stay the same. The Fourier transform of the solute-ion Ornstein-Zernike equation, (91), becomes

$$\underline{\hat{H}}(k) = \left(\underline{\underline{I}} - \underline{\underline{\hat{C}}}(k)\right)^{-1}\underline{\hat{C}}(k). \tag{100}$$

The pole that determines the asymptotic behaviour of the solute-ion total correlation function corresponds to the singularity in the inverted matrix. This consists solely of the bulk ion direct correlation functions, and hence may be explicitly seen to be unchanged by the solute; the determinant vanishes at the same $k = i\kappa$ as in the bulk electrolyte. Hence the pole of the solute-solvent total correlation functions have the same residue as in the bulk electrolyte, with an effective solute charge $\tilde{q}_0$ appearing. One ends up with

$$\underline{\hat{H}}(k) \sim \frac{-4\pi\beta/\epsilon}{k^2 + \Lambda(k)^2} \tilde{q}_0 \underline{\tilde{q}}, \quad k \to i\kappa, \tag{101}$$

where the effective charge on the solute is related to the short-range part of the solute-solvent direct correlation functions by

$$\begin{aligned} \tilde{q}_0 &= \underline{\tilde{q}}^T \underline{\hat{C}}(i\kappa) \\ &= q_0 + \underline{\tilde{q}}^T \underline{\hat{\chi}}(i\kappa) \end{aligned} \tag{102}$$

The asymptote is

$$h_{0\gamma}(r) \sim 2\mathrm{Re}' \left\{ \frac{-\beta \tilde{q}_0 \tilde{q}_\gamma}{\epsilon\nu} \frac{e^{-\kappa r}}{r} \right\}, \quad r \to \infty. \tag{103}$$

It is emphasised that κ, ν, and $\tilde{q}_\gamma$, $\gamma > 0$, are all properties of the bulk electrolyte and are unaffected by the solute. Only $\tilde{q}_0$ depends on the nature of the solute, via the short-ranged part of the solute-solvent direct correlation functions. The solute-solute total correlation function follows by setting $\gamma = 0$ in this result, and depends on the square of the effective solute charge.

A point worth emphasising about this result is that the rate at which the ion densities in the double layer about an isolated solute decay to their bulk concentrations (the decay length κ) is the same as the decay length of the bulk electrolyte. One of the earliest analyses to show this effect was that of Stillinger and Kirkwood[65]. (This behaviour is predicted generally by the singlet approach[70,77,78]; it holds also for the liquid-vapour interface[70,71].) Amongst other things this means that the ion profiles will become oscillatory at a point determined by the bulk electrolyte concentration, and similarly for the interaction between the solutes. This point has been emphasised in the context of the modified Poisson-Boltzmann theory[60,79,80].

The amplitude of decay of the ion densities in the double layer about a solute is determined by the nature of the solute via $\tilde{q}_0$, and the interaction between two identical solutes scales with the square of their effective charge. In consequence the force between two identical macroions must be repulsive at large separations in the monotonic regime. This follows because all quantities are real, $\tilde{q}_0$ occurs as a square, and $\nu > 0$. (At low coupling, $\nu \to 1$, the Debye-Hückel result, and at the monotonic-oscillatory transition, $\nu \to 0$, Eq. (82).) In other words, asymptotically the force between identical charged solutes is either monotonic repulsive, or oscillatory. *It cannot be monotonicly attractive.* In the oscillatory regime it is periodically attractive, and the attractive regions can be quite large since the period of oscillations becomes infinite as one approaches the bulk oscillatory-monotonic transition.

In the core-dominated regime, the analysis proceeds as in the bulk. Under the same assumption that the electrolyte ions have identical short-range interactions, one obtains for the spherical solute

$$\underline{\hat{H}}(k) \sim \frac{-2i\xi x(i\xi)}{\underline{\rho}^T \underline{\rho}\, x'(i\xi)(k^2 + \xi^2)} \underline{\rho}\, \underline{\rho}^T \underline{\hat{\chi}}(i\xi), \quad k \to i\xi, \tag{104}$$

with corresponding asymptote

$$h_{0\alpha}(r) \sim 2\mathrm{Re}' \left\{ \frac{-2i\xi}{4\pi\rho^2 x'(i\xi)} \frac{e^{-\xi r}}{r} \sum_{\gamma>0} \rho_\gamma \hat{\chi}_\gamma(i\xi) \right\}, \; r \to \infty. \tag{105}$$

Since the right hand side is independent of the index of the left hand side, whatever the direct solute-ion interaction for each species is, the solute-ion profiles become identical at large separations in this core-dominated regime, (provided that the correlations of the ions themselves are asymptotically identical in the bulk).

The solute-solute total correlation function goes like

$$\begin{aligned} \hat{h}_{00}(k) &= \hat{c}_{00}(k) + \underline{\hat{H}}^T(k) \underline{\hat{C}}(k) \\ &\sim \frac{-2i\xi x(i\xi)}{\underline{\rho}^T \underline{\rho}\, x'(i\xi)(k^2 + \xi^2)} \underline{\hat{\chi}}^T(i\xi) \underline{\rho}\, \underline{\rho}^T \underline{\hat{\chi}}(i\xi), \; k \to i\xi, \end{aligned} \tag{106}$$

since the solute-solute direct correlation function is more short-ranged than the total correlation function, and since $\underline{\rho}^T\underline{\hat{C}} = \underline{\rho}^T\underline{\hat{\chi}}$ because $\underline{\rho}^T\underline{q} = 0$. One obtains the asymptote

$$h_{00}(r) \;\sim\; 2\mathrm{Re}'\left\{\frac{-2i\xi}{4\pi\rho^2 x'(i\xi)}\frac{e^{-\xi r}}{r}\left(\sum_{\gamma>0}\rho_\gamma\hat{\chi}_\gamma(i\xi)\right)^2\right\},\quad r\to\infty. \tag{107}$$

The sum evidently represents the effective 'charge' of the solute; it gives the magnitude of the ion density profile in the double layer about the isolated solute, and its square gives the magnitude of their pairwise interaction.

B. Isolated planar solutes

1. *Wall-ion Ornstein-Zernike equation*

Originally the wall-solvent Ornstein-Zernike equation was derived from the large solute radius limit[81], and in the case of the electric double layer the derivation was modified to take care of the long range Coulomb potential[18,82–84]. Based on that experience, the singlet approach has come to be interpreted quite generally, and the existence of the solute-solvent Ornstein-Zernike equation is taken for granted, with the solute being characterised by the geometrical factors manifest in the symmetry of the arguments of the correlation functions. This is the approach taken here for a solute that represents a planar wall.

The wall-ion correlation functions depend only upon the perpendicular distance from the surface of the wall, and the distance convention is such that contact occurs at $z = 0$ for all ions,

$$h_{0\alpha}(z) = -1,\; z < 0. \tag{108}$$

Although a more realistic model could allow for ion-specific distances of closest approach to the surface, due for example to variation in size or solvation, the consequent complication in the algebra obscures the subsequent analysis without any new features emerging. Therefore a single contact plane is assumed in all that follows. The wall is here a semi-infinite half-space; it is also possible to deal with a wall of finite thickness, but in this case one should be aware that correlations can occur between ions across the wall, and the properties of the coupled double layers are not identical to those at an isolated infinitely thick wall. Electroneutrality was shown above to hold for a spherical solute of arbitrary radius, and it also holds for the planar wall. In the present geometry the condition is

$$-\sigma = \int_0^\infty \underline{q}^T\underline{H}(z)\,dz. \tag{109}$$

This electroneutrality constraint is also known as the constant charge condition. An alternative is instead to specify the surface potential, since this mimics the effects of charge regulation at some or other level of approximation. The constant charge case is the easiest to deal with theoretically, and one can in practice obtain any desired surface potential by empirical adjustments of the charge. One has to exercise some care when dealing with interacting double layers at constant potential because the free energy differs from that taken at constant charge due to the variation in charge with separation. Comparison between the two models at finite separations generally refer to double layers that are identical at infinite separation. The interaction pressure is the same at any separation provided the two models have the same surface potential and charge at that separation. In what follows only the constant charge model will be treated.

In view of the symmetry, the Ornstein-Zernike convolution integral may be expressed in cylindrical coordinates,

$$\begin{aligned}\underline{H}(z) &= \underline{C}(z) + 2\pi\int_0^\infty ds\,s\int_{-\infty}^\infty dz'\,\underline{\underline{C}}\left(\sqrt{(z'-z)^2+s^2}\right)\underline{H}(z'), &(110)\\ &= -\beta\psi(z)\underline{q} + \underline{\chi}(z) + 2\pi\int_0^\infty ds\,s\int_{-\infty}^\infty dz'\,\underline{\underline{\chi}}\left(\sqrt{(z'-z)^2+s^2}\right)\underline{H}(z'). &(111)\end{aligned}$$

Here the vector of wall-ion total correlation functions has components $\{\underline{H}(z)\}_\alpha = \rho_\alpha^{1/2}h_\alpha(z)$, and similarly for the wall-ion direct correlation function $\underline{C}(z)$ and its short ranged part $\underline{\chi}(z)$. As before one has

$$c_{0\alpha}(z) = \chi_{0\alpha}(z) - \beta q_\alpha V_0^{\mathrm{Coul}}(z), \tag{112}$$

where the Coulomb part of the solute-ion potential may be written in general as

$$V_0^{\rm Coul}(\mathbf{r}) = \int \frac{\sigma(\mathbf{s})}{\epsilon|\mathbf{r}-\mathbf{s}|}\, d\mathbf{s}. \tag{113}$$

In the present particular, the wall charge density is $\sigma(\mathbf{r}) = \sigma\delta(z)$, where σ is the surface charge per unit area located at the plane $z = 0$. In view of this the mean electrostatic potential is defined by the passage from the first to the second form of the Ornstein-Zernike equation. It is

$$\begin{aligned}
\psi(z) &= \frac{2\pi}{\epsilon}\int_{-\infty}^{\infty} dz' \int_0^{\infty} ds\; s[\sigma\delta(z') + \underline{q}^T\underline{H}(z')]\frac{1}{\sqrt{s^2+(z-z')^2}} \\
&= \frac{-2\pi}{\epsilon}\int_{-\infty}^{\infty}[\sigma\delta(z') + \underline{q}^T\underline{H}(z')]|z-z'|\, dz' \\
&= \frac{2\pi}{\epsilon}\int_0^{\infty}\underline{q}^T\underline{H}(z')z'\, dz' + \frac{4\pi}{\epsilon}\int_z^{\infty}\underline{q}^T\underline{H}(z')(z-z')\, dz', \quad z>0,
\end{aligned} \tag{114}$$

and $\psi(z) = \psi(0), \quad z < 0$. (The electroneutrality condition has been used to cancel the upper limit of the first integration.) In this form the mean electrostatic potential goes to a non-zero constant in the bulk electrolyte far from the wall, $\psi(z) \to -\psi(0),\ z \to \infty$. This is undesirable because in order for the density to decay to its bulk value far from the wall, the second form of the Ornstein-Zernike equation implies that $\underline{\chi}(z) \to -\beta\underline{q}\psi(0),\ z \to \infty$, (and the closure below implies the same limiting behaviour for the bridge function). By adding an appropriate constant one can set the zero of the potential to be in the bulk,

$$\psi(z) = \begin{cases} \psi(0), & z \le 0, \\ \dfrac{4\pi}{\epsilon}\displaystyle\sum_\gamma q_\gamma\rho_\gamma\int_z^{\infty} h_{0\gamma}(z')(z-z')\, dz', & z \ge 0, \end{cases} \tag{115}$$

and now $\psi(z),\ \underline{\chi}(z),$ and $\underline{d}(z) \to 0$ all go to zero in the bulk far from the wall. (It is possible to include a Stern layer, $-\delta < z < 0$, which is the region between the plane of closest approach of the ions and the plane in which the surface charge is located, in which the potential is linear, but this has no effect on the properties of the double layer and so is not treated here.) This choice of zero is equivalent to choosing the constant of the wall-ion Coulomb potential such that

$$V_0^{\rm Coul}(z) = -\frac{2\pi\sigma}{\epsilon}|z| + \frac{2\pi\sigma}{\epsilon}S + \frac{\psi(0)}{2}, \text{ all } z, \tag{116}$$

where $S \to \infty$ is the lateral extent of the wall. The potential drop across the double layer is

$$\psi(0) = \frac{-4\pi}{\epsilon}\sum_\gamma q_\gamma\rho_\gamma\int_0^{\infty} h_{0\gamma}(z')z'\, dz', \tag{117}$$

and it is the variation of this with surface charge that is the differential capacitance. The first moment of the total correlation function represents the dipole moment of the double layer, and $\psi(0)$ is just the drop in electrostatic potential across a dipole layer.

The diagrammatic definitions of the wall-ion correlation functions are identical to the usual ion-ion ones, and the exact closure is

$$h_{0\alpha}(z) = -1 + \exp\left[-\beta q_\alpha V_0(z) + h_{0\alpha}(z) - c_{0\alpha}(z) + d_\alpha(z)\right] \tag{118}$$

$$= -1 + \exp\left[h_{0\alpha}(z) - \chi_{0\alpha}(z) + d_{0\alpha}(z)\right], \tag{119}$$

where $d_{0\alpha}(z)$ is the wall-ion bridge function. Here and henceforth it is assumed that the ions interact with the wall only via the Coulomb potential, for $z > 0$, and that there is an infinite repulsion (hard-core) for $z < 0$. Note that the second form of the closure, Eq. (119), with the second form of the Ornstein-Zernike equation, Eq. (111), reduce to the non-linear Boltzmann approximation when $\chi_{\alpha\gamma}(r)$ and $d_{0\alpha}(z)$ are set to zero. Also, the surface charge density does not explicitly appear in the expression for the mean electrostatic potential, Eq. (115), or in the alternate forms for the Ornstein-Zernike and closure equations, (111) and (119); it must be determined by the electroneutrality condition, Eq. (109).

The wall-ion total correlation function that appears here may be identified with the solute-ion total correlation function of the preceding section in the limit that the radius of the macroionic solute goes to infinity,

$$\lim_{R\to\infty} h_{0\alpha}(R+z;R) = h_{0\alpha}(z), \tag{120}$$

where on the left side macroion-ion total correlation function appears with its dependence on the macroion radius shown explicitly, and the right side defines the wall-ion total correlation function. An identical limit holds for $\chi_{0\alpha}(z)$, but in the case of $c_{0\alpha}(z)$, $V_0(z)$, and $\psi(z)$ the limiting equality only holds up to an arbitrary constant.

As in the case of the spherical solute, the short range part of the wall-ion direct correlation function is exponentially short-ranged, and assumed to have a shorter decay length than the total correlation function. This is true of the electrolyte side of the wall, but within the wall it goes to a constant. This can be seen from the Ornstein-Zernike equation (111), where in the limit that $z \to -\infty$ the convolution integral is dominated by regions $z' \approx z$, because $\underline{\underline{\chi}}(r)$ is exponentially short-ranged, and hence $\underline{H}(z')$ may be replaced by -1 and taken out of the integral. The result is

$$\lim_{z\to-\infty} \chi_{0\alpha}(z) = -1 + \beta q_\alpha \psi(0) + \sum_\gamma \rho_\gamma \hat{\chi}_{\alpha\gamma}(0), \tag{121}$$

or using Eq. (21),

$$\underline{\rho}^T \underline{\chi}(z) \to -\beta\chi_T^{-1}, \;\; z \to -\infty. \tag{122}$$

The fact that $\chi_{0\alpha}(z)$ goes to a constant means that its one-dimensional Fourier transform is well-defined in the upper half of the complex plane.

2. Asymptotics of the isolated planar double layer

The asymptotic behaviour of the planar electric double can be obtained from the preceding analysis and the large radius limit of the solute asymptotes in §IIA. The radial Fourier transforms for spherical symmetric functions become one dimensional Fourier transforms in the planar case. In the large radius limit the relationship between them is

$$\begin{aligned}
\hat{f}(k;R) &= \frac{4\pi}{k}\int_0^\infty f(r;R)\sin kr\, r\, dr \\
&= \frac{4\pi}{k}\int_{-R}^\infty f(R+z;R)\sin\left[k(R+z)\right]\,(R+z)\,dz \\
&= \frac{4\pi}{ik}\int_{-R}^\infty f(R+z;R)\sinh\left[ik(R+z)\right]\,(R+z)\,dz \\
&\sim \frac{-2\pi R e^{-ikR}}{ik}\int_{-\infty}^\infty f(z)e^{-ikz}\,dz, \;\; R\to\infty, \;\; \mathrm{Im}\{k\}>0, \\
&= \frac{-2\pi R e^{-ikR}}{ik}\overline{f}(k),
\end{aligned} \tag{123}$$

which defines the one-dimensional Fourier transform, denoted by an overline.

The one-dimensional Fourier transform of the Coulomb part of the wall potential will also be required. This turns out to be a generalised function, which may be treated by rewriting Eq. (116) in terms of Heaviside step functions

$$V_0^{\mathrm{Coul}}(z) = \frac{-2\pi\sigma}{\epsilon}[z\theta(z) - z\theta(-z)] + \frac{2\pi\sigma}{\epsilon}S + \frac{\psi(0)}{2}. \tag{124}$$

Now the Fourier transform of $z\theta(z)$ is k^{-2}, provided $\mathrm{Im}\{k\} < 0$, and the Fourier transform of $-z\theta(-z)$ is also k^{-2}, but for $\mathrm{Im}\{k\} > 0$. Hence analytic continuation is necessary, and the transform of the wall-ion Coulomb potential in the whole complex plane is

$$\overline{V}_0^{\mathrm{Coul}}(k) = \frac{-4\pi\sigma}{\epsilon k^2} + \left[\frac{2\pi\sigma}{\epsilon}S + \frac{\psi(0)}{2}\right]2\pi\delta(k), \;\; \text{all } k. \tag{125}$$

This result was obtained in Ref.[18] by using Poisson's equation, $V_0''(z) = -(4\pi\sigma/\epsilon)\delta(z)$, and the fact that the Fourier transform of $f''(z)$ is $-k^2\overline{f}(k)$.

With these results the effective charge on the macroion, Eq. (102), becomes

$$\begin{aligned}\tilde{q}_0(R) &= \underline{\tilde{q}}^T \underline{\hat{C}}(i\kappa; R) \\ &\sim \frac{2\pi R e^{\kappa R}}{\kappa} \left[\underline{\tilde{q}}^T \underline{\overline{\chi}}(i\kappa) - \beta \underline{\tilde{q}}^T \underline{q} \overline{V}_0^{\mathrm{Coul}}(i\kappa) \right], \quad R \to \infty \\ &= \frac{2\pi R e^{\kappa R}}{\kappa} \left[\sigma + \underline{\tilde{q}}^T \underline{\overline{\chi}}(i\kappa) \right], \end{aligned} \tag{126}$$

where the fact that $\kappa^2 = (4\pi\beta/\epsilon)\underline{\tilde{q}}^T \underline{q}$ has been used. In view of this one defines the effective surface charge density[18]

$$\tilde{\sigma} = \frac{1}{2} \left[\sigma + \underline{\tilde{q}}^T \underline{\overline{\chi}}(i\kappa) \right], \tag{127}$$

where a factor of a half is included in the definition to preserve the Poisson-Boltzmann form for the asymptote, and so that at low concentrations $\tilde{\sigma} = \sigma$. This last fact follows because in the Poisson-Boltzmann limit $\chi_{\alpha\gamma}(r) = 0$, and hence $\kappa = \kappa_D$ and $\tilde{\underline{q}} = \underline{q}$. In this regime the linear Poisson-Boltzmann profile holds, $\underline{H}(z) = -\beta \underline{q} \psi(z), \quad z > 0$, and Eq. (111) shows that $\chi_{0\alpha}(z) = 0, \ z > 0$, and that $\chi_{0\alpha}(z) = -1 + \beta q_\alpha \psi(0), \ z < 0$. In this limit $\underline{q}^T \underline{\chi}(z) = \kappa_D^2 \epsilon \psi(0)/4\pi = \kappa_D \sigma, \ z < 0$, and hence $\underline{q}^T \underline{\overline{\chi}}(i\kappa_D) = \sigma$. Note that this expression for the effective surface charge holds when there is no Stern layer; if one has a Stern layer of width δ, then one simply replaces σ by $\sigma e^{-\kappa\delta}$ in this result; the expressions given below remain formally unchanged.

Inserting these results into the solute-ion total correlation function, Eq. (103),

$$h_{0\gamma}(R+z; R) \sim 2\mathrm{Re}' \left\{ \frac{-\beta \tilde{q}_0(R) \tilde{q}_\gamma}{\epsilon\nu} \frac{e^{-\kappa(R+z)}}{R+z} \right\}, \quad z \to \infty, \tag{128}$$

one obtains in the planar limit

$$h_{0\gamma}(z) \sim 2\mathrm{Re}' \left\{ \frac{-4\pi\beta \tilde{q}_\gamma \tilde{\sigma}}{\epsilon\nu\kappa} e^{-\kappa z} \right\}, \quad z \to \infty. \tag{129}$$

The limiting procedure is $R \to \infty, \ z \to \infty, \ z/R \to 0$. (The factor of $4\pi/\kappa$ comes from the prefactor of $\tilde{q}_0(R)$ and the factor of $1/2$ in the definition of $\tilde{\sigma}$.) As before, $\mathrm{Re}'\{z\}$ means to take the real part of z if z is complex, and to take half of z if z is real, a consequence of the two mutually conjugate poles located in the upper half of the complex plane. The fact that the decay length for the planar double layer is the same as for the spherical double layer and for the bulk electrolyte is not unexpected, and obviously the transition from monotonic to oscillatory double layer profiles will occur at the same point as in the bulk electrolyte. This was pointed out for the planar double layer by Stillinger and Kirkwood[65], who gave approximate expressions for the decay length, the transition point, and also the mean electrostatic potential drop across the double layer. (See also the modified Poisson-Boltzmann results[60,79,80].) Note that in planar geometry the Yukawa-form of the spherical case has become a pure exponential decay, a consequence of the fact that the three-dimensional Fourier transform of the short-ranged direct correlation function has been replaced by a one-dimensional one. Substituting this asymptote into the expression for the mean electrostatic potential, Eq. (115), one obtains

$$\psi(z) \sim 2\mathrm{Re}' \left\{ \frac{4\pi\tilde{\sigma}}{\epsilon\nu\kappa} e^{-\kappa z} \right\}, \quad z \to \infty. \tag{130}$$

Again one sees that the effective charges give the response to the mean electrostatic potential, and that in the asymptotic regime the latter is proportional to the effective surface charge density.

Since electrostatics don't enter in the core-dominated regime, one can immediately take the planar limit of the core-dominated spherical solute result, Eq. (105), to obtain

$$h_{0\alpha}(z) \ \sim \ 2\mathrm{Re}' \left\{ \frac{-2ie^{-\xi z}}{\rho^2 x'(i\xi)} \sum_{\gamma>0} \rho_\gamma \overline{\chi}_{0\gamma}(i\xi) \right\}, \quad \alpha > 0, \ z \to \infty. \tag{131}$$

Despite the charge on the wall, this shows that all of the ion profiles are asymptotically identical in the core-dominated regime.

Figure 3 shows the asymptotic behaviour of the isolated planar double layer in the monotonic regime. After several screening lengths the counterion total correlation function has gone over to its asymptotic form, Eq. (129). In this

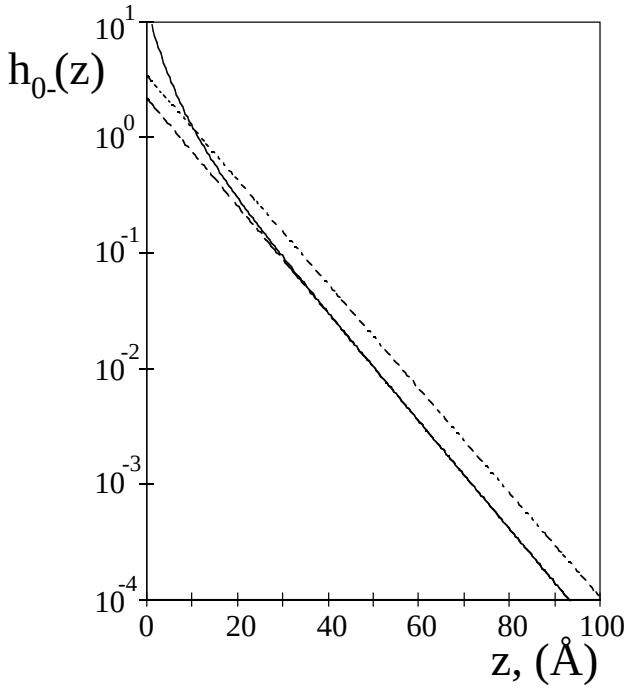

FIG. 3: The counterion density distribution for the planar double layer for an area per surface charge of 250Å^2, in contact with a 0.1M monovalent restricted primitive model electrolyte ($\epsilon_r = 78.358$, $T = 298.15$K, $d = 4.25$Å), with Debye length of 9.61Å, and an actual decay length of 9.31Å, and $\nu = 1.0007$. The curve is the hypernetted chain result, which is well fitted by the straight line asymptote, Eq. (129), with effective charge obtained from Eq. (127) equal to 405.2Å^2 per unit surface charge. The remaining straight line is the linear Poisson-Boltzmann prediction using the actual surface charge density.

case the Debye length, $\kappa_D^{-1} = 9.61$Å, is quite close to the actual screening length of the electrolyte, $\kappa^{-1} = 9.32$Å, and it would be hard to measure the discrepancy experimentally. (It would in fact be impossible to do so without a precise independent measure of the actual electrolyte concentration; the measured screening length is often used to determine the electrolyte concentration via the Debye-Hückel formula.) However the magnitude of the density profile does show a significant discrepancy from the classical prediction. In this case the effective surface charge given by Eq. (127) in hypernetted chain approximation is 405.2Å^2, (401.8Å^2 when bridge diagrams are included). which is about two thirds of the actual surface charge. In other words, if one were to analyse the measured profiles with the linear Poisson-Boltzmann theory, one would obtain quite a good fit to the data using a substantially decreased surface charge density, which one would presumably attribute to physico-chemical binding of counterions to the surface, thereby deducing an erroneous binding constant. Similar conclusions hold for the non-linear Poisson-Boltzmann theory, which could be used with an area per unit charge of 290Å^2 to fit the asymptotic tail, about 15% too large. For a quantitative analysis of experimental data, one should use an accurate theory that includes ion size and correlations. Alternatively one may fit the data with the mean-field Poisson-Boltzmann approximation, provided that one corrects the fitted surface charge density to obtain the actual surface charge density. Data for such a correction is given in §IV.

3. Algebraic correlations along a wall

The singlet approach that has been used so far gives the wall-ion distribution function, which corresponds to the density profile in the double layer. It does not directly give the correlation between ions in the presence of the wall, (although these are implicitly contained in the diagrams comprising the wall-ion correlation functions). These ion-ion distribution functions near a wall are given by the inhomogeneous Ornstein-Zernike equation, and it will now be demonstrated that they decay as inverse cubics parallel to the wall, which contrasts with the exponential asymptotes of the bulk correlation functions and of the density profiles in the double layer.

For the planar geometry of an isolated charged wall, the density depends only upon the distance from the wall, $\rho_\alpha(\mathbf{r}) = \rho_\alpha(z)$, and the pair correlation functions depend upon the distances of the two ions from the wall and upon their separation in the direction parallel to the wall, $h_{\alpha\gamma}(\mathbf{r}_1, \mathbf{r}_2) = h_{\alpha\gamma}(s_{12}, z_1, z_2)$. The matrix of distribution

functions becomes $\left\{\underline{\underline{H}}(s_{12},z_1,z_2)\right\}_{\alpha\gamma}=\rho_\alpha^{1/2}(z_1)h_{\alpha\gamma}(s_{12},z_1,z_2)\rho_\gamma^{1/2}(z_2)$. In this planar geometry the inhomogeneous Ornstein-Zernike equation is

$$\underline{\underline{H}}(s_{12},z_1,z_2)=\underline{\underline{C}}(s_{12},z_1,z_2)+\int d\mathbf{s}_3\int_0^\infty dz_3\;\underline{\underline{\hat{H}}}(s_{13},z_1,z_3)\underline{\underline{\hat{C}}}(s_{32},z_3,z_2), \tag{132}$$

which partially factorises upon Fourier transformation in the lateral direction,

$$\underline{\underline{\hat{H}}}(k,z_1,z_2)=\underline{\underline{\hat{C}}}(k,z_1,z_2)+\int_0^\infty \underline{\underline{\hat{H}}}(k,z_1,z_3)\underline{\underline{\hat{C}}}(k,z_3,z_2)\;dz_3. \tag{133}$$

In this section the circumflex signifies the two-dimensional Fourier transform of a function with cylindrical symmetry, which is just the Hankel transform of order zero,

$$\hat{f}(k)=2\pi\int_0^\infty f(r)J_0(kr)r\,dr, \tag{134}$$

with inverse

$$f(r)=\frac{1}{2\pi}\int_0^\infty \hat{f}(k)J_0(kr)k\,dk. \tag{135}$$

In this cylindrical coordinate system the ion-ion potential is

$$\underline{\underline{u}}^{\mathrm{Coul}}(s_{12},z_1,z_2)=\frac{1/4\pi\beta}{\sqrt{s_{12}^2+(z_1-z_2)^2}}\underline{\underline{Q}}(z_1,z_2), \tag{136}$$

which has transform

$$\underline{\underline{\hat{u}}}^{\mathrm{Coul}}(k,z_1,z_2)=\frac{e^{-k|z_1-z_2|}}{2\beta k}\underline{\underline{Q}}(z_1,z_2). \tag{137}$$

(The charge matrix has a spatial dependence through the densities that it contains.) It is assumed without proof that the inhomogeneous ion-ion direct correlation function decays like the Coulomb potential, and hence that the function $\underline{\underline{\chi}}(s_{12},z_1,z_2)=\underline{\underline{C}}(s_{12},z_1,z_2)+\beta\underline{\underline{u}}^{\mathrm{Coul}}(s_{12},z_1,z_2)$ is at least integrable. The alternative form of the Ornstein-Zernike equation is

$$\begin{aligned}\underline{\underline{\hat{H}}}(k,z_1,z_2) \;=\; & \underline{\underline{\hat{\chi}}}(k,z_1,z_2)+\int_0^\infty \underline{\underline{\hat{H}}}(k,z_1,z_3)\underline{\underline{\hat{\chi}}}(k,z_3,z_2)\;dz_3 \\ & -\underline{\underline{Q}}(z_1,z_2)\frac{e^{-k|z_1-z_2|}}{2k}-\int_0^\infty \underline{\underline{\hat{H}}}(k,z_1,z_3)\underline{\underline{Q}}(z_3,z_2)\frac{e^{-k|z_3-z_2|}}{2k}\;dz_3.\end{aligned} \tag{138}$$

The last two terms represent the transform of the fluctuation potential; $\phi_\alpha(s_{12},z_1;z_2)$ is the change in the mean electrostatic potential at $\mathbf{s}_2,z_2$ due to an ion of type α being at $(\mathbf{s}_1,z_1)$,

$$\phi_\alpha(s_{12},z_1;z_2)=\frac{q_\alpha}{\epsilon r_{12}}+\sum_\gamma\int h_{\alpha\gamma}(s_{13},z_1,z_3)\frac{q_\gamma}{\epsilon r_{32}}\rho_\gamma(z_3)\;d\mathbf{r}_3. \tag{139}$$

The fluctuation potential in the double layer plays the rôle of the mean electrostatic potential about an ion in the bulk electrolyte.

Now a moment expansion will be performed. As in the analysis of the bulk electrolyte, (§IB), for an exponentially short-ranged function all moments exist and the odd moments are zero. Since in this planar geometry the transform of the Coulomb potential contains odd powers of k (whereas only $1/k^2$ appeared in the bulk) one anticipates that the correlation functions will exhibit power-law decay parallel to the wall. One defines the moments to be

$$\underline{\underline{\hat{H}}}(k,z_1,z_2)=\underline{\underline{H}}^{(0)}(z_1,z_3)+|k|\underline{\underline{H}}^{(1)}(z_1,z_3)+\dots\,, \tag{140}$$

and similarly for $\underline{\underline{\hat{\chi}}}$. Note that the absolute value of k appears because by definition $\underline{\underline{H}}(r,z_1,z_2)$ is a real even function of r. One now takes the limit that $k\to 0$ in the Ornstein-Zernike equation and equates coefficients. (For finite $|z_1-z_2|$

it is permissible to expand the various exponentials since z_3 is kept finite by the short range of the total correlation function in the integrand.) Equating the coefficients of k^{-1} one has

$$0 = 0 + 0 - \frac{1}{2}\underline{\underline{Q}}(z_1, z_2) - \frac{1}{2}\int_0^\infty \underline{\underline{H}}^{(0)}(z_1, z_3)\underline{\underline{Q}}(z_3, z_2)\, dz_3, \tag{141}$$

or

$$-q_\alpha = \sum_\gamma q_\gamma \int h_{\alpha\gamma}(s_{12}, z_1, z_2)\rho_\gamma(z_2)\, dz_2\, d\mathbf{s}_2. \tag{142}$$

This is just the local electroneutrality condition, Eq. (46), in planar geometry.

Equating the coefficient of k^0 one obtains

$$\begin{aligned}\underline{\underline{H}}^{(0)}(z_1, z_2) = \\ \underline{\underline{\chi}}^{(0)}(z_1, z_2) + \int_0^\infty \underline{\underline{H}}^{(0)}(z_1, z_3)\underline{\underline{\chi}}^{(0)}(z_3, z_2)\, dz_3 + \underline{\underline{Q}}(z_1, z_2)\frac{|z_1 - z_2|}{2} \\ + \int_0^\infty \underline{\underline{H}}^{(0)}(z_1, z_3)\underline{\underline{Q}}(z_3, z_2)\frac{|z_3 - z_2|}{2}\, dz_3 - \frac{1}{2}\int_0^\infty \underline{\underline{H}}^{(1)}(z_1, z_3)\underline{\underline{Q}}(z_3, z_2)\, dz_3.\end{aligned} \tag{143}$$

By pre-multiplying by $\underline{\underline{Q}}(z_0, z_1)$ and integrating over z_1, one can cancel most of these terms by the local electroneutrality condition, and one is left with

$$-\underline{\underline{Q}}(z_0, z_2) = \frac{-1}{2}\int_0^\infty dz_1 \int_0^\infty dz_3\, \underline{\underline{Q}}(z_0, z_1)\underline{\underline{H}}^{(1)}(z_1, z_3)\underline{\underline{Q}}(z_3, z_2) \tag{144}$$

or

$$1 = \frac{2\pi\beta}{\epsilon}\sum_{\alpha\gamma} q_\alpha q_\gamma \int_0^\infty dz_1 \int_0^\infty dz_2\, \rho_\alpha(z_1)\rho_\gamma(z_2)h^{(1)}_{\alpha\gamma}(z_1, z_2) \tag{145}$$

This proves that the first moment of the total correlation function is non-zero. Now if $\hat{f}(k) \sim \text{constant} + A|k|,\ k \to 0$, then $f(r) \sim -A/2\pi r^3,\ r \to \infty$. That is

$$h_{\alpha\gamma}(r, z_1, z_2) \sim \frac{-h^{(1)}_{\alpha\gamma}(z_1, z_2)}{2\pi r^3},\ r \to \infty, \tag{146}$$

where the numerator obeys the sum rule Eq. (145). The asymptote and the sum rule for an electrolyte next to a planar wall were first given by Jancovici[85,86] and have been discussed by others[87–89]. The fact that the ion-ion correlations decay as inverse cubics in the direction parallel to a planar wall is in marked contrast to the exponential decay of the bulk electrolyte. It is a consequence of the inability of the electrolyte to screen the charge on an ion equally on all sides due to the presence of the wall. The ion and its counter-charge cloud has a net dipole moment, and the r^{-3} behaviour results from the dipole-dipole interaction. Identical decay occurs for an electrolyte confined to a two-dimensional planar surface[90–94]; in this case the densities that appear in Eq. (145) become δ-functions and the two-dimensional charge-charge correlation function has a universal asymptote[93,94]. Note that an r^{-3} tail is an integrable function in the two-dimensional sub-space parallel to the wall.

This behaviour does not depend upon the charge on the wall but only that it excludes electrolyte from a semi-infinite half-space. For a wall of finite thickness t with electrolyte on both sides, it may be the dominant behaviour for $r << t$, but in the asymptotic limit the correlations parallel to the surface will decay exponentially with the bulk correlation length[88,95]. For the semi-infinite half-space treated in detail above, if the asymptotic limit is taken such that the perpendicular distance of the ions from the wall always remains much greater than their lateral separation, than one expects them to behave like the bulk correlation function and to decay exponentially. The existence of algebraic correlations depends upon the inability of ions to be screened on all sides; the correlations between ions confined to an infinite cylinder decay like[96] $(z \ln|z|)^{-2},\ |z| \to \infty$.

In addition to the local electroneutrality condition and the sum rule on the first moment of the inhomogeneous total correlation function, there is also the second moment condition, which can be written as a sum-rule for the fluctuation potential,[30,31]

$$1 = -\beta\sum_\alpha q_\alpha \int d\mathbf{s}\, dz_1\, \rho_\alpha(z_1)\phi_\alpha(s, z_1; z_2), \tag{147}$$

which follows from the alternate form of the Ornstein-Zernike equation, Eq. (138), upon multiplication by the charge matrix, integration, k-limitation, and invocation of the local electroneutrality condition, Eq. (142). Finally, a dipole sum rule for the inhomogeneous total correlation function of the planar double layer was derived by Blum et al.[97], (see Refs[6,89] for an alternative derivation), and Carnie[98] showed that it was related to the second moment condition.

C. Analysis of interacting charged walls

1. *Wall-wall Ornstein-Zernike equation*

The singlet approach can be applied to the problem of interacting planar walls[77]. In the general case of interacting solutes, the solute-solute Ornstein-Zernike equation exists (c.f. Eq. (96) above), as do the solute-solute pair correlation functions. However for two walls of infinite cross sectional area, the solute-solute pair correlation functions do not exist except as generalised functions (e.g. the pair distribution function is a set of delta functions). In this case the physical entity is the interaction free energy per unit area. In diagrammatic terms, this is the wall-wall potential, minus the connected pair diagrams that have the walls as non-adjacent root points not forming an articulation pair, per unit area. This simply corresponds to the solute-solute potential of mean force per unit area, which is just the exponent of the closure equation. One has

$$\beta w_{00}^{\rm int}(z) = \beta V_{00}(z) - d_{00}(z) - \int_{-\infty}^{\infty} \underline{H}^T(z')\underline{C}(z-z')\,dz', \tag{148}$$

where $\beta = 1/k_BT$, and where the wall-wall quantities per unit area symbolised by w, V, and d are the interaction free energy, potential, and the bridge function, respectively. The convolution integral, which is clearly just the series function per unit area, contains the wall-ion pair correlation functions discussed in §IIB1. It will be assumed that the walls interact only with the Coulomb potential, and that one is only interested in the region $z > 0$, where z represents the width of the region available to the centers of the ions, (c.f. Eq. (108) above). In order to express this interaction free energy in terms of short range functions, one needs to remove the wall-ion Coulomb potential from the integral of the wall-ion direct correlation function, (c.f. Eq. (112)). One has

$$\int_0^{\infty} \underline{H}^T(z')\underline{q}V_0^{\rm Coul}(z-z')\,dz' = \sigma\psi(z) + \frac{2\pi\sigma^2}{\epsilon}z - \frac{2\pi\sigma^2}{\epsilon}S - \sigma\psi(0), \quad z > 0, \tag{149}$$

where the single wall electroneutrality condition, Eq. (109), the mean electrostatic potential due to a charged wall, Eq. (115), the wall-ion Coulomb potential, Eq. (116), and the potential drop across an isolated double layer, Eq. (117), have all been used. In view of this one chooses the arbitrary constants in the Coulomb part of the wall-wall potential to cancel these, leaving only the mean electrostatic potential outside of the integral. Accordingly one chooses

$$V_{00}(z) = \frac{2\pi\sigma^2}{\epsilon}S + \sigma\psi(0) - \frac{2\pi\sigma^2}{\epsilon}z, \quad z > 0, \tag{150}$$

and the interaction free energy per unit area becomes

$$\beta w_{00}^{\rm int}(z) = \beta\sigma\psi(z) - d_{00}(z) - \int_{-\infty}^{\infty} \underline{H}^T(z')\underline{\chi}(z-z')\,dz', \quad z > 0. \tag{151}$$

In the case of a Stern layer of width $\delta > 0$, one replaces $\psi(z)$ by $\psi(z+\delta)$ in this expression. Note that $w_{00}^{\rm int}(z) \to 0$, $z \to \infty$, (see below), and hence no surface or bulk contributions are included in this free energy expression. The net pressure (force per unit area) between the walls is

$$p^{\rm net}(z) = \frac{-\partial w_{00}^{\rm int}(z)}{\partial z}. \tag{152}$$

This corresponds to the total pressure of the confined electrolyte less the osmotic pressure of the bulk electrolyte, which is imagined to be pressing on the far sides of the walls (at infinity).

The above expressions are for two identical walls, but the generalisation to the non-symmetric situation is immediate. If one uses the subscripts '1' and '2' to denote the two walls, then one has

$$\begin{aligned} \beta w_{12}^{\rm int}(z) &= \beta\sigma_1\psi_2(z) - d_{12}(z) - \int_{-\infty}^{\infty} \underline{H}_1^T(z')\underline{\chi}_2(z-z')\,dz' \\ &= \beta\sigma_2\psi_1(z) - d_{12}(z) - \int_{-\infty}^{\infty} \underline{H}_2^T(z')\underline{\chi}_1(z-z')\,dz'. \end{aligned} \tag{153}$$

2. The Derjaguin approximation

The Derjaguin approximation[99] relates the total force between particles with curved surfaces to the interaction free energy per unit area between planar walls, and has found extensive application in colloid science[1], including to non-spherical particles[100]. Its utility lies in the fact that it subsumes one degree of freedom, the curvature, into a single geometric parameter times the planar free energy. In general the free energy is difficult to obtain, and considerable efficiency can result if one need calculate it only for the simplest case, namely planar geometry, which has the greatest symmetry. The Derjaguin approximation allows the planar result to be applied to interacting particles of arbitrary curvature. What is perhaps obscure is the precise nature and regime of validity of the approximation. Attard and coworkers[77,101] proceeded by comparing the formally exact Ornstein-Zernike results for planes and for spheres in the large radius limit of the latter. That approach is modified here for the electric double layer.

For macrospheres, the solute-solute potential of mean force may be written

$$\begin{aligned}\beta w_{00}^{\rm int}(x+2R;R) &= \beta\int\sigma(\mathbf{s};R)\,\psi(|\mathbf{s}-\mathbf{r}|;R)\,d\mathbf{s}\\ &\quad - d_{00}(x+2R;R) - b_{00}^{\rm sr}(x+2R;R),\end{aligned}\tag{154}$$

where the macroion has surface charge $\sigma(\mathbf{s};R)=\sigma\delta(s-R)$, and where $\mathbf{r}=(x+2R)\hat{\mathbf{x}}$. The modified series function is

$$\begin{aligned}b_{00}^{\rm sr}(r;R) &= \int\underline{H}^T(s;R)\underline{\chi}(|\mathbf{r}-\mathbf{s}|;R)\,d\mathbf{s}\\ &= \frac{2\pi}{r}\int_0^\infty ds\,s\underline{H}^T(s;R)\int_{|r-s|}^{r+s}dt\,t\underline{\chi}(t;R).\end{aligned}\tag{155}$$

In the last line bispherical coordinates are used, and s and t measure the radial distances from the centers of the macroions. Let the surface separation of the macroions be $x\equiv r-2R$, and define $y\equiv s-R$ and $z\equiv t-R$. The planar limit is obtained as $R\to\infty$, with the separations of interest being $0<x\ll R$. Because the correlation functions are exponentially short-ranged on the electrolyte side of the interface, the integral is dominated by regions $y\ll R$ and $z\ll R$. Changing the variables of integration, the lower limit of the t integral becomes $|2R+x-y-R|-R=x-y$, and the upper limit may be extended to infinity. This gives

$$b_{00}^{\rm sr}(x+2R;R)=\frac{2\pi}{x+2R}\int_{-R}^\infty dy\,(y+R)\underline{H}^T(y+R;R)\int_{x-y}^\infty dz\,(z+R)\underline{\chi}(z+R;R).\tag{156}$$

Now as $y\to-R$, $z\to\infty$ and $\chi_{0\alpha}(z+R;R)\to 0$. Therefore the integrals are dominated by $y\gg -R$ and $|z|\ll R$. Accordingly the large radius limit yields

$$\lim_{R\to\infty}b_{00}^{\rm sr}(x+2R;R)=\pi R\int_{-\infty}^\infty dy\,\underline{H}^T(y)\int_{x-y}^\infty dz\,\underline{\chi}(z),\tag{157}$$

where wall-ion correlation functions appear in the integrand. Differentiating one obtains

$$\begin{aligned}\lim_{R\to\infty}\frac{-1}{\pi R}\frac{\partial b_{00}^{\rm sr}(x+2R;R)}{\partial x} &= \int_{-\infty}^\infty\underline{H}^T(y)\underline{\chi}(x-y)\,dy\\ &\equiv b_{00}^{\rm sr}(x),\end{aligned}\tag{158}$$

where the last quantity is the modified wall-wall series function per unit area. This result for interacting macrospheres was derived by Attard et al.[77] and by Henderson[102].

The treatment of the bridge function is very similar. Since it consists of $h_{0\gamma}(r;R)$ and $h_{\alpha\gamma}(r)$ bonds, which are exponentially short-ranged, the convolution integrals are dominated by regions with the field points in the electrolyte between the two surfaces. One field point can be singled out, and the bridge function can be written as an integral over $\mathbf{s}_\alpha$ and sum over α of $c_{\underline{00}\alpha}(r,s,t;R)$, which is that part of the triplet direct correlation function with non-adjacent solutes not forming an articulation pair[101]. Transforming to bispherical coordinates, one concludes as above that $|y|\ll R$ and that $|z|\ll R$, and hence that

$$\begin{aligned}\lim_{R\to\infty}\frac{-1}{\pi R}\frac{\partial d_{00}(x+2R;R)}{\partial x} &= \sum_\alpha\rho_\alpha\int_{-\infty}^\infty c_{\underline{00}\alpha}(y,x-y)\,dy\\ &\equiv d_{00}(x),\end{aligned}\tag{159}$$

where the last quantity is the wall-wall bridge function per unit area.

The final contribution to the macrospherical solute-solute potential of mean force, Eq. (154), is the charge times the mean electrostatic potential, which is written as an integral over the surface charge density. Now the distance between the center of one macroion and the surface of the other at a perpendicular distance τ from the central axis is $t(\tau) = \sqrt{\tau^2 + (R + x + \tau^2/2R)^2} \to R + x + \tau^2/R + x^2/2R,\ R \to \infty$, and hence $\psi(t(\tau); R) \to \psi(x + \tau^2/R + x^2/2R),\ R \to \infty$. One has

$$\begin{aligned} 2\pi\sigma \int_0^\infty \psi(t(\tau); R)\tau\, d\tau &\sim 2\pi\sigma \int_0^\infty \psi(x + \tau^2/R + x^2/2R)\tau\, d\tau, \\ &\sim \pi R\sigma \int_x^\infty \psi(z)\, dz,\ R \to \infty. \end{aligned} \tag{160}$$

When differentiated with respect to x this yields a contribution of the same form as for the bridge function and for the short range part of the series function.

Now the negative derivative of the potential of mean force is the force between the solutes $F_{00}(x + 2R; R)$, and one concludes that

$$\begin{aligned} \lim_{R\to\infty} \frac{\beta}{\pi R} F_{00}(x + 2R; R) &= \beta\sigma\psi(x) - d_{00}(x) - b_{00}^{\rm sr}(x) \\ &= \beta w_{00}^{\rm int}(x). \end{aligned} \tag{161}$$

In words, the force between spherical solutes, divided by π times their radius, equals the interaction free energy per unit area between planar walls. This is the Derjaguin approximation, and the present analysis shows that it is exact in the asymptotic limit $R \to \infty$. Certain assumptions made in this derivation remain valid for solutes of large but finite radius if the surface separation is small compared to the radius, $x \ll R$, and, implicitly, if the range of the macroion-ion correlation functions in the electrolyte is less than the radius, $\kappa^{-1} \ll R$. (This last condition was used to find the dominant regions of the integrals, and to extend the ranges of integration.) Hence one concludes that it is legitimate to apply the Derjaguin approximation to colloid particles of finite radius whenever these two conditions are fulfilled.

This derivation of the Derjaguin approximation is based upon the formally exact Ornstein-Zernike expressions for the solute-solute interaction free energy, and it is worthwhile to compare it with the more heuristic approach that is generally used[99,100]. In this approach one postulates that the potential of mean force between two solutes of large radius and close separation is the sum of a free energy per unit area acting between elements of area on their surface. Since the surfaces are nearly flat, this free energy density is taken to be that for infinite planar walls at the local surface separation. At a distance r from the central axis the latter is $h(r) = x + r^2/R$, where x is the surface separation on the central axis and R is the radius of the two spherical solutes. Consequently one has

$$\begin{aligned} \beta w_{00}^{\rm int}(2R + x; R) &= 2\pi \int_0^\infty w_{00}^{\rm int}(x + r^2/R)\, r\, dr \\ &= \pi R \int_x^\infty w_{00}^{\rm int}(h)\, dh, \end{aligned} \tag{162}$$

and differentiation yields Eq. (161). The quantitative accuracy of the Derjaguin approximation for interacting macroions has been explored within the context of the linear[51,52] and the non-linear[53,55] Poisson-Boltzmann approximations. It has also been tested for hard-sphere fluids using the hypernetted chain approximation, with and without bridge diagrams[77,103].

3. Asymptotics of overlapping planar double layers

The asymptotic behaviour of two interacting walls is most easily extracted from the interaction free energy written in the form of Eq. (151). As previously for the bulk electrolyte and for the isolated double layer, one assumes the bridge function to be more short ranged than the rest. Consequently the wall-ion mean electrostatic potential and the short range series function dominate asymptotically, and both have range κ. From the transforms of Eq. (129) and of Eq. (130), one respectively obtains

$$\overline{\underline{H}}(k) \sim \frac{-4\pi\beta\tilde{\sigma}}{\epsilon\nu\kappa} \underline{\tilde{q}} \frac{1}{\kappa + ik},\ \ k \to i\kappa, \tag{163}$$

and

$$\overline{\psi}(k) \sim \frac{4\pi\tilde{\sigma}}{\epsilon\nu\kappa}\frac{1}{\kappa+ik}, \;\; k \to i\kappa, \tag{164}$$

assuming for the present that κ is real. Hence near the pole the wall-wall interaction free energy per unit area, Eq. (151), goes like

$$\begin{aligned}\beta\overline{w}_{00}^{\rm int}(k) &\sim \left[\frac{4\pi\beta\sigma\tilde{\sigma}}{\epsilon\nu\kappa} + \frac{4\pi\beta\tilde{\sigma}}{\epsilon\nu\kappa}\underline{\tilde{q}}^T\underline{\overline{\chi}}(i\kappa)\right]\frac{1}{\kappa+ik}, \;\; k \to i\kappa, \\ &= \frac{8\pi\beta\tilde{\sigma}^2}{\epsilon\nu\kappa}\frac{1}{\kappa+ik},\end{aligned} \tag{165}$$

where the expression for the effective surface charge density, Eq. (127), has been used. Consequently the asymptote is[18]

$$w_{00}^{\rm int}(r) \sim \frac{8\pi\tilde{\sigma}^2}{\epsilon\nu\kappa}e^{-\kappa z}, \; z \to \infty, \; {\rm Im}\{\kappa\} = 0, \tag{166}$$

and

$$w_{00}^{\rm int}(r) \sim 2{\rm Re}\left\{\frac{8\pi\tilde{\sigma}^2}{\epsilon\nu\kappa}e^{-\kappa z}\right\}, \; z \to \infty, \; {\rm Im}\{\kappa\} \neq 0, \tag{167}$$

This depends only on properties of the bulk electrolyte, κ and ν, and the effective surface charge of the isolated double layer, $\tilde{\sigma}$. This result reduces to the linear Poisson-Boltzmann theory in the Debye-Hückel limit, $\chi_{\alpha\gamma} = 0$. As for the interaction between identical macroions, because the effective surface charge occurs as a square, and because κ and ν are both positive, in the monotonic regime the force between identically charged walls is repulsive. That is the interaction between two similar double layers is either monotonically repulsive, or oscillatory, and any attractions measured or predicted cannot persist for all separations, (although there can be a very large period of oscillation near the bulk transition).

Finally, in the core-dominated bulk regime it follows from the wall-wall Ornstein-Zernike equation that the interaction free energy per unit area is

$$\beta w^{\rm int}(z) \sim 2{\rm Re}'\left\{\frac{-2ie^{-\xi z}}{\rho^2 x'(i\xi)}\left(\sum_{\gamma>0}\rho_\gamma\overline{\chi}_{0\gamma}(i\xi)\right)^2\right\}, \;\; z \to \infty, \tag{168}$$

where again the effective surface 'charge' that described the amplitude of the decay of the density profiles away from the isolated wall appears as the square in their interaction.

Figure 4 shows the double layer interaction between two identical planar walls that have the same parameters as the isolated wall described in Fig. 3. It is evident that the asymptotic regime extends to separations as small as several screening lengths, and that the effective charge for the isolated wall, Eq. (142), describes the asymptote for two interacting walls accurately. The linear Poisson-Boltzmann theory using the actual area per unit surface charge of 250Å^2 significantly overestimates the repulsion, but it would fit the data with the effective surface charge of 405.2Å^2, from which one might erroneously conclude that 1/3 of the surface charge had been neutralised by bound counterions.

D. Other solute geometries

One of the great advantages of the singlet method is the flexibility that it allows in the interpretation of a solute. So far results have been given for macrospherical solutes and for planar walls. In what remains of this section three generic types of solutes will be treated: cylinders, pores, and multi-molecular species. These illustrate the range of problems that may be treated within the singlet approach.

1. Cylinders

As mentioned in the introduction to §IIB for isolated walls, the modern singlet approach is predicated upon the assumption that the solute-ion Ornstein-Zernike equation exists, and the properties of the solute-ion correlation

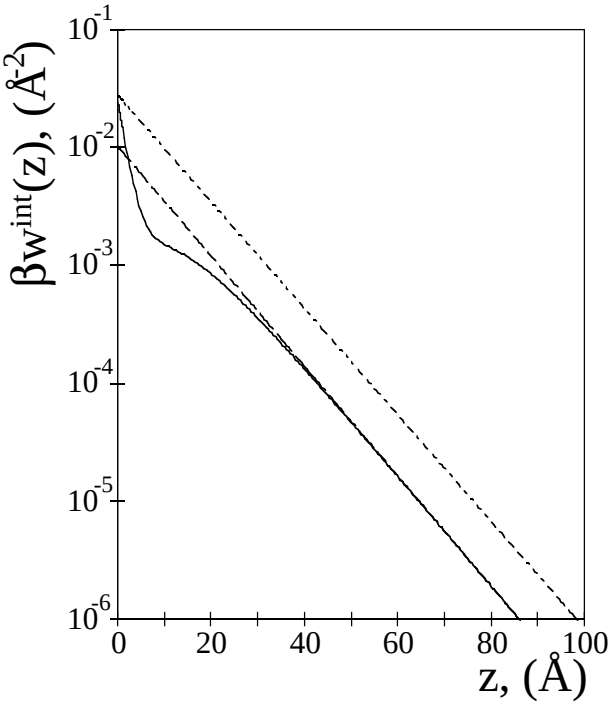

FIG. 4: The interaction free energy for the same case as Fig. 3. The hypernetted chain curve goes rapidly to its asymptote, Eq. (166), with $|e/\tilde{\sigma}| = 405.2\text{Å}^2$ from Eq. (127), but the linear Poisson-Boltzmann equation with the actual surface charge density $|e/\sigma| = 250\text{Å}^2$ significantly overestimates the repulsion.

functions are deduced from the symmetry of the solute, and from the behaviour of the Coulomb potential. The procedure holds for arbitrary shaped solutes, and here it is illustrated for cylinders. Previous work on the singlet method for the ion distributions about an isolated cylinder was in the context of the hypernetted chain approximation (i.e. neglect of the cylinder-ion bridge function), and Lozada-Cassou has reviewed these derivations and results[4]. Discussion of the approximate methods is deferred until §III, whereas in this section the object is to give formally exact singlet expressions for an isolated cylinder, and to extend them to two interacting cylinders. Asymptotic results are also given, including a formal microscopic expression for the amount of counterion condensation that occurs on a charged cylinder.

For an infinitely long cylinder of radius R, the solute-ion total correlation function depends only upon r, the distance from the axis of the cylinder, and one has

$$h_{0\gamma}(r) = -1, \quad r < R, \tag{169}$$

where the surface of closest approach has been taken to be the same for all the ions. The cylinder-ion Ornstein-Zernike equation is

$$\begin{aligned} \underline{H}(r) &= \underline{C}(r) + \int \underline{\underline{C}}(|\mathbf{r}-\mathbf{s}|)\underline{H}(s_r)\, d\mathbf{s} \\ &= \underline{C}(r) + \int_{-\infty}^{\infty} dz \int_0^{2\pi} d\theta \int_0^{\infty} ds\, s\, \underline{\underline{C}}\left(\sqrt{z^2+r^2+s^2-2rs\cos\theta}\right) \underline{H}(s), \end{aligned} \tag{170}$$

where s_r is the radial component of $\mathbf{s}$.

For a cylinder with surface charge density σ, (i.e. with an axial length per unit charge of $|e/2\pi R\sigma|$, where e is the charge on an electron) the electroneutrality condition is

$$-\sigma = \frac{1}{R}\int_R^{\infty} \underline{q}^T \underline{H}(r)\, r\, dr, \tag{171}$$

and the cylinder-ion Coulomb potential is (up to an arbitrary constant)

$$V_0^{\rm Coul}(r) = \begin{cases} \dfrac{-4\pi\sigma R}{\epsilon}\ln r, & r > R, \\ \dfrac{-4\pi\sigma R}{\epsilon}\ln R, & r < R. \end{cases} \tag{172}$$

The mean electrostatic potential becomes

$$\begin{aligned} \psi(r) &= V_0^{\rm Coul}(r) - \frac{4\pi}{\epsilon}\int_R^r \underline{q}^T\underline{H}(r')\ln r\, r'\, dr' - \frac{4\pi}{\epsilon}\int_r^\infty \underline{q}^T\underline{H}(r')\ln r'\, r'\, dr' \\ &= \begin{cases} \psi(R) & r \le R, \\ \dfrac{4\pi}{\epsilon}\displaystyle\int_r^\infty \underline{q}^T\underline{H}(r')\ln[r/r']\, r'\, dr' & r \ge R. \end{cases} \end{aligned} \tag{173}$$

Here the electroneutrality condition has been used, and it may be seen that as $r \to \infty$, $\psi(r)$ vanishes with the same decay length as $\underline{H}(r)$.

Analogously to the spherical and planar solutes treated above, the cylinder-ion Ornstein-Zernike equation may be rewritten in terms of short-range functions,

$$\underline{H}(r) = -\beta\underline{q}\psi(r) + \underline{\chi}(r) + \int \underline{\underline{\chi}}(|\mathbf{r}-\mathbf{s}|)\underline{H}(s_r)\, d\mathbf{s}, \tag{174}$$

where $\underline{\chi}(r)$ is the short range part of the cylinder-ion direct correlation function. Similarly the formally exact closure beyond contact is

$$h_{0\alpha}(r) = -1 + \exp\left[h_{0\alpha}(r) - \chi_{0\alpha}(r) + d_{0\alpha}(r)\right], \tag{175}$$

where $d_{0\alpha}(r)$ is the cylinder-ion bridge function.

The asymptotic behaviour of the ions far from the cylinder is obtained from the Fourier transform of the Ornstein-Zernike equation, Eq. (170),

$$\overline{\underline{H}}(k_r)\delta(k_z) = \overline{\underline{C}}(k_r)\delta(k_z) + \hat{\underline{\underline{C}}}\left(\sqrt{k_r^2+k_z^2}\right)\overline{\underline{H}}(k_r)\delta(k_z). \tag{176}$$

Here the overline denotes the two-dimensional Fourier transform of a circularly symmetric function (Hankel transform of order zero), k_r and k_z are the radial and axial components of the three-dimensional Fourier vector, and the Dirac deltas appear because of the constancy of the cylinder functions in the axial direction. Integrating both sides with respect to k_z, setting $k = k_r$, and rearranging, one obtains

$$\overline{\underline{H}}(k) = \left(\underline{\underline{I}} - \hat{\underline{\underline{C}}}(k)\right)^{-1}\left[\overline{\underline{\chi}}(k) - \beta\overline{V}_0^{\rm Coul}(k)\underline{q}\right]. \tag{177}$$

As always the transform of the cylinder-ion Coulomb potential is problematic. As in Ref.[18] (see also Eq. (125) above) the analytic part can be extracted from Poisson's equation, $\nabla^2 V_0^{\rm Coul}(r) = -(4\pi\sigma/\epsilon)\delta(r-R)$, and the fact that the transform of $f''(r)$ is $-k^2\overline{f}(k)$. Hence

$$\begin{aligned} -k^2\overline{V}_0^{\rm Coul}(k) &= 2\pi\int_0^\infty \frac{-4\pi\sigma}{\epsilon}\delta(r-R)J_0(kr)\, r\, dr \\ &= \frac{-8\pi^2\sigma R}{\epsilon}J_0(kR). \end{aligned} \tag{178}$$

One sees that the pole that occurs in the Ornstein-Zernike equation is just that of the bulk electrolyte, and hence the analysis of §IIA2 goes through unchanged. The result is

$$\overline{\underline{H}}(k) \sim \frac{-4\pi\beta/\nu\epsilon}{k^2+\kappa^2}\left[\tilde{\underline{q}}^T\overline{\underline{\chi}}(i\kappa) + 2\pi\sigma R I_0(\kappa R)\right]\tilde{\underline{q}}, \quad k \to i\kappa, \ \mathrm{Im}\{\kappa\} = 0. \tag{179}$$

where $I_0(z) = J_0(iz)$ is the modified Bessel function of the first kind. Now

$$\frac{1}{2\pi}\int_0^\infty \frac{1}{k^2+\kappa^2}J_0(kr)\, k\, dk = \frac{1}{2\pi}K_0(\kappa r), \tag{180}$$

where $K_0(z)$ is the modified Bessel function of the second kind, and hence

$$\underline{H}(r) \sim \frac{-2\beta}{\epsilon\nu}\left[\tilde{\underline{q}}^T\overline{\underline{\chi}}(i\kappa) + 2\pi\sigma R I_0(\kappa R)\right] K_0(\kappa r)\tilde{\underline{q}}, \;\; r\to\infty, \quad \mathrm{Im}\{\kappa\}=0. \tag{181}$$

Since

$$K_0(\kappa r) \sim \sqrt{\frac{\pi}{2\kappa r}}\left[1 - \frac{1}{8\kappa r} + \ldots\right] e^{-\kappa r}, \;\; r\to\infty, \tag{182}$$

one sees that the concentrations of ions in the double layer about a charged cylinder decay to their bulk values exponentially, over distances typified by the bulk screening length.

In order to identify the effective surface charge of the cylinder, the asymptote should be compared with the linear Poisson-Boltzmann result[104]

$$\underline{H}(r) = \frac{-4\pi\beta\sigma}{\epsilon\kappa_D K_1(\kappa_D R)} K_0(\kappa_D r)\underline{q}, \tag{183}$$

where $K_1(z) = -K_0'(z)$ is the first order modified Bessel function of the second kind. Hence one should take

$$\tilde{\sigma} = \frac{\kappa K_1(\kappa R)}{2\pi}\left[\tilde{\underline{q}}^T\overline{\underline{\chi}}(i\kappa) + 2\pi\sigma R I_0(\kappa R)\right], \; \mathrm{Im}\{\kappa\}=0, \tag{184}$$

as the effective surface charge. In the linear Poisson-Boltzmann limit, $[\underline{\underline{\chi}}(r)=0,\; \tilde{\underline{q}}=\underline{q},\; \kappa=\kappa_D]$, one has $\underline{H}(r) = -\beta\underline{q}\psi(r)$, and Eq. (174) shows that $\underline{q}^T\underline{\chi}(r)=0,\; r>R$, and that $\underline{q}^T\underline{\chi}(r) = \kappa_D\sigma K_0(\kappa_D R)/K_1(\kappa_D R),\; r<R$. It may be verified that the Hankel transform is $\underline{q}^T\overline{\underline{\chi}}(i\kappa_D) = 2\pi\sigma R K_0(\kappa_D R) I_1(\kappa_D R)/K_1(\kappa_D R)$, and hence in this limit

$$\begin{aligned}\tilde{\sigma} &= \sigma\kappa_D R\left[K_0(\kappa_D R)I_1(\kappa_D R) + I_0(\kappa_D R)K_1(\kappa_D R)\right] \\ &= \sigma,\end{aligned} \tag{185}$$

where the Wronskian for the modified Bessel functions has been used. Thus one recovers the Poisson-Boltzmann limit as one should, which persuades that the correct form for the effective surface charge density has been found. Manning[105,106] has put forward a theory for linear macroions based on counterion condensation in the cylindrical double layer; Eq.(184) represents a formal microscopic expression for the effective surface charge density that could presumably be used to characterise unambiguously the amount of condensation that occurs. With these definitions the asymptote is

$$\underline{H}(r) \sim \frac{-4\pi\beta\tilde{\sigma}}{\epsilon\nu\kappa K_1(\kappa R)} K_0(\kappa r)\tilde{\underline{q}}, \;\; r\to\infty, \; \mathrm{Im}\{\kappa\}=0, \tag{186}$$

and presumably one takes twice the real part if it is complex.

The interaction between two parallel cylinders can also be treated at the singlet level. As in the case of walls, for infinitely long cylinders the cylinder-cylinder pair correlation functions do not exist, and the quantity of physical import is the free energy per unit length. By analogy with the planar result this is

$$\begin{aligned}\beta w_{00}^{\mathrm{int}}(r) &= -d_{00}(r) + \beta\sigma R\int_0^{2\pi}\psi\left(\sqrt{r^2+R^2-2rR\cos\theta}\right)d\theta \\ &\quad - \int_0^{2\pi}d\theta\int_0^{\infty}ds\, s\,\underline{H}^T(s)\underline{\chi}\left(\sqrt{r^2+s^2-2rs\cos\theta}\right),\end{aligned} \tag{187}$$

where $d_{00}(r)$ is the bridge function per unit length for parallel cylinders, and the other functions pertain to an isolated cylinder. For the case of non-parallel cylinders, the total interaction free energy exists, and hence so do the pair correlation functions. Although fundamentally no different to the case of aligned cylinders, geometric factors appear in the more general case that make the result appear more complicated. The result for identical cylinders, one on the z-axis, and the other lying in the plane $x=r$ inclined at an angle $\theta\neq 0$ is

$$\begin{aligned}\beta w_{00}^{\mathrm{int}}(r,\theta) &= -d_{00}(r,\theta) + \beta\sigma R\int_{-\infty}^{\infty}dz'\int_0^{2\pi}d\phi\,\psi(t(x',y',z')) \\ &\quad - \int_{-\infty}^{\infty}dx\,dy\,dz\,\underline{H}^T\left(\sqrt{x^2+y^2}\right)\underline{\chi}(t(x,y,z)),\end{aligned} \tag{188}$$

where $x' = R\cos\phi$, $y' = R\sin\phi$, and

$$t(x,y,z) = \left((x-r)^2 + y^2\cos^2\theta - 2yz\sin\theta\cos\theta + z^2\sin^2\theta\right)^{1/2} \tag{189}$$

is the perpendicular distance between a point (x,y,z) and the axis of the inclined cylinder. Differentiation of this result with respect to r gives the force between the cylinders, and differentiation with respect to θ gives the torque. In both cases this free energy (potential of mean force) goes to zero at large separations because the cylinders are surrounded by electrolyte.

The final question to be addressed for cylinders is whether or not the Derjaguin approximation can be applied to two parallel cylinders. In §IIC2 it was shown that the force between two macrospheres, divided by π times their radius, equalled the interaction free energy between two walls in the limit that the radius of the spheres went to infinity. For finite radii this was the Derjaguin approximation, and for interacting non-parallel cylinders a corresponding result is known[99,100]. The case of perfectly aligned cylinders is important because of its relevance to hexagonal phases of rod-like polyions and to the interaction between curved particles adsorbed on a surface or confined to a membrane. The simplest way to make the point is by the heuristic derivation, Eq. (162). That is, one postulates that the potential of mean force (per unit length) for solutes of radius R can, at close separations, be written as the sum of free energy densities acting between elements of area on their surface. In the large radius limit the cylinders are virtually flat, and the free energy density is taken to be that between planar walls at a local separation of $h(y) = x + y^2/R$, where x is the closest separation of their surfaces, and y is the perpendicular distance from the plane containing the cylinders. One has

$$\begin{aligned} \beta w_{00}^{\rm int}(x+2R;R) &= \int_{-\infty}^{\infty} w_{00}^{\rm int}(x+y^2/R)\,dy \\ &= \sqrt{R}\int_x^{\infty} \frac{w_{00}^{\rm int}(h)}{\sqrt{h-x}}\,dh. \end{aligned} \tag{190}$$

This shows that the potential of mean force per unit length between parallel cylinders scales with the square root of their radius, and that it is a weighted integral of the interaction free energy per unit area of planar walls. (The weight function has an integrable singularity.) As such it represents an efficient computational procedure, but unlike the interaction between spheres, differentiation does not yield a simple expression for the force. This is rather different to the case of two spheres (or to a sphere and a plane, or to two crossed cylinders), where the Derjaguin approximation gives the total force as a geometric factor times the interaction free energy per unit area between planar walls. For parallel cylinders, or for particles adsorbed on a surface or confined to a membrane, the Derjaguin approximation only exists in the sense of Eq. (190).

The cylindrical double layer has been studied fairly extensively because of its relevance for rod-like polyelectrolytes such as DNA, and also because of its application to channels and pores in membranes and zeolites. In cylindrical geometry it is possible to obtain an analytic solution to the non-linear Poisson-Boltzmann equation for the case when there are only counterions in the double layer (no added salt)[107–109]. In the presence of added electrolyte, the linear Poisson-Boltzmann equation has solution in terms of modified Bessel functions[104,110,111]; solutions of the non-linear version have also been discussed[112]. Anderson and Record[113] have reviewed the cylindrical double layer as applied to DNA, and discussed the comparative advantages of the Poisson-Boltzmann theory and Manning's counterion condensation approach[105,106].

The singlet cylinder-ion hypernetted chain approximation was given by Lozada-Cassou[114]. Numerical results were obtained using the mean spherical approximation[115] and the hypernetted chain approximation[116] for the bulk ion-ion direct correlation function. Vlachy and co-workers[117–119] obtained simulation and integral equation results for cylindrical pores, and Yeomans et al.[120] have recently compared the HNC/MSA approximation for that system with simulations and with the double layer at a planar wall. Das et al.[121] have treated linear polyelectrolytes within the cell model by Monte Carlo, modified Poisson-Boltzmann (MBP5[122]), and non-linear Poisson-Boltzmann approximations. The cylindrical double layer has been reviewed[4,123].

2. Membranes and pores

The spherical, planar, and cylindrical macroions that have so far been analysed illustrate the variety of solute geometries that can be utilised. A conceptually different system, namely a confined electrolyte, can also be treated by the singlet method by considering the solute to be a pore. Spherical and planar geometries are the simplest. The planar slit pore will be treated in the next section, and this section will initially focus upon an isolated spherical pore of radius R, for which one has

$$\underline{H}(r) = -1,\ r > R. \tag{191}$$

Here $\{\underline{H}(r)\}_\alpha = \rho_\alpha^{1/2} h_{0\alpha}(r)$ is the pore-ion total correlation function. The ions are in equilibrium with a bulk electrolyte where they have number density ρ_α, and a common surface of closest approach, which defines the surface of the pore, has been used. If the pore has surface charge density σ, then the electroneutrality condition is

$$-4\pi R^2\sigma = \int \underline{q}^T \underline{H}(r)\, d\mathbf{r} = 4\pi \sum_\alpha q_\alpha \rho_\alpha \int_0^R h_{0\alpha}(r) r^2\, dr. \tag{192}$$

In the event that one wants to model a fixed number of ions inside the pore, one can adjust the bulk concentrations until the integrals of the individual pore-ion distribution functions give the specified number of ions; average quantities (but not their fluctuations) will then be the same as if the canonical ensemble had been used.

As usual the solute-ion Ornstein-Zernike equation is

$$\underline{H}(r) = \underline{C}(r) + \int \underline{\underline{C}}(|\mathbf{r}-\mathbf{s}|)\underline{H}(s)\, d\mathbf{s} \tag{193}$$

$$= \underline{\chi}(r) - \beta \underline{q}\psi(r) + \int \underline{\underline{\chi}}(|\mathbf{r}-\mathbf{s}|)\underline{H}(s)\, d\mathbf{s}. \tag{194}$$

The expression for the mean electrostatic potential follows from the integral of the Coulomb contribution to the bulk direct correlation function

$$-\beta \int \underline{q}\,\underline{q}^T \underline{H}(s) \frac{1}{\epsilon|\mathbf{r}-\mathbf{s}|}\, d\mathbf{s} = \frac{-4\pi\beta}{\epsilon} \underline{q} \left[\frac{1}{r} \int_0^r \underline{q}^T \underline{H}(s) s^2\, ds + \int_r^R \underline{q}^T \underline{H}(s) s\, ds \right]. \tag{195}$$

Hence the mean electrostatic potential may be written

$$\psi(r) = \begin{cases} \psi(0) + \dfrac{4\pi}{\epsilon r} \displaystyle\int_0^r \underline{q}^T \underline{H}(s)[s-r] s\, ds, & r \le R, \\ \psi(0) - \dfrac{4\pi R\sigma}{\epsilon} - \dfrac{4\pi}{\epsilon} \displaystyle\int_0^R \underline{q}^T \underline{H}(s) s\, ds, & r \ge R, \end{cases} \tag{196}$$

and consequently the pore-ion Coulomb potential is

$$V_0^{\mathrm{Coul}}(r) = \begin{cases} \psi(0) - \dfrac{4\pi}{\epsilon} \displaystyle\int_0^R \underline{q}^T \underline{H}(s) s\, ds + \dfrac{4\pi R\sigma}{\epsilon}, & r \le R, \\ \psi(0) - \dfrac{4\pi}{\epsilon} \displaystyle\int_0^R \underline{q}^T \underline{H}(s) s\, ds + \dfrac{4\pi R^2\sigma}{\epsilon r}, & r \ge R. \end{cases} \tag{197}$$

There is an arbitrary constant here, signified by the mean electrostatic potential at the origin. In open geometries the zero of potential is chosen to lie in the bulk electrolyte far from the solute, and then all correlation functions decay to zero; no such principle exists for closed geometries. For analytic results the constant is immaterial, and it is convenient to choose the potential to be zero outside of the net neutral pore, but one does not have the same freedom in numerical approaches. Changing the value of the arbitrary constant of the potential implies corresponding changes in the constant contribution to the pore-ion short-ranged direct correlation function and the bridge function. However approximate numerical approaches usually implicitly set the value of these functions (for example, the hypernetted chain approximation discussed below sets the bridge function to zero), and hence one can no longer arbitrarily set the zero of the potential. In practice $\psi(0)$ can be found by satisfying the electroneutrality condition; if there are too many counterions it is decreased, and if too many coions it is increased (negative feedback). (This method is described in more detail in §IVB.) These two equations for the mean electrostatic and Coulomb potentials combine to give the second form of the Ornstein-Zernike equation, Eq. (194), with the short range part of the pore-ion direct correlation function being $\underline{\chi}(r) = \underline{C}(r) + \beta \underline{q} V_0^{\mathrm{Coul}}(r)$. One may verify that $\chi_\alpha(r) \to -1 + \beta q_\alpha \psi(R) + \sum_\gamma \rho_\gamma \hat{\chi}_{\alpha\gamma}(0)$, $r \to \infty$. The exact closure is formally identical to those given above.

Electrolyte confined to spherical pores in this fashion is perhaps the simplest model of a reverse micelle. This consists of an aqueous core bounded by a spherical shell of amphiphilic molecules, all immersed in a bulk oil phase. (At this level image charges, which arise from the oil-water dielectric disparity, are ignored, which may be an unrealistic approximation in this system.) Interactions can occur between a pair of such reverse micelles, due to the correlated fluctuations of the ions they contain, even though the ions themselves are excluded from the oil phase and there is no net charge on the micelles[124,125]. Now the pore-pore Ornstein-Zernike convolution integral consists of pore-ion

correlation functions, which are constant as $r \to \infty$. One can subtract these constants to obtain the short-range contribution

$$\begin{aligned}\int \underline{H}^T(s)\underline{\chi}(|\mathbf{r}-\mathbf{s}|)\,d\mathbf{s} &= \int \underline{H}^{\mathrm{sr}\,T}(s)\underline{\chi}^{\mathrm{sr}}(|\mathbf{r}-\mathbf{s}|)\,d\mathbf{s} \\ &\quad + \hat{\underline{H}}^{\mathrm{sr}\,T}(0)\underline{\chi}(\infty) + \underline{H}^T(\infty)\hat{\underline{\chi}}^{\mathrm{sr}}(0) + \underline{H}^T(\infty)\underline{\chi}(\infty)V, \end{aligned} \tag{198}$$

where V is the volume. Here $h_{0\alpha}(\infty) = -1$, and $h^{\mathrm{sr}}_{0\alpha}(r) = h_{0\alpha}(r) + 1$ is just the pore-ion radial distribution function, which vanishes for $r > R$, and $\chi_{0\alpha}(\infty) = -1 + \beta q_\alpha \psi(R) + \sum_\gamma \rho_\gamma \hat{\chi}_{\alpha\gamma}(0)$, with $\chi^{\mathrm{sr}}_{0\alpha}(r) = \chi_{0\alpha}(r) - \chi_{0\alpha}(\infty)$. Similarly the pore-pore bridge function, which consists of pore-ion and ion-ion total correlation functions, goes to a constant at large separations. The constant can be eliminated by replacing two of the pore-ion h-bonds by pore-ion g-bonds (one connected to each pore, and not connected to the same field point), which leaves a short-ranged part that decays exponentially with the decay length of the bulk electrolyte. All of these constants can be discarded to give a formally exact expression for the pore-pore potential of mean force, (for $r > 2R$),

$$\begin{aligned} w^{\mathrm{int}}_{00}(r) &= -d^{\mathrm{sr}}_{00}(r) - \int \underline{H}^{\mathrm{sr}\,T}(s)\underline{\chi}^{\mathrm{sr}}(|\mathbf{r}-\mathbf{s}|)\,d\mathbf{s} \\ &= -d^{\mathrm{sr}}_{00}(r) - 2\pi \sum_\alpha \rho_\alpha \int_0^R ds\, s^2 g_{0\alpha}(s) \int_0^\pi d\theta\, \chi^{sr}_{0\alpha}(\sqrt{r^2+s^2-2rs\cos\theta}). \end{aligned} \tag{199}$$

There is no contribution to the interaction from the mean electrostatic potential because the micelle (pore plus confined ions) has no net charge. One expects that in the asymptotic limit the correlated fluctuations between the two confined electrolytes will give a van der Waals attraction[124,125], $w^{\mathrm{int}}_{00}(r) \sim \mathcal{O}(r^{-6})$, $r \to \infty$.

This method of treating the interaction between two pores can also be applied to the thickness-dependent free energy of a planar membrane. The wall-wall Ornstein-Zernike equation of §IIC1 gives the interaction free energy per unit area of two planar walls separated by an electrolyte (i.e. $z > 0$). But as in the case of reverse micelles there is no fundamental impediment to applying the result for $z < 0$, which could model a charged bilayer membrane with liquid-like interior, of thickness $|z|$ and with electrolyte on either side. Again one has to account for the fact that the wall-ion correlation functions tend to constants deep inside the wall, and so one has to work with short-range functions. Using similar arguments to the above, the interaction free energy per unit area is

$$w^{\mathrm{int}}_{00}(z) = d^{\mathrm{sr}}_{00}(z) + \int_0^\infty \underline{H}^{\mathrm{sr}\,T}(z')\underline{\chi}^{\mathrm{sr}}(z-z')\,dz',\ z < 0, \tag{200}$$

where the first function in the integrand is the wall-ion distribution function, which vanishes for $z' < 0$, and the second term has been made short-ranged by subtracting the constant given by Eq. (121). Again the bridge function has had two non-contiguous wall-ion h-bonds replaced by g-bonds, and it is exponentially short-ranged. Note that there is no bulk free energy contribution to this, which would be just the osmotic pressure of the bulk electrolyte times the thickness of the membrane, nor any surface free energy part. This is purely the interaction free energy per unit area, which arises from correlations between ions in the electrolyte on the two sides of the membrane. It represents a van der Waals force, and hence for large thicknesses it should approach zero from below, $w^{\mathrm{int}}_{00}(z) \sim \mathcal{O}(z^{-2})$, $z \to -\infty$.

In some ways this method that treats the membrane as two interacting walls at negative separations is not the most obvious way of analysing the problem. What is perhaps more intuitive is to consider the membrane as a single planar wall of finite thickness t. Then all of the analysis for the isolated wall of §IIB1 holds, with minor modifications due to the replacement of the core exclusion condition, Eq. (108), by

$$h_{0\alpha}(z) = -1, \quad |z| < t/2. \tag{201}$$

This method and the one of the preceding paragraph treat the same problem, and each has its own advantages. The membrane free energy is obtained directly in the first approach, but not in the second, whereas the ion profiles on both sides of the membrane are given directly by the second approach, but not the first. The two approaches illustrate another aspect of the singlet method, namely that it is possible to regard two interacting solutes as a single species, and this is the next subject.

3. Dumb-bells

The flexibility of the singlet Ornstein-Zernike approach is nowhere more evident than when the solute is a cluster of ions or particles. The membrane example at the end of the preceding section showed the fundamental equivalence of

treating interacting walls either as two solutes or as a single molecular species. More generally the solute can be the n-ion of §IB3, and then the solute-ion density profile simply corresponds to the $(n+1)$-ion distribution function. When the solute is taken to be two particles, the method will be called the dumb-bell singlet approach; it is based upon the solute-ion Ornstein-Zernike equation, and has to be distinguished from the method explored in detail above that utilises the solute-solute Ornstein-Zernike equation for the same problem. The dumb-bell approach is due to Lozada-Cassou, (it is termed by him a three point extension), and a number of applications have been reviewed[4]. Essentially the dumb-bell can be formed from any two particles at a fixed separation. A particularly interesting example is for a solute comprised of two ions, because this gives the triplet distribution function of the bulk electrolyte. In the dumb-bell method one has to take care of additional geometric factors in formulating the solute-ion Ornstein-Zernike integral, which may then become complicated in detail though it remains conceptually straightforward. The simplest geometry is the planar case, and this section will focus upon two infinitely thick walls, which corresponds to the wall-wall analysis of §IIC1, and which can also be considered as a slit pore. In §IV the merits of the two singlet methods for interacting solutes will be compared.

A solute comprised of two semi-infinite half-spaces separated by t has for the solute-ion total correlation function

$$h_{0\alpha}(z;t) = -1, \ |z| > t/2, \tag{202}$$

which manifests the confinement of the electrolyte between the walls. That the solute actually consists of two walls will be explicitly signified by the separation appearing in the argument of the solute-ion correlation functions. Attention will be restricted to the symmetric system, $h_{0\alpha}(-z;t) = h_{0\alpha}(z;t)$, and if each wall has surface charge density σ, then the electroneutrality condition is

$$-2\sigma = \int_{-\infty}^{\infty} \underline{q}^T \underline{H}(z;t)\, dz = \sum_\alpha q_\alpha \rho_\alpha \int_{-t/2}^{t/2} h_{0\alpha}(z;t)\, dz. \tag{203}$$

As usual the solute-ion Ornstein-Zernike equation is

$$\begin{aligned} \underline{H}(z;t) &= \underline{C}(z;t) + \int \underline{\underline{C}}(|\mathbf{r}-\mathbf{r}'|)\underline{H}(r'_z;t)\, d\mathbf{r}' \\ &= \underline{C}(z;t) + 2\pi \int_0^\infty dr'\, r' \int_{-\infty}^{\infty} dz'\, \underline{\underline{C}}\left(\sqrt{r'^2+(z-z')^2}\right) \underline{H}(z';t). \end{aligned} \tag{204}$$

From the Coulomb contribution to the bulk ion-ion direct correlation function one obtains the mean electrostatic potential,

$$\psi(z;t) = \psi(0;t) - \frac{4\pi}{\epsilon} \int_0^z \underline{q}^T \underline{H}(z';t)(z-z')\, dz', \ \ |z| \le t/2, \tag{205}$$

and the potential is constant and equal to its contact value within each wall. The arbitrary constant is signified by the appearance of the potential at the mid-plane, $\psi(0;t)$. In practice its value may be determined from the electroneutrality condition; if neutralisation is not satisfied, it should be increased or decreased in proportion to the extra coions or counterions, respectively, (see §IVB below). In the limit $t \to \infty$, $\psi(0;t) \to 0$, since there is bulk electrolyte in the central region between the walls, and it may be verified by a shift in the coordinate system that this expression reduces to that for an isolated planar wall, Eq. (115). Now the Coulomb potential of an ion between two planes with identical charges is a constant, and this may be discarded along with the constant from the mean electrostatic potential to give the alternative formulation of the solute-ion Ornstein-Zernike equation,

$$\underline{H}(z;t) = -\beta \underline{q}\psi(z;t) + \underline{\chi}(z;t) + 2\pi \int_0^\infty dr'\, r' \int_{-\infty}^{\infty} dz'\, \underline{\underline{\chi}}\left(\sqrt{r'^2+(z-z')^2}\right) \underline{H}(z';t). \tag{206}$$

As above, $\chi_{0\alpha}(z;t) \to -1 + \beta q_\alpha \psi(t/2;t) + \sum_\gamma \rho_\gamma \hat{\chi}_{\alpha\gamma}(0), \ |z| \to \infty$. The formally exact closure equation is

$$h_{0\alpha}(z;t) = -1 + \exp\left[h_{0\alpha}(z;t) - \chi_{0\alpha}(z;t) + d_{0\alpha}(z;t)\right], \tag{207}$$

where $d_{0\alpha}(z;t)$ is the solute-ion bridge function. These equations correspond to a confined electrolyte in equilibrium with the bulk; by adjusting the bulk concentrations one can mimic a closed system with a specified number of ions, and the ion and potential profiles will then be identical to their counterparts in the canonical ensemble.

The equations above determine the ion and potential profiles between two charged walls separated by t. For the study of slit pores these are the two main quantities of interest. The wall-wall Ornstein-Zernike equation of §IIC1 did not determine the density profiles between the two walls, and so for the study of slit pores the dumb-bell approach is

preferable. What the wall-wall approach did give was the interaction free energy per unit area, a quantity that is not directly available from the formally exact dumb-bell equations given above. The separation-dependent free energy is an important quantity in the study of solute-solute interactions, (it determines, for example, whether particles stick together or remain dispersed), and can be more or less directly measured. The pressure, which when integrated gives the free energy, can be obtained for the dumb-bell geometry from the contact theorem, as is now shown.

As mentioned above the density profile around a solute n-ion corresponds to the $(n+1)$-particle distribution function. The Born-Green-Yvon hierarchy also relates these two levels of distribution functions. For the dumb-bell solute the first member of the hierarchy is required. Usually the Born-Green-Yvon equation expresses the gradient of the pair distribution function as the average direct force plus the indirect force mediated by a third particle. By dividing by the pair distribution function one can rewrite it as an expression for the gradient of the potential of mean force. For two spherical solutes it is

$$w'_{00}(r_{12}) = V'_{00}(r_{12}) + \sum_\alpha \rho_\alpha \int u'_{0\alpha}(r_{13}) \cos\theta \frac{g_{00\alpha}(r_{12}, r_{13}, \cos\theta)}{g_{00}(r_{12})}\, d\mathbf{r}_3, \tag{208}$$

where V_{00} is the solute-solute potential, and $u_{0\alpha}$ is the isolated solute-ion potential. The ion density times the solute-solute-ion triplet distribution function divided by the solute-solute pair distribution function is the probability of finding an ion conditional upon the solutes being at $\mathbf{r}_1$ and $\mathbf{r}_2$. This is just the dumb-bell–ion distribution function and one has

$$\begin{aligned} \frac{g_{00\alpha}(r_{12}, r_{13}, \cos\theta)}{g_{00}(r_{12})} &= g_{0\alpha}(r_{13}) g_{0\alpha}(r_{23}) \exp -\beta\tau_{00\alpha}(r_{12}, r_{13}, \cos\theta) \\ &= 1 + h_{0\alpha}(\mathbf{r}_3; r_{12}). \end{aligned} \tag{209}$$

Strictly speaking the numerator and the denominator of the left side do not individually exist for planar walls of infinite area (c.f. the discussion of the wall-wall Ornstein-Zernike equation, Eq. (148), above), but the right sides are well defined for both finite and infinite solutes. (τ is the solute-solute-ion triplet potential of mean force, which is the set of connected, non-parallel diagrams with non-adjacent root points.) Inserting the dumb-bell distribution function into the Born-Green-Yvon equation gives the mean solute-solute force, (and upon integration their interaction free energy), as was originally given by Lozada-Cassou[126]. This enables the interaction of spherical and other finite solutes to be characterised.

For infinite planar solutes the analogue of the Born-Green-Yvon equation reduces to the contact theorem, as is now shown. Equation (208) says that the mean force between solutes is the sum of a direct part and an indirect part due to the mediation of the ions. In the planar case one has to deal with the force per unit area, but the same situation holds: the mean force per unit area is the direct pressure between the walls plus the force on one wall due to the ions, summed over species and integrated over space, weighted with their probability. The indirect contribution clearly scales with the area of the plates, and hence it is the axial integration that gives the indirect force per unit area. That is

$$w'_{00}(t) = V'_{00}(t) + \sum_\alpha \rho_\alpha \int_{-t/2}^{t/2} u'_{0\alpha}(z)[1 + h_{0\alpha}(z;t)]\, dz. \tag{210}$$

Note that $\cos\theta$ has been set equal to 1 because in this planar geometry the component of force is always parallel to the line connecting the walls. Its worth mentioning that this result can be derived directly from Eq. (208) by taking the infinite solute radius limit, and by invoking the relationships of §IIC2. Because there is no electrolyte on the far side of these plates, the left side represents the total pressure of the double layer, $p^{\text{total}}(t) = -w'_{00}(t)$. To obtain the net pressure one subtracts the osmotic pressure due to the bulk electrolyte, $p^{\text{net}}(t) = p^{\text{total}}(t) - p_\infty$, and thence the interaction free energy per unit area follows by integration,

$$w^{\text{int}}(t) = \int_t^\infty p^{\text{net}}(t')\, dt', \tag{211}$$

with $w^{\text{int}}(t) \to 0$, $t \to \infty$. For the electrolyte confined between walls, the wall-ion potential consists of the Coulomb part, Eq. (116), plus the hard-wall term, which gives a Dirac-δ when differentiated,

$$u'_{0\alpha}(z) = -\frac{2\pi\sigma q_\alpha}{\epsilon} - k_B T \delta(z - t/2). \tag{212}$$

With the wall-wall Coulomb potential given by Eq. (150), the wall-wall Born-Green-Yvon equation becomes

$$\begin{aligned} p^{\rm total}(t) &= \frac{2\pi\sigma^2}{\epsilon} - \sum_\alpha \rho_\alpha \int_{-\infty}^{\infty} \left[-\frac{2\pi\sigma q_\alpha}{\epsilon} - k_B T \delta(z - t/2) \right] [1 + h_{0\alpha}(z;t)]\, dz \\ &= -\frac{2\pi\sigma^2}{\epsilon} + k_B T \sum_\alpha \rho_\alpha [1 + h_{0\alpha}(t/2;t)], \end{aligned} \tag{213}$$

where the electroneutrality condition, Eq. (203), has been used. This says that the total pressure (force per unit area) acting between the walls consists of the kinetic term due to the thermal motion of the ions in contact with the wall less a constant electrostatic contribution. This is known as the contact theorem[127–131]. Although formally exact, taking the difference of the two positive terms could be problematic in an approximate implementation of the dumb-bell–ion scheme. The problems may be exacerbated by subtracting the bulk pressure to obtain the exponentially decaying net pressure; this will be tested by comparison with simulation results in §IVB.

III. APPROXIMATE METHODS

In Sections I and II the focus was on the formally exact expressions that could be used to analyse electrolytes and the electric double layer. Now attention shifts to numerical approaches, and in practice this means that one has to introduce approximations. The two computational schemes in current usage are simulation (molecular dynamics and Monte Carlo) and integral equation. The approximations are fundamentally different for the two approaches. Simulations set out to evaluate ensemble averages by generating all configurations of the ensemble. The limitations are the finite system-size, the amount of equilibration, and the finite number of configurations used to generate the statistics, assuming numerical errors to be negligible. The accuracy of any simulation can be improved by running the simulation for a longer time with more particles. In contrast integral equations are constructed to be at equilibrium and at the thermodynamic limit, and their limitation is due to having to close the set of formally exact relations between the correlation functions with an approximation. Whereas the numerical errors in solving an integral equation can be made negligible, (by using finer grids and larger cut-offs), the approach itself is fundamentally approximate and can only be improved by changing the closure. Simulations are said to be exact, (the above limitations notwithstanding), and they are used to generate benchmark results to test approximate theories. (The tests are carried out on well-defined model systems, which is the reason that one does not test the accuracy of an approximate theory by comparing it with experimental data.) Integral equations may be solved very efficiently, and results can be generated relatively quickly, which allows for direct application to experimental data in any regime where one is satisfied of the reliability of the approximation.

This section sets out the various integral equation approximations –singlet, inhomogeneous, density functional– and describes the relationship between them. The discussion of density functional theory will be limited; although closely related to Ornstein-Zernike based theories, and although the results are often accurate, reliable and tractable, in some ways the approximations used in density functional theory are of a more ad hoc nature. The approximation in theories based upon the hypernetted chain closure is generally the neglect of the bridge function, and hence systematic improvements can be made by including bridge diagrams of increasing complexity, which seems an advantage. Inhomogeneous integral equations in general are the most accurate and the most reliable of the approximate methods, and they have been used to generate benchmark results in cases where simulations aren't feasible, such as fluids around macrospheres. However they are rather complex to program and require heavy computational resources, in contrast to singlet integral equations. One is ultimately aiming for a practical theory that can be used for the quantitative interpretation of measurements, including data fitting. Accordingly the major emphasis in this section will be on the solute-ion Ornstein-Zernike equation (singlet method) with hypernetted chain closure, and the systematic improvement to that approximation that includes the first bridge diagram.

A. Singlet hypernetted chain approximation

The solute-ion Ornstein-Zernike equation, Eq. (91), relates the solute-ion total and direct correlation functions, and uses the bulk ion-ion direct correlation function. The latter may be obtained by any of the methods used to treat a bulk electrolyte, such as the hypernetted chain approximation, without[132] or with[133–137] the first bridge diagram. The mean spherical approximation is also used, since it has the advantage of providing an analytic polynomial expression for the ion-ion direct correlation function[62–64]. The second formally exact equation that relates the two solute-ion correlation functions is the closure equation. It is identical to that for the bulk electrolyte, Eq. (35), and it requires

a new unknown, the solute-ion bridge function. One needs to introduce an approximation, and most attention has focussed upon the hypernetted chain closure, which appears the most reliable. (For example, the Percus-Yevick approximation gives negative solute-solute distribution functions for large macrospheres, whereas the hypernetted chain approximation is guaranteed to remain positive[138].) The bridge function consists of an infinite sum of highly connected cluster diagrams, which are difficult to calculate. The hypernetted chain approximation simply neglects the bridge function,

$$d_{0\alpha}^{\rm HNC}(r) = 0. \tag{214}$$

This approximation is quite reliable and relatively accurate for bulk electrolytes, except possibly for divalent aqueous electrolytes at low concentrations. However the electric double layer represents a more severe test, and it is known to be inaccurate for certain quantities and in certain regimes. For example, the contact theorem relates the ion density at a planar wall to the pressure of the bulk electrolyte[127–131],

$$k_BT\sum_\alpha \rho_\alpha[1+h_{0\alpha}(0^+)] = p + \frac{2\pi\sigma^2}{\epsilon}, \tag{215}$$

which may be compared to Eq. (213). However the hypernetted chain approximation gives for the contact density[83]

$$k_BT\sum_\alpha \rho_\alpha[1+h_{0\alpha}(0^+)] = k_BT\sum_\alpha \rho_\alpha - \frac{k_BT}{2}\sum_{\alpha\gamma}\rho_\alpha\rho_\gamma\hat{\chi}_{\alpha\gamma}(0) + \frac{2\pi\sigma^2}{\epsilon}. \tag{216}$$

Using the formal expression for the isothermal compressibility

$$\chi_T \equiv \rho\left(\frac{\partial p}{\partial\rho}\right)_T = k_BT\rho - k_BT\sum_{\alpha\gamma}\rho_\alpha\rho_\gamma\hat{\chi}_{\alpha\gamma}(0), \tag{217}$$

where $\rho = \sum_\alpha \rho_\alpha$, the hypernetted chain result implies

$$p^{\rm ex} \equiv p - \rho k_BT = \frac{\rho}{2}\left(\frac{\partial p^{\rm ex}}{\partial\rho}\right)_T. \tag{218}$$

Hence if the hypernetted chain contact densities were used to obtain the pressure, then this is exact for the second virial coefficient for a simple fluid; for an electrolyte this route does not give exactly even the first correction to the ideal gas equation of state. In contrast the hypernetted chain approximation used in the virial theorem for a bulk simple fluid would yield the third virial coefficient exactly. The results persuade that the contact densities at a planar wall are not a good thermodynamic pathway to the bulk pressure.

A systematic correction to the hypernetted chain is to approximate the bridge function by the first bridge diagram. It is best to resum the f-bonds, which are individually non-integrable, in terms of the exponentially short-ranged h-bonds, and the first resummed bridge diagram is[17]

$$\begin{aligned} d_{0\alpha}^{\rm HNCD}(r_{12}) &= \frac{1}{2}\sum_{\gamma\lambda}\rho_\gamma\rho_\lambda\int h_{0\gamma}(r_{13})h_{0\lambda}(r_{14})h_{\gamma\lambda}(r_{34}) \\ &\quad\times h_{\gamma\alpha}(r_{23})h_{\lambda\alpha}(r_{24})\,d\mathbf{r}_3\,d\mathbf{r}_4. \end{aligned} \tag{219}$$

This first bridge diagram alone significantly improves the hypernetted chain closure and extends its regime of applicability for the bulk electrolyte[133–137]. Usually one solves the hypernetted chain approximation for the total correlation functions, which are then used to evaluate this bridge diagram. One then iterates the Ornstein-Zernike and closure equations with fixed bridge function to obtain the new total correlation function; in most cases recalculating the bridge function to obtain self-consistency has negligible effect. The numerical evaluation of this bridge diagram is facilitated by expansion in Legendre polynomials[139,140]

$$\begin{aligned} d_{0\alpha}^{\rm HNCD}(r_{12}) &= 2\pi^2\sum_{\gamma\lambda}\rho_\gamma\rho_\lambda\sum_{n=0}^{\infty}\left(\frac{2}{2n+1}\right)^2\int_0^\infty dr_3 r_3^2\int_0^\infty dr_4 r_4^2 \\ &\quad\times h_{\gamma\alpha}(r_3)h_{\lambda\alpha}(r_4)\hat{h}_{0\gamma}^{(n)}(r_1,r_3)\hat{h}_{0\lambda}^{(n)}(r_1,r_4)\hat{h}_{\gamma\lambda}^{(n)}(r_3,r_4), \end{aligned} \tag{220}$$

where the ion α has been placed at the origin, $\mathbf{r}_2 = \mathbf{0}$. Here the solute has been taken to be spherically symmetric, and the Legendre coefficients are

$$\hat{f}^{(n)}(r,s) = \frac{2n+1}{2}\int_{-1}^{1} P_n(x) f\left(\sqrt{r^2+s^2-2rsx}\right)\,dx, \tag{221}$$

where $P_n(x)$ is the Legendre polynomial of order n. For the case where the solute is a single planar wall one has

$$d_{0\alpha}^{\rm HNCD}(z_2) \;=\; 2\pi^2 \sum_{\gamma\lambda} \rho_\gamma \rho_\lambda \sum_{n=0}^{\infty} \left(\frac{2}{2n+1}\right)^2 \int_0^\infty dr_3 r_3^2 \int_0^\infty dr_4 r_4^2 \\ \times h_{\gamma\alpha}(r_3) h_{\lambda\alpha}(r_4) \hat{h}_{0\gamma}^{(n)}(z_2, r_3) \hat{h}_{0\lambda}^{(n)}(z_2, r_4) \hat{h}_{\gamma\lambda}^{(n)}(r_3, r_4), \tag{222}$$

where the Legendre coefficients of the bulk ion-ion total correlation functions were given in above, Eq. (221), and those of the wall-ion total correlation function are[84]

$$\hat{h}_{0\alpha}^{(n)}(z, r) = \frac{2n+1}{2} \int_{-1}^{1} P_n(x) h_{0\alpha}(z - rx)\, dx. \tag{223}$$

It is convenient to evaluate the Legendre coefficients by an orthogonal technique[141], which corresponds to a Gaussian quadrature; typically only 10-20 terms are needed in the expansion. Expressions for the Legendre expansion of the bridge diagrams with three field points have been given by Attard and Patey[138]. These authors found that the hypernetted chain approximation was increasingly improved as more bridge diagrams were added to the closure, especially for the solute-solute interaction[77,138]. These results were for hard-sphere solutes in a hard-sphere fluid; to date bridge diagrams with three field points have not been used for electrolytes or for the electric double layer. An alternative expansion is the hydrostatic hypernetted chain approximation of Zhou and Stell[142]. The theory amounts to a formula for the bridge function that involves the bulk chemical potential and the bulk compressibility evaluated at either a local or a weighted density, and it has been shown to improve upon the singlet hypernetted chain approximation for hard spheres at and between hard-walls[142].

The singlet hypernetted chain approximation has been used to obtain the properties of the electric double about an isolated solute, with much attention focussed on a charged planar wall[2,3]. At higher surface charge densities there occurs numerical instabilities in the solution of the approximation; the most efficient and robust algorithm appears to be the one given by Ballone et al.[143], which is based upon earlier work on the one-component plasma[144,145]. The variational method of Feller and McQuarrie[146] also appears quite robust. Carnie and Torrie[2] give an extensive review and comparison of results for the isolated planar double layer prior to 1984, including the modified Poisson-Boltzmann approximation. Blum[3] compares various theories in detail for the case of 1M monovalent electrolyte ($d = 4.25$Å) against a wall with surface charge density $\sigma = 0.7e/d^2$. This is a demanding test case where the simulations[143,147,148] show a secondary peak in the counterion profile at about one diameter from contact, which is not predicted by the bare hypernetted chain approximation. However inclusion of the first bridge diagram does give this peak[143]. Nielaba, Forstmann and co-workers[149,150] use the singlet hypernetted chain approach with a local density approximation which invokes the bulk ion-ion direct correlation function of a jellium and obtain the secondary peak. It is also given by certain density functional approximations; local[151] and weighted[152–154] densities have been used. Inhomogeneous integral equations (discussed below) are perhaps the most accurate of all approaches, and include the Born-Green-Yvon approach of Caccamo and co-workers[155,156], and the inhomogeneous Ornstein-Zernike approach of Kjellander and Marčelja[157] and of Plischke and Henderson[158].

The singlet hypernetted chain approximation has been used in other geometries. Bratko[159] treated ions confined to a spherical pore, and results have also been obtained for cylinders and cylindrical pores[115–117,120]. The dumb-bell approach, which uses the hypernetted chain approximation for an isolated solute composed of two particles (§IID3), has been used to obtain the interaction between planar walls[160–164].

The singlet equation for interacting solutes, (e.g. the macrospheres of §IIA, or the walls of §IIC), can also be solved with the hypernetted chain approximation, with or without the first bridge diagram. Patey[165] obtain hypernetted chain results for charged spherical colloids at infinite dilution, and found an attraction at small separations between identically charged macroions with high surface charge densities. (Teubner's[166] argument that this attraction was spurious and an artifact of the hypernetted chain approximation is based on a theorem of Bell and Levine[167] that is only valid in Poisson-Boltzmann approximation.) Henderson also used the hypernetted chain approximation for two charged spherical macroions[102], and others have studied highly asymmetric electrolytes[168–173]. For interacting walls, singlet hypernetted chain results have been obtained for hard-walls in Lennard-Jones and in dipolar fluids[77], and for the electric double layer interaction between charged walls without[174,175], and with[84] the first bridge diagram.

1. Solvation free energy

A peculiar advantage of the hypernetted chain approximation is that one can perform the coupling constant integrations to obtain the chemical potential and the Helmholtz free energy as spatial integrals of the fully coupled pair correlation functions[176,177]. This holds in a variety of applications besides bulk electrolytes, and this section derives

the hypernetted chain approximation for the solvation free energy. This is a useful quantity that determines, for example, the electric double layer contribution to the solvation of charged particles and how it changes with curvature or surface charge. Also, for the case of the dumb-bell singlet approach, the solvation free energy of the dumb-bell gives the interaction free energy of the two solutes, and hence for the case of two planes the results of the present section provide an alternative to the contact theorem of §IID3 for calculating the pressure. The following derivation of the hypernetted chain solvation free energy and its extension to include the first bridge diagram is based upon that of Kiselyov and Martynov[178], (see also Ref.[179]).

The solvation free energy is the change in the grand potential of the electrolyte when there is a solute fixed at the origin. Formally this is

$$\begin{aligned}
\mu_0 &\equiv \Omega^{(1)}(\underline{\mu}, V, T) - \Omega^{(0)}(\underline{\mu}, V, T) \\
&= \int_0^1 \frac{\partial \Omega^{(\lambda)}(\underline{\mu}, V, T)}{\partial \lambda}\, d\lambda \\
&= \mu_0^{\text{self}} + \int_0^1 \left\langle \sum_{\alpha,i} u_{0\alpha}(r_{\alpha i}) \right\rangle^{(\lambda)} d\lambda \\
&= \mu_0^{\text{self}} + \int_0^1 d\lambda \sum_\alpha \rho_\alpha \int d\mathbf{r}\; u_{0\alpha}(r) g_{0\alpha}^{(\lambda)}(r).
\end{aligned} \tag{224}$$

Here the superscript indicates that the solute-ion distribution function is partially coupled; the solute-ion potential is $u_{0\alpha}^{(\lambda)}(r) = \lambda u_{0\alpha}(r)$. The quantity μ_0^{self} represents the self-energy of the solute, a zero-body term that must be added since the coupling integral represents only the contribution of the ions to the solvation free energy. For simplicity spherical solutes have been assumed, although the results will apply to any geometry in an obvious fashion, and a pair-wise additive solute-ion potential has been invoked, which excludes image charge interactions. Using the exact closure, (c.f. Eq. (35)), one can perform two integrations by parts to obtain

$$-\beta \int_0^1 u_{0\alpha}(r) g_{0\alpha}^{(\lambda)}(r)\, d\lambda = \tag{225}$$

$$\begin{aligned}
&h_{0\alpha}(r) - [h_{0\alpha}(r) - c_{0\alpha}(r) + d_{0\alpha}(r)] g_{0\alpha}(r) \\
&\quad + \int_0^1 [h_{0\alpha}^{(\lambda)}(r) - c_{0\alpha}^{(\lambda)}(r) + d_{0\alpha}^{(\lambda)}(r)] \frac{\partial h_{0\alpha}^{(\lambda)}(r)}{\partial \lambda}\, d\lambda,
\end{aligned} \tag{226}$$

where the correlation functions without superscript are fully coupled.

Now for the hypernetted chain approximation, $d_{0\alpha}^{\text{HNC}}(r) = 0$, and the coupling constant integral involves the series function, which is just the Ornstein-Zernike convolution integral. One has

$$\begin{aligned}
&\sum_\alpha \rho_\alpha \int d\mathbf{r}_\alpha \int_0^1 d\lambda\, [h_{0\alpha}^{(\lambda)}(r_\alpha) - c_{0\alpha}^{(\lambda)}(r_\alpha)] \frac{\partial h_{0\alpha}^{(\lambda)}(r_\alpha)}{\partial \lambda} \\
&\qquad = \sum_{\alpha\gamma} \rho_\alpha \rho_\gamma \int d\mathbf{r}_\alpha\, d\mathbf{r}_\gamma \int_0^1 d\lambda\, h_{0\gamma}^{(\lambda)}(r_\gamma) c_{\gamma\alpha}(r_{\gamma\alpha}) \frac{\partial h_{0\alpha}^{(\lambda)}(r_\alpha)}{\partial \lambda} \\
&\qquad = \sum_{\alpha\gamma} \rho_\alpha \rho_\gamma \int d\mathbf{r}_\alpha\, d\mathbf{r}_\gamma \int_0^1 d\lambda\, \frac{1}{2} \frac{\partial}{\partial \lambda} \left[h_{0\gamma}^{(\lambda)}(r_\gamma) c_{\gamma\alpha}(r_{\gamma\alpha}) h_{0\alpha}^{(\lambda)}(r_\alpha) \right] \\
&\qquad = \frac{1}{2} \sum_{\alpha\gamma} \rho_\alpha \rho_\gamma \int d\mathbf{r}_\alpha\, d\mathbf{r}_\gamma\, h_{0\gamma}(r_\gamma) c_{\gamma\alpha}(r_{\gamma\alpha}) h_{0\alpha}(r_\alpha) \\
&\qquad = \frac{1}{2} \sum_\alpha \rho_\alpha \int d\mathbf{r}_\alpha\, [h_{0\alpha}(r_\alpha) - c_{0\alpha}(r_\alpha)] h_{0\alpha}(r_\alpha).
\end{aligned} \tag{227}$$

Here the product rule has been invoked to give the factor of one half, because the right side is symmetric in the two solute-ion bonds. Note that the ion-ion correlation functions are always fully coupled and independent of λ. With this result the hypernetted chain solvation free energy may be written

$$-\beta \mu_0^{\text{HNC}} = -\beta \mu_0^{\text{self}} + \sum_\alpha \rho_\alpha \int \left[c_{0\alpha}(r) - \frac{1}{2} \{h_{0\alpha}(r) - c_{0\alpha}(r)\} h_{0\alpha}(r) \right] d\mathbf{r}. \tag{228}$$

In some cases (e.g. planar walls), it is desirable to replace the direct correlation function by its short-ranged counterpart, $\chi_{0\alpha}(\mathbf{r}) = c_{0\alpha}(\mathbf{r}) + \beta q_\alpha V_0^{\rm Coul}(\mathbf{r})$. For the most general solute with charge distribution $\sigma(\mathbf{r})$, one may write

$$V_0^{\rm Coul}(\mathbf{r}) = \text{ const.} + \int \frac{\sigma(\mathbf{s})}{\epsilon|\mathbf{r}-\mathbf{s}|}\, d\mathbf{s}. \tag{229}$$

Using the definition of the mean electrostatic potential, $\psi(\mathbf{r}) = V_0^{\rm Coul}(\mathbf{r}) + \sum_\alpha \rho_\alpha q_\alpha \int d\mathbf{s}\; h_{0\alpha}(\mathbf{s})/\epsilon|\mathbf{r}-\mathbf{s}|$, it follows that the hypernetted chain solvation free energy may be rewritten

$$-\beta\mu_0^{\rm HNC} = \frac{-\beta}{2}\int \sigma(\mathbf{s})\psi(\mathbf{s})\, d\mathbf{s} + \sum_\alpha \rho_\alpha \int \left[\chi_{0\alpha}(\mathbf{r}) - \frac{1}{2}\left\{h_{0\alpha}(\mathbf{r}) - \chi_{0\alpha}(\mathbf{r})\right\} h_{0\alpha}(\mathbf{r})\right]\, d\mathbf{r}. \tag{230}$$

Note that the solute self-energy,

$$\mu_0^{\rm self} = \frac{1}{2}\int \sigma(\mathbf{s}) V_0^{\rm Coul}(\mathbf{s})\, d\mathbf{s}, \tag{231}$$

is explicitly cancelled in this final result.

It also possible to perform the coupling constant integral when one goes beyond the bare hypernetted chain approximation and includes bridge diagrams. The first solute-ion bridge diagram is given explicitly by Eq. (219), which can be represented as

$d_{0\alpha}^{\rm HNCD}(r) =$ 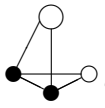 (232)

Here the empty circles represent the solute and the ion α, the filled circles represent the ions that are integrated and summed over, and the lines represent total correlation function bonds. The solvation free energy in this approximation is

$$\begin{aligned} -\beta\mu_0^{\rm HNCD} &= -\beta\mu_0^{\rm HNC} - \sum_\alpha \rho_\alpha \int d_{0\alpha}(r) g_{0\alpha}(r)\, d\mathbf{r} \\ &\quad + \int_0^1 d\lambda \sum_\alpha \rho_\alpha \int d\mathbf{r}\; d_{0\alpha}^{(\lambda)}(r) \frac{\partial h_{0\alpha}^{(\lambda)}(r)}{\partial\lambda}. \end{aligned} \tag{233}$$

As for the series function, which was treated in hypernetted chain approximation above, equivalence of the solute-ion bonds allows the coupling integrand to be expressed as the differential of a product. This is clear in the diagrammatic representation,

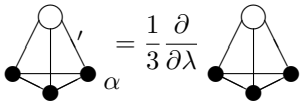 (234)

where the prime in the first diagram denotes the differentiated solute-ion h-bond. The factor of 1/3 arises because only the solute-ion bonds depend upon λ, and the three of them are identical. There is no change in symmetry number in passing to the final diagram because of the label α; this integration will be now be done explicitly. The final result is

$$-\beta\mu_0^{\rm HNCD} = -\beta\mu_0^{\rm HNC} - \sum_\alpha \rho_\alpha \int \left[d_{0\alpha}^{\rm HNCD}(r) + \frac{2}{3} d_{0\alpha}^{\rm HNCD}(r) h_{0\alpha}(r)\right]\, d\mathbf{r}. \tag{235}$$

This procedure may be extended to the higher order bridge diagrams[179,180].

It is worthwhile to give explicit expressions for the solvation free energy for planar walls. For an isolated wall, $\sigma(\mathbf{r}) = \sigma\delta(z)$, and the solvation free energy per unit area becomes

$$-\beta\mu_0^{\rm HNC} = \frac{-\beta\sigma\psi(0)}{2} + \sum_\alpha \rho_\alpha \int_{-\infty}^{\infty} \left[\chi_{0\alpha}(z) - \frac{1}{2}\left\{h_{0\alpha}(z) - \chi_{0\alpha}(z)\right\} h_{0\alpha}(z)\right]\, dz. \tag{236}$$

This is in fact infinite because neither correlation function vanishes inside the wall; $h_{0\alpha}(z) \to -1$ and $\chi_{0\alpha}(z) \to -1 - \beta q_\alpha \psi(0)/2 + \rho_\alpha \sum_\gamma \rho_\gamma \hat{\chi}_{\alpha\gamma}(0)$ as $z \to -\infty$. The physical origin of the divergence is that to make a wall of thickness L one has to displace bulk electrolyte and thus do work against the bulk pressure, which gives a contribution $\mu_0 \sim pL$. The divergent contribution in the above is

$$-\beta\mu_0^{\rm HNC} \sim -\left[\sum_\alpha \rho_\alpha - \frac{1}{2}\sum_{\alpha\gamma}\rho_\alpha\rho_\gamma\hat{\chi}_{\alpha\gamma}(0)\right] L, \quad L \to \infty. \tag{237}$$

The bracketed term is just the hypernetted chain contact density expression for the bulk pressure, Eq. (216).

One can avoid this divergence by dealing with the electrostatic free energy, and the most convenient reference state is that of an uncharged wall. If one denotes the solute-ion correlation functions for an uncharged wall by the superscript zero, and if one defines difference functions such as $\Delta h_{0\alpha}(z) \equiv h_{0\alpha}(z) - h_{0\alpha}^{(0)}(z)$ that are short-ranged inside the wall, then one can form a well-defined expression for the surface charge dependent part of the free energy

$$\begin{aligned} -\beta[\mu_0^{\rm HNC}(\sigma) - \mu_0^{\rm HNC}(0)] &= \frac{-\beta\sigma\psi(0)}{2} + \frac{1}{2}\sum_\alpha \rho_\alpha \int_0^\infty \Big[2\Delta\chi_{0\alpha}(z) + \Delta\chi_{0\alpha}(-z) \\ &\quad - \Delta\left\{h_{0\alpha}(z)^2\right\} + \Delta\left\{\chi_{0\alpha}(z)h_{0\alpha}(z)\right\}\Big]\, dz. \end{aligned} \tag{238}$$

Because $\underline{\rho}^T \underline{\chi}(z) \to -\beta\chi_T^{-1}, \quad z \to -\infty$, which is independent of surface charge, it is clear that the above integral is convergent. One has a similar situation for the hypernetted chain approximation that includes the first bridge diagram, and the solution is analogous. In this case deep inside the wall the bridge function goes to a constant that is given by

$$\begin{aligned} \lim_{z\to-\infty} d_{0\alpha}^{\rm HNCD}(z) &= \frac{1}{2}\sum_{\gamma\lambda}\rho_\gamma\rho_\lambda \int d\mathbf{r}\, d\mathbf{s}\; h_{\alpha\gamma}(r)h_{\alpha\lambda}(s)h_{\gamma\lambda}(|\mathbf{r}-\mathbf{s}|) \\ &= \frac{1}{4\pi^2}\sum_{\gamma\lambda}\rho_\gamma\rho_\lambda \int_0^\infty \hat{h}_{\alpha\gamma}(k)\hat{h}_{\alpha\lambda}(k)\hat{h}_{\gamma\lambda}(k)\, k^2\, dk, \end{aligned} \tag{239}$$

which is clearly independent of the surface charge.

For the dumb-bell solute that consists of two identical walls separated by t, $\sigma(\mathbf{r}) = \sigma[\delta(t/2+z) + \delta(t/2-z)]$, one has for the free energy per unit area

$$\begin{aligned} -\beta\mu_0^{\rm HNC}(t) &= -\beta\sigma\psi(t/2;t) + \sum_\alpha \rho_\alpha \int_{-\infty}^{\infty} \\ &\quad \left[\chi_{0\alpha}(z;t) - \frac{1}{2}\left\{h_{0\alpha}(z;t) - \chi_{0\alpha}(z;t)\right\} h_{0\alpha}(z;t)\right] dz. \end{aligned} \tag{240}$$

Again this is divergent, and again only a free energy difference is meaningful. This time the zero of free energy is chosen to be at infinite separation, which corresponds to two isolated walls. One has

$$\lim_{t\to\infty} h_{0\alpha}(z;t) = h_{0\alpha}(t/2+z) + h_{0\alpha}(t/2-z), \tag{241}$$

and

$$\lim_{t\to\infty} \chi_{0\alpha}(z;t) = \chi_{0\alpha}(t/2+z) + \chi_{0\alpha}(t/2-z). \tag{242}$$

On the left dumb-bell–ion functions occur, and on the right wall-ion functions. As usual one defines difference functions that vanish for large plate separations,

$$\Delta h_{0\alpha}(z;t) \equiv h_{0\alpha}(z;t) - h_{0\alpha}(t/2+z) - h_{0\alpha}(t/2-z), \tag{243}$$

and

$$\Delta\chi_{0\alpha}(z;t) \equiv \chi_{0\alpha}(z;t) - \chi_{0\alpha}(t/2+z) - \chi_{0\alpha}(t/2-z). \tag{244}$$

These also go to zero deep within the walls,

$$\Delta h_{0\alpha}(z;t) \to 0, \ |z| \to \infty, \tag{245}$$

and

$$\Delta\left\{\underline{\rho}^T\underline{\chi}(z;t)\right\}\to 0,\ \ |z|\to\infty. \tag{246}$$

Similarly, the difference in the surface potential vanishes for large separations,

$$\Delta\psi(t/2;t)\equiv\psi(t/2;t)-\psi(0)\to 0,\ \ t\to\infty. \tag{247}$$

Finally, the product of ion-wall total correlation functions from each isolated wall vanishes for large distances or separations,

$$h_{0\alpha}(t/2+z)\,h_{0\alpha}(t/2-z)\to 0,\ \ |z|\to\infty,\ \text{or}\ t\to\infty, \tag{248}$$

and similarly for the product of h and χ. In view of these definitions it is straightforward to show that the dumb-bell hypernetted chain approximation for the interaction free energy per unit area, (see the corresponding wall-wall result in §IIC), is

$$\begin{aligned}
-\beta w_{00}^{\rm int}(t) &\equiv -\beta[\mu_0(t)-2\mu_0]\\
&= -\beta\sigma\Delta\psi(t/2;t)+\sum_\alpha\rho_\alpha\int_{-\infty}^{\infty}\Delta\chi_{0\alpha}(z;t)\,dz\\
&\quad-\frac{1}{2}\sum_\alpha\rho_\alpha\int_{-\infty}^{\infty}[h_{0\alpha}(z;t)-\chi_{0\alpha}(z;t)]\,\Delta h_{0\alpha}(z;t)\,dz\\
&\quad-\sum_\alpha\rho_\alpha\int_{-\infty}^{\infty}[\Delta h_{0\alpha}(z;t)-\Delta\chi_{0\alpha}(z;t)]\,h_{0\alpha}(t/2+z)\,dz\\
&\quad-\sum_\alpha\rho_\alpha\int_{-\infty}^{\infty}[h_{0\alpha}(t/2+z)-\chi_{0\alpha}(t/2+z)]\,h_{0\alpha}(t/2-z)\,dz.
\end{aligned} \tag{249}$$

This expression contains both dumb-bell–ion and wall-ion correlation functions and their differences. (Note that the dumb-bell potential and the consistent short-ranged direct correlation function are given in §IID3. Also, a formally identical expression holds for a non-zero Stern layer, and it may be shown that the value of the interaction free energy is independent of the width of the Stern layer.) Differentiating this free energy provides an alternative to the contact theorem for calculating the net pressure between two walls in the dumb-bell approach, §IID3. This result holds for the hypernetted chain approximation, but an analogous result can be derived when the first bridge diagram is included. Feller and McQuarrie[163] formulated the singlet dumb-bell hypernetted chain approximation as a variational principle. They did not use the free energy directly, but rather obtained the pressure from the contact theorem, and they avoided any divergences by dealing with plates of finite thickness.

B. Inhomogeneous integral equations

The singlet integral equation and the inhomogeneous integral equation represent two alternative viewpoints of the electric double layer. In the first the charged particles are treated on the same footing as the ions of the electrolyte, and the solute-ion distribution function corresponds to the density profile of the double layer. In the second the charged particles are treated as fixed and as the source of an external field, which causes the non-uniform density of the ions that is the double layer. In the inhomogeneous approach one applies the closure approximation to the inhomogeneous ion-ion correlation functions, whereas in the singlet approach the closure is applied to the density profile itself. Other things being equal one would expect a given closure approximation to be more accurate and reliable when used in the inhomogeneous method than when used in the singlet method. For example, it is necessary to include the first bridge diagram in the singlet approach to obtain results comparable to the bare hypernetted chain closure in the inhomogeneous approach. This is certainly true for the simplest singlet methods, such as the wall-ion Ornstein-Zernike equation, but the boundaries between the two approaches become blurred for dumb-bells and n-ions. For example, the ion density profile around a dumb-bell consisting of a wall and a fixed ion corresponds to the inhomogeneous ion-ion correlation function next to a wall.

The inhomogeneous Ornstein-Zernike equation is

$$\underline{\underline{H}}(\mathbf{r}_1,\mathbf{r}_2)=\underline{\underline{C}}(\mathbf{r}_1,\mathbf{r}_2)+\int\underline{\underline{H}}(\mathbf{r}_1,\mathbf{r}_3)\underline{\underline{C}}(\mathbf{r}_3,\mathbf{r}_2)\,d\mathbf{r}_3, \tag{250}$$

where the elements of the inhomogeneous total correlation function matrix are

$$\left\{\underline{\underline{H}}(\mathbf{r}_1,\mathbf{r}_2)\right\}_{\alpha\gamma} = \rho_\alpha(\mathbf{r}_1)^{1/2} h_{\alpha\gamma}(\mathbf{r}_1,\mathbf{r}_2)\rho_\gamma(\mathbf{r}_2)^{1/2}, \tag{251}$$

and similarly for the inhomogeneous direct correlation function. One has $\underline{\underline{H}}(\mathbf{r}_1,\mathbf{r}_2) = \underline{\underline{H}}^T(\mathbf{r}_2,\mathbf{r}_1)$.

The diagrammatic definitions of the total and direct correlation functions are formally the same as for the uniform electrolyte; the densities that weight the field points are no longer constant but vary in space. Consequently the formally exact closure remains

$$h_{\alpha\gamma}(\mathbf{r}_1,\mathbf{r}_2) = -1 + \exp -\beta u_{\alpha\gamma}(\mathbf{r}_1,\mathbf{r}_2) + h_{\alpha\gamma}(\mathbf{r}_1,\mathbf{r}_2) - c_{\alpha\gamma}(\mathbf{r}_1,\mathbf{r}_2) + d_{\alpha\gamma}(\mathbf{r}_1,\mathbf{r}_2), \tag{252}$$

where d is the inhomogeneous bridge function, and the pair potential u need not depend solely on separation (as do the hard-sphere and direct Coulomb potential), but can depend upon position. Electrostatic images due to dielectric disparities are an example of a position-dependent contribution that is readily incorporated into the inhomogeneous approach; a discussion of these is deferred until the conclusion.

The remaining unknown function in the above is the density, and there are several formally exact expressions for its gradient. The oldest is the first member of the Born-Green-Yvon hierarchy for an inhomogeneous fluid, which balances the gradient of the density with the force due to an external potential, $V_\alpha(\mathbf{r})$, and the internal forces in the double layer[181–184],

$$\nabla\rho_\alpha(\mathbf{r}_1) = -\beta\rho_\alpha(\mathbf{r}_1)\nabla V_\alpha(\mathbf{r}_1) - \beta\rho_\alpha(\mathbf{r}_1)\sum_\gamma \int g_{\alpha\gamma}(\mathbf{r}_1,\mathbf{r}_2)\nabla_1 u_{\alpha\gamma}(\mathbf{r}_1,\mathbf{r}_2)\rho_\gamma(\mathbf{r}_2)\, d\mathbf{r}_2, \tag{253}$$

where the inhomogeneous pair distribution function is $g = h + 1$. An alternative result may be derived from the Born-Green-Yvon hierarchy for an homogeneous fluid mixture. For the case of a solute, the first member relates the solute-ion pair distribution function to the solute-ion-ion triplet distribution function,

$$\nabla_0 g_{0\alpha}(\mathbf{r}_{01}) = -\beta g_{0\alpha}(\mathbf{r}_{01})\nabla_0 u_{0\alpha}(\mathbf{r}_{01}) - \beta\sum_\gamma \rho_\gamma \int \nabla_0 u_{0\gamma}(\mathbf{r}_{02}) g_{0\alpha\gamma}(\mathbf{r}_{01},\mathbf{r}_{02})\, d\mathbf{r}_2. \tag{254}$$

If the solute is taken to be fixed and is considered as the source of an external field, then these may be rewritten in terms of the density profile and the inhomogeneous pair total correlation function, (since the integral of the force over the unconnected diagrams vanishes)[185,186],

$$\nabla\rho_\alpha(\mathbf{r}_1) = -\beta\rho_\alpha(\mathbf{r}_1)\nabla V_\alpha(\mathbf{r}_1) - \beta\rho_\alpha(\mathbf{r}_1)\sum_\gamma \int h_{\alpha\gamma}(\mathbf{r}_1,\mathbf{r}_2)\rho_\gamma(\mathbf{r}_2)\nabla V_\gamma(\mathbf{r}_2)\, d\mathbf{r}_2. \tag{255}$$

This equation is eponymously referred to as the WLMB equation. Note that the external potential that appears here will usually contain in addition to the Coulomb potential a volume exclusion term, whose gradient contributes a δ-function; this accounts for the boundary terms that some authors explicitly include in the WLMB equation[6,187]. In actual fact an equation equivalent to the WLMB equation was earlier given by Triezenberg and Zwanzig[188]

$$\nabla\rho_\alpha(\mathbf{r}_1) = -\beta\rho_\alpha(\mathbf{r}_1)\nabla V_\alpha(\mathbf{r}_1) + \rho_\alpha(\mathbf{r}_1)\sum_\gamma \int c_{\alpha\gamma}(\mathbf{r}_1,\mathbf{r}_2)\nabla\rho_\gamma(\mathbf{r}_2)\, d\mathbf{r}_2. \tag{256}$$

(This equation, which with the external potential set to zero is Eq. (19) of Ref.[188], is also called by some the WLMB equation.) The two equations are related by the Ornstein-Zernike equation. Any one of these three equations for the density gradient, together with the Ornstein-Zernike and closure equations, are sufficient to determine the three unknown functions (the density profile, and the total and direct correlation functions), provided one has some prescription or approximation for the bridge function.

As in the bulk and singlet equations, the simplest approximation for the bridge function is to neglect it altogether, which is just the hypernetted chain closure applied to the inhomogeneous correlation functions,

$$d^{\mathrm{HNC}}_{\alpha\gamma}(\mathbf{r}_1,\mathbf{r}_2) = 0. \tag{257}$$

As in the singlet case discussed in §IIIA1, within the inhomogeneous hypernetted chain approximation it is possible to perform the coupling integral, which gives an explicit expression for the local chemical potential. Enforcing the constancy of this yields an alternative to the three formally exact equations given above for determining the density profile[189]. The numerical evaluation of the first bridge diagram appears formidable for the inhomogeneous fluid, and to

date systematic corrections to the hypernetted chain approximation have not been attempted. Various ansatz for the inhomogeneous bridge function have been explored for a Lennard-Jones fluid between two walls[190], and Percus-Yevick hard-sphere bridge functions have been used for ions in the planar electric double layer[191]. In the latter approximation the results are good but the computation appears rather demanding.

As in the bulk fluid, the direct correlation function decays as the pair potential for large separations between the ions, as was assumed in §IIB3 above. Hence one defines the short-ranged part to be

$$\underline{\underline{\chi}}(\mathbf{r}_1,\mathbf{r}_2) = \underline{\underline{C}}(\mathbf{r}_1,\mathbf{r}_2) + \frac{1}{4\pi r_{12}}\underline{\underline{Q}}(\mathbf{r}_1,\mathbf{r}_2), \tag{258}$$

where the dyadic charge matrix now depends upon the positions of the ions due to densities that are incorporated into its definition, $\underline{\underline{Q}}(\mathbf{r}_1,\mathbf{r}_2) = (4\pi\beta/\epsilon)\underline{q}(\mathbf{r}_1)\underline{q}^T(\mathbf{r}_2)$, with $\left\{\underline{q}(\mathbf{r})\right\}_\alpha = q_\alpha\rho_\alpha^{1/2}(\mathbf{r})$. (The pair potential due to dielectric images, if present, should also be subtracted.) The mean spherical approximation sets the short-ranged part of the direct correlation function to zero beyond contact,

$$\chi_{\alpha\gamma}^{\mathrm{MSA}}(\mathbf{r}_1,\mathbf{r}_2) = 0, \quad |\mathbf{r}_1-\mathbf{r}_2| > d_{\alpha\gamma}. \tag{259}$$

One of course enforces the exact condition $h_{\alpha\gamma}(\mathbf{r}_1,\mathbf{r}_2) = -1, \quad |\mathbf{r}_1-\mathbf{r}_2| < d_{\alpha\gamma}$. This corresponds to neglecting the bridge function and to linearising the hypernetted chain closure (apart from the mean electrostatic potential). For the case of zero-size ions, $d_{\alpha\gamma} = 0$, this is just the Debye-Hückel approximation, which sets the inhomogeneous total correlation function to the exponential of the fluctuation potential and is known as Loeb's closure[192]; it has been used to extract some analytic results for the planar double layer[88,193,194]. The analysis of Attard et al.[193,194] was termed the extended Poisson-Boltzmann approximation, which is the same name as that given to the earlier analysis at a similar level of approximation by Podgornik and Žekš[195]. Solutions to Loeb's closure (inhomogeneous mean spherical approximation for ions of zero size) were obtained by Blum et al.[196] for the case when the density profile can be expressed as a sum of exponentials.

The modified Poisson-Boltzmann theory, originally due to Bell and Levine[197,198], represents one of the earliest inhomogeneous integral equation approaches. Loeb's closure was used, but instead of the inhomogeneous Ornstein-Zernike equation the Kirkwood hierarchy was invoked. The modified Poisson-Boltzmann theory has been used to study the electric double layer at an isolated wall, and it includes volume exclusion effects due to ion-size, correlation effects due to the fluctuation potential, and the effects of images due to the dielectric constant of the wall. The various approximations used have been refined several times, (see Ref.[199] and references therein); the most recent version remains one of the more accurate theories for the isolated double layer at all but the highest surface charge densities[2].

The first member of the Born-Green-Yvon hierarchy for an inhomogeneous fluid, Eq. (253), was applied to the electric double layer by Croxton and McQuarrie[200], who approximated the inhomogeneous pair distribution function by the bulk one, with certain correction factors to ensure electroneutrality.

What makes the Ornstein-Zernike approach so popular for bulk fluids is that the convolution integral factorises upon Fourier transformation; the consequent algebraic equation is readily 'solved' for either the total or the direct correlation function. The availability of the fast Fourier transform is a significant advantage because one alternately iterates the closure in real space and the Ornstein-Zernike equation in Fourier space. For inhomogeneous fluids there are just two geometries in which the Ornstein-Zernike equation partially factorises: planar, and spherical. As mentioned in §IIB3, in planar geometry a zero order Hankel transform yields

$$\underline{\underline{\hat{H}}}(k,z_1,z_2) = \underline{\underline{\hat{C}}}(k,z_1,z_2) + \int_0^\infty \underline{\underline{\hat{H}}}(k,z_1,z_3)\underline{\underline{\hat{C}}}(k,z_3,z_2)\,dz_3. \tag{260}$$

The one dimensional integral that remains is readily evaluated, and hence the transformed equation is in a form suitable for iteration. Because one has to transform back and forth from Hankel space many times, from the numerical point of view it is desirable to have a discrete orthogonal transform. Lado has given an 'almost' orthogonal transform, which appears to be quite robust in practice[201]. Unfortunately it does not appear possible to formulate a fast version of this. The density profile equations are also simplified by a Hankel transform. The planar inhomogeneous Ornstein-Zernike equation was solved by Sokolowski[202,203] for a hard-sphere fluid with Percus-Yevick closure, and by Nieminen, Ashcroft, and co-workers[204–206] for a Lennard-Jones fluid with modified hypernetted chain closure. For the electric double layer Kjellander, Marčelja and co-workers[157,189,191,207–214] used the hypernetted chain approximation for two walls (slit pore). Plischke and Henderson[158,215,216] used that approximation and also the mean spherical approximation for the double layer at an isolated wall.

For the case of a spherically inhomogeneous fluid, the density depends upon the distance from the origin and the pair correlations depend upon the two distances of the ions from the origin and the angle between them. The Ornstein-Zernike equation is

$$\underline{\underline{H}}(r_1,r_2,\theta_{12}) = \underline{\underline{C}}(r_1,r_2,\theta_{12}) + \int \underline{\underline{H}}(r_1,r_3,\theta_{13})\underline{\underline{C}}(r_3,r_2,\theta_{32})\,d\mathbf{r}_3, \tag{261}$$

which partially factorises upon Legendre transformation[141,217],

$$\underline{\underline{\hat{H}}}^{(n)}(r_1,r_2) = \underline{\underline{\hat{C}}}^{(n)}(r_1,r_2) + \frac{4\pi}{2n+1}\int_0^\infty \underline{\underline{\hat{H}}}^{(n)}(r_1,r_3)\underline{\underline{\hat{C}}}^{(n)}(r_3,r_2)\; r_3^2\, dr_3. \tag{262}$$

(The equations for the density profile in spherical geometry also simplify upon Legendre transform[141].) The Legendre transforms are essentially the same as those used for the evaluation of the bridge function,

$$\hat{f}^{(n)}(r_1,r_2) = \frac{2n+1}{2}\int_0^\pi f(r_1,r_2,\theta)\sin\theta\; d\theta. \tag{263}$$

A discrete orthogonal version of the Legendre transform performs well in practice[141]. A quick (but not fast) version has been tested[218], and a fast (but not orthogonal) algorithm is known[219]. The spherically inhomogeneous Ornstein-Zernike equation has been solved for hard-sphere fluids with Percus-Yevick closure[141], and for Lennard-Jones fluids with hypernetted chain closure[218,220]. Fushiki has also solved it for a charged spherical pore containing counterions only[159,217]. Outhwaite and Bhuiyan[221] have used the modified Poisson-Boltzmann theory (Kirkwood hierarchy with Loeb's closure) to study the electric double layer around a spherical macroion.

The planar and spherical geometries are the only two geometries in which the inhomogeneous pair correlation functions depends upon three variables, one of them in an homogeneous fashion. In contrast, for example, for systems with cylindrical symmetry they depend upon the two distances from the axis, the mutual angle, and the mutual separation along the axis. Currently it does not appear feasible to solve the inhomogeneous Ornstein-Zernike equation in any but planar and spherical geometry (or circular or linear geometry in two dimensions), although Bhuiyan and Outhwaite[122] have formulated their modified Poisson-Boltzmann theory in cylindrical geometry.

In concluding this section on the inhomogeneous approach, it is now shown that if the inhomogeneous direct correlation function is replaced by the bulk one in the equations for the density profile, then one recovers the singlet hypernetted chain approximation, as was pointed out by Badiali et al.[144]. Replacing the inhomogeneous $c_{\alpha\gamma}(\mathbf{r}_1,\mathbf{r}_2)$ by the bulk $c_{\alpha\gamma}(r_{12})$, the Triezenberg-Zwanzig equation for the density profile, Eq. (256), may be rewritten

$$\begin{aligned}
\frac{1}{\rho_\alpha(\mathbf{r}_1)}\frac{\partial\rho_\alpha(\mathbf{r}_1)}{\partial\mathbf{r}_1} &= -\beta\frac{\partial V_\alpha(\mathbf{r}_1)}{\partial\mathbf{r}_1} + \sum_\gamma\int\frac{\partial\rho_\gamma(\mathbf{r}_2)}{\partial\mathbf{r}_2}c_{\gamma\alpha}(r_{12})\; d\mathbf{r}_2 \\
&= -\beta\frac{\partial V_\alpha(\mathbf{r}_1)}{\partial\mathbf{r}_1} - \sum_\gamma\int\rho_\gamma(\mathbf{r}_2)\frac{\partial c_{\gamma\alpha}(r_{12})}{\partial\mathbf{r}_2}\; d\mathbf{r}_2 \\
&= -\beta\frac{\partial V_\alpha(\mathbf{r}_1)}{\partial\mathbf{r}_1} + \sum_\gamma\int\rho_\gamma(\mathbf{r}_2)\frac{\partial c_{\gamma\alpha}(r_{12})}{\partial\mathbf{r}_1}\; d\mathbf{r}_2 \\
&= -\beta\frac{\partial V_\alpha(\mathbf{r}_1)}{\partial\mathbf{r}_1} + \frac{\partial}{\partial\mathbf{r}_1}\sum_\gamma\rho_\gamma\int h_{0\gamma}(\mathbf{r}_2)c_{\alpha\gamma}(r_{12})\; d\mathbf{r}_2.
\end{aligned} \tag{264}$$

The second equality follows an integration by parts, the integrated portion vanishing, the third equality arises because $\partial f(r_{12})/\partial\mathbf{r}_2 = -\partial f(r_{12})/\partial\mathbf{r}_1$, and the final equality is due to the fact that $\rho_\gamma(\mathbf{r}_2) = \rho_\gamma[1+h_{0\gamma}(\mathbf{r}_2)]$, where the constant part gives a contribution that is independent of $\mathbf{r}_1$. Integrating this one obtains

$$\begin{aligned}
\ln 1 + h_{0\alpha}(\mathbf{r}_1) &= -\beta V_\alpha(\mathbf{r}_1) + \sum_\gamma\rho_\gamma\int h_{0\gamma}(\mathbf{r}_2)c_{\gamma\alpha}(r_{12})\; d\mathbf{r}_2 \\
&= -\beta q_\alpha\psi(\mathbf{r}_1) + \sum_\gamma\rho_\gamma\int h_{0\gamma}(\mathbf{r}_2)\chi_{\gamma\alpha}(r_{12})\; d\mathbf{r}_2,
\end{aligned} \tag{265}$$

both sides vanishing as $\mathbf{r}_1\to\infty$. This is just the singlet hypernetted chain approximation; in planar geometry it is equivalent to Eqs (111) and (119), with $d_{0\alpha}(z) = 0$. Colmenares and Olivares[222] used this method to treat the electric double layer using hypernetted chain and mean spherical approximation bulk direct correlation functions.

For the Debye-Hückel closure to the bulk correlation functions, which is also the mean spherical approximation for ions with zero size, $\chi_{\alpha\gamma}(r) = 0$, this evidently reduces to the non-linear Poisson-Boltzmann approximation for the density profile. This closure and profile approximation have been used in the inhomogeneous approach to analyse the electrostatic correlation contribution to the double layer interaction between planar surfaces. For the planar electric double with counterions only[193], and with a restricted primitive model electrolyte[194], Attard et al. solved the zero-sized mean spherical approximation for the inhomogeneous pair correlation functions using the non-linear Poisson-Boltzmann density profile, and obtained analytic expressions for the double layer interaction free energy. The same approximation was solved by Blum et al.[196] for exponential density profiles.

C. Density functional theory

The hypernetted chain solvation free energy, Eq. (228), may be rewritten

$$\begin{aligned}
&-\beta[\mu_0^{\mathrm{HNC}} - \mu_0^{\mathrm{self}}] \\
&= -\sum_\alpha \rho_\alpha \int \{[h_{0\alpha}(r_1) - c_{0\alpha}(r_1)]\,[1 + h_{0\alpha}(r_1)] - h_{0\alpha}(r_1)\}\; d\mathbf{r}_1 \\
&\quad + \frac{1}{2}\sum_\alpha \rho_\alpha \int [h_{0\alpha}(r_1) - c_{0\alpha}(r_1)]\, h_{0\alpha}(r_1)\; d\mathbf{r}_1 \\
&= -\sum_\alpha \rho_\alpha \int \Big[\{\beta u_{0\alpha}(r_1) + \ln[1 + h_{0\alpha}(r_1)]\}\,[1 + h_{0\alpha}(r_1)] - h_{0\alpha}(r_1)\Big]\; d\mathbf{r}_1 \\
&\quad + \frac{1}{2}\sum_{\alpha\gamma} \rho_\alpha \rho_\gamma \int d\mathbf{r}_1\; d\mathbf{r}_2\; h_{0\alpha}(r_1) c_{\alpha\gamma}(r_{12}) h_{0\gamma}(r_2).
\end{aligned} \tag{266}$$

The solute-ion direct correlation function has been eliminated by using the hypernetted chain closure on the first term, and by using the Ornstein-Zernike equation on the second. One may confirm that this particular form of the free energy is optimised by the hypernetted chain approximation,

$$\begin{aligned}
&\frac{-\beta\delta\mu_0^{\mathrm{HNC}}}{\rho_\alpha \delta h_{0\alpha}(r_1)} \\
&= -\beta u_{0\alpha}(r_1) - \ln[1 + h_{0\alpha}(r_1)] - 1 + 1 + \sum_\gamma \rho_\gamma \int c_{\alpha\gamma}(r_{12}) h_{0\gamma}(r_2)\; d\mathbf{r}_2 \\
&= -[h_{0\gamma}(r_1) - c_{0\gamma}(r_1)] + h_{0\gamma}(r_1) - c_{0\gamma}(r_1) \\
&= 0.
\end{aligned} \tag{267}$$

In other words, minimising the solvation free energy in the form of Eq. (266) with respect to the double layer about the solute is equivalent to solving the singlet hypernetted chain approximation. (Olivares and McQuarrie[223] give systematic methods for deriving variational principles for closure approximations.) The advantage of the variational approach is that one can use physically appropriate analytic functions to describe the density profile, and the free energy minimisation by parameter variation is rather efficient. Moreover, the errors in the free energy are second order compared to the errors in the density profiles, and hence one only has to solve the minimisation problem approximately.

By considering the solute as fixed and the source of an external field, the solute-ion distribution function may be replaced by the density profile, and it is clear that Eq. (266) gives the grand potential as an explicit functional of the density. This is an example of a density functional approximation, in which the equilibrium density profile is given by the optimisation of a grand potential functional. The various versions and applications of density functional theory have been reviewed by Evans[224,225]. Normally one writes the grand potential as a functional of the configurational part of the Hamiltonian (the pair potential, and the chemical potential and any other one-body external potentials). The functional derivative of the grand potential with respect to the one-body potential yields the density profile, and successive differentiation yields the density-density and higher order correlation functions. There is in fact a one-to-one relationship between the one-body potential and the density profile, and one may alternatively regard the free energy as a functional of the density. The Legendre transform of the grand potential yields the so-called intrinsic part of the Helmholtz free energy[224,225],

$$\mathcal{F}[\underline{\rho}] = \Omega + \sum_\alpha \int [\mu_\alpha - V_\alpha(\mathbf{r})]\rho_\alpha(\mathbf{r})\; d\mathbf{r}. \tag{268}$$

For the case treated above of a spherical solute fixed at the origin, the external field is $V_\alpha(\mathbf{r}) = u_{0\alpha}(r)$ and the density profile is $\rho_\alpha(\mathbf{r}) = \rho_\alpha[1 + h_{0\alpha}(r)]$. Provided that one has a recipe for $\mathcal{F}$ as a functional of the density profile, one may regard this equation as giving the grand potential as a functional of the density, $\tilde{\Omega}[\underline{\rho}]$, which functional is minimised by the equilibrium density profile, at which point it equals the actual grand potential. (It is easiest to develop approximations directly for $\mathcal{F}$, which does not depend upon the specific external field, and then to use these to obtain Ω).

The intrinsic Helmholtz free energy may be split into ideal and excess parts. The former is

$$\mathcal{F}^{\mathrm{id}}[\underline{\rho}] = \sum_\alpha \int f_\alpha^{\mathrm{id}}(\rho_\alpha(\mathbf{r}))\; d\mathbf{r}, \tag{269}$$

where $f_\alpha^{\rm id}(\rho) = k_BT\rho(\ln[\rho\Lambda_\alpha^3] - 1)$ is the ideal Helmholtz free energy density, and Λ_α is the de Broglie thermal wavelength. The functional derivatives of the excess part of the intrinsic Helmholtz free energy with respect to the density profile yield the hierarchy of direct correlation functions[224,225]. Specifically, the one-body direct correlation function is

$$c_\alpha(\mathbf{r}_1;[\underline{\rho}]) = -\frac{\delta\mathcal{F}^{\rm ex}[\underline{\rho}]}{\delta\rho_\alpha(\mathbf{r}_1)}, \tag{270}$$

and the two-body direct correlation function is

$$c_{\alpha\gamma}(\mathbf{r}_1,\mathbf{r}_2;[\underline{\rho}]) = \frac{\delta c_\alpha(\mathbf{r}_1;[\underline{\rho}])}{\delta\rho_\gamma(\mathbf{r}_2)} = -\frac{\delta^2\mathcal{F}^{\rm ex}[\underline{\rho}]}{\delta\rho_\alpha(\mathbf{r}_1)\delta\rho_\gamma(\mathbf{r}_2)}. \tag{271}$$

In view of these expressions, $\mathcal{F}$ as a functional of the density profile can be obtained by functional integration of the direct correlation function, and the resultant formally exact formulae provide a basis for a number of approximation schemes. If one introduces a coupling constant for the density profile, $\underline{\rho}^{(\lambda)}(\mathbf{r}) = \underline{\rho}^{(0)}(\mathbf{r}) + \lambda\Delta\underline{\rho}(\mathbf{r})$, then one obtains[224,225]

$$\begin{aligned}
&\beta\mathcal{F}^{\rm ex}[\underline{\rho}^{(1)}] \\
&= \beta\mathcal{F}^{\rm ex}[\underline{\rho}^{(0)}] - \sum_\alpha \int_0^1 d\lambda \int d\mathbf{r}\ \Delta\rho_\alpha(\mathbf{r}) c_\alpha(\mathbf{r};[\underline{\rho}^{(\lambda)}]) \qquad (272)\\
&= \beta\mathcal{F}^{\rm ex}[\underline{\rho}^{(0)}] - \sum_\alpha \int d\mathbf{r}\ \Delta\rho_\alpha(\mathbf{r}) c_\alpha(\mathbf{r};[\underline{\rho}^{(0)}]) \\
&\quad + \sum_{\alpha\gamma} \int_0^1 d\lambda\,(\lambda-1) \int d\mathbf{r}_1\, d\mathbf{r}_2\ \Delta\rho_\alpha(\mathbf{r}_1)\Delta\rho_\gamma(\mathbf{r}_2) c_{\alpha\gamma}(\mathbf{r}_1,\mathbf{r}_2;[\underline{\rho}^{(\lambda)}]). \qquad (273)
\end{aligned}$$

A convenient starting point for the functional integration is the uniform electrolyte, $\rho_\alpha^{(0)}(\mathbf{r}) = \rho_\alpha$, in which case the grand potential functional becomes

$$\begin{aligned}
&\beta\Omega[\underline{\rho}^{(1)}] - \beta\Omega[\underline{\rho}^{(0)}] = \\
&\quad \beta\sum_\alpha \int V_\alpha(\mathbf{r})\rho_\alpha(\mathbf{r})\ d\mathbf{r} + \sum_\alpha \int \left[\rho_\alpha(\mathbf{r}) \ln\frac{\rho_\alpha(\mathbf{r})}{\rho_\alpha} - \rho_\alpha(\mathbf{r}) + \rho_\alpha\right] d\mathbf{r} \\
&\quad + \sum_{\alpha\gamma} \int_0^1 d\lambda\,(\lambda-1) \int d\mathbf{r}_1\, d\mathbf{r}_2\ \Delta\rho_\alpha(\mathbf{r}_1)\Delta\rho_\gamma(\mathbf{r}_2) c_{\alpha\gamma}(\mathbf{r}_1,\mathbf{r}_2;[\underline{\rho}^{(\lambda)}]). \qquad (274)
\end{aligned}$$

When the external field represents a solute fixed at the origin, the left side is the solvation free energy, $\beta\mu_0$, (less the self term).

This formally exact result gives the grand potential as a functional of the density profile. Obviously one has to give some formula for the two-body direct correlation function that appears. The simplest approximation is to ignore the dependence upon the coupling constant and to take it to be equal to the corresponding quantity of the bulk electrolyte,

$$c_{\alpha\gamma}(\mathbf{r}_1,\mathbf{r}_2;[\underline{\rho}^{(\lambda)}]) = c_{\alpha\gamma}(r_{12};[\underline{\rho}^{(0)}]). \tag{275}$$

In this case one obtains[224–226]

$$\begin{aligned}
&\beta\Omega[\underline{\rho}^{(1)}] - \beta\Omega[\underline{\rho}^{(0)}] = \\
&\quad \beta\sum_\alpha \int V_\alpha(\mathbf{r})\rho_\alpha(\mathbf{r})\ d\mathbf{r} + \sum_\alpha \int \left[\rho_\alpha(\mathbf{r}) \ln\frac{\rho_\alpha(\mathbf{r})}{\rho_\alpha} - \rho_\alpha(\mathbf{r}) + \rho_\alpha\right] d\mathbf{r} \\
&\quad - \frac{1}{2}\sum_{\alpha\gamma} \int d\mathbf{r}_1\, d\mathbf{r}_2\ [\rho_\alpha(\mathbf{r}_1) - \rho_\alpha][\rho_\gamma(\mathbf{r}_2) - \rho_\gamma] c_{\alpha\gamma}(r_{12};[\underline{\rho}^{(0)}]). \qquad (276)
\end{aligned}$$

For the case when the external field represents a solute fixed at the origin, this is evidently identical to Eq. (266). Hence mimimising the approximate grand potential functional that has the inhomogeneous partially coupled direct

correlation function replaced by the fully coupled bulk one is equivalent to solving the singlet hypernetted chain approximation.

An obvious improvement is to retain the next term in the functional Taylor expansion, which will give an expression that involves the triplet direct correlation function of the bulk electrolyte[227,228]. This is equivalent to retaining bridge diagrams in the hypernetted chain approximation, since the bridge function can be written as an expansion over the three-body and higher direct correlation functions[38,39,179].

Perturbation approximations are perhaps the most popular form of density functional theory[224,225]. One typically uses the short-range repulsive part of the pair potential to define a reference fluid, which is predominantly responsible for the double layer structure, and one usually treats the attractive part in mean-field or other approximate fashion. The reference intrinsic free energy may be that of a bulk hard-sphere fluid using a simple local density approximation[229], or more sophisticated weighted versions[230–232]; see the review of Evans[225] for a discussion of these and other recipes for the reference free energy.

Density functional theory has been applied to the electric double layer at an isolated planar wall. Groot[151] used a density functional approximation that invoked the mean spherical bulk direct correlation function evaluated at a local density. A similar approach was earlier used by Nielaba, Forstmann and co-workers[149,150], who instead inserted a bulk direct correlation function, evaluated at a local non-neutral density, into the singlet hypernetted chain equation. Davis and co-workers[152,233,234] used a perturbation approach that invoked the hard-sphere free energy density evaluated at a density determined by a weighting due to Tarazona[232], together with a hard-sphere/Coulomb correction to the direct correlation function evaluated at the bulk density. They also studied interacting planar double layers in the primitive model[235] and with added hard sphere solvent[236]. Very similar approaches were used by Kierlik and Rosinberg[153], who give a transparent derivation of the electrostatic contributions, and by Patra and Ghosh[154], who evaluated the Coulomb correction at the effective rather than the bulk density. The latter authors tested as well the weighting due to Denton and Ashcroft[237], and obtained very good results for the restricted primitive model double layer[154,238]. They also included a hard-sphere solvent[154], which is the solvent primitive model similarly treated by Tang et al.[234], and went on to treat an asymmetric binary electrolyte[239], the double layer at a metallic electrode within a jellium model[240], and the solvation force due to overlapping double layers[241]. Penfold et al.[242] obtained a correction to the Poisson-Boltzmann equation using a local density approximation and tested it for a spherical macroion (cell model). Feller and McQuarrie[146] formulated the singlet hypernetted chain approximation as a variational principle, and solved it for the isolated planar double layer.

For interacting walls, Stevens and Robins[243] obtained good results for the pressure for the counterions-only double layer using a local density approximation and the known free energy of the bulk, point-ion, one component plasma. Attard et al.[193,194] obtained an analytic expression for the free energy of interacting planar double layers, (counterions-only and restricted primitive model, including dielectric images), using the non-linear Poisson-Boltzmann approximation for the density profile and the mean spherical approximation for ions of zero-size for the inhomogeneous ion-ion direct correlation function. Podgornik and Žekš[195] used a similar level of approximation in the context of a functional integral description of the effects of ion correlations in the double layer. Feller and McQuarrie[163,164] used variational techniques to obtain the interaction of two walls and the electric double layer between them (equivalent to the singlet dumb-bell hypernetted chain approximation). As mentioned above, Davis and co-workers[235,236] and Patra and Ghosh[241] applied used weighted density approximations for interacting planar double layers.

D. Simulations

The isolated planar double layer has been simulated for a restricted primitive model confined between two identically charged walls[244–246] and between one charged and one neutral wall[147,247], which has the advantages of attaining bulk concentrations for smaller system sizes, and of avoiding time-consuming sums due to multiple image charges. (Ballone et al.[143] used two walls of equal and opposite charge, obtaining agreement with the results of Torrie and Valleau[147], which were for a smaller system.) Zhang et al.[236] simulated an electrolyte in a hard-sphere solvent confined between a neutral and a charged wall using (essentially) the canonical ensemble. Two-dimensional Ewald sums were used by these authors and by others[248–253]; for conducting metal walls the usual three dimensional Ewald sum can be used[254]. Torrie and Valleau[147] argue that Ewald sums exaggerate the correlations in the planar double layer, and that it is preferable to include only the mean field contribution to the potential from ions external to the central simulation cell. Caillol and Levesque[148] avoided periodic boundary conditions in their simulations of the isolated planar double layer by placing the system on the surface of a 4-sphere.

The pressure due to the interaction of two planar double layers at small separations has been obtained for counterions only[214,255–260] and for binary primitive model electrolytes[214,259–262], and for molten salts[263]. The paper by Guldbrand et al.[256] is noteworthy for being the first simulation to show attractive double layer forces between similarly charged surfaces. In some cases the canonical ensemble was used and Widom's method was applied to determine the chemical

potential and hence the concentration of the bulk electrolyte in equilibrium with the double layer. It is probably preferable to use grand canonical Monte Carlo, as this sets the desired equilibrium directly[147,260]. For example, Bratko et al.[264] were able to study the adsorption excess of a restricted primitive model electrolyte confined between two neutral walls as a function of separation, and the consequent number of confined ions were used in canonical simulations for the net pressure between the neutral walls[265]. Grand canonical and isobaric Monte Carlo studies of relatively realistic models of a mica-clay slit pore with counterions in an aqueous solvent have been carried out[266–269]. Molecular dynamics have been performed in the canonical ensemble for water and mobile counterions between two ionic surfactant monolayers[270]. The solvation of Sodium Chloride at a platinum electrode has been reported[271], as has the structure of water between neutral and charged planar walls[272]. Results have also been reported for pure water between clay and surfactant lamellae[273–275]. Lee et al.[276] used molecular dynamics with Ewald summation to study a dipolar fluid confined between charged Lennard-Jones walls. The interaction of charged surfaces with grafted polyelectrolyte counterions has been simulated[277–281].

Simulations deal with finite sized samples, and except for fully closed pores one has to attend to the boundaries. Periodic boundary conditions with Ewald summation have been used for bulk electrolytes. As mentioned above, Ewald summation has also been used for planar slits, although it has been argued that mean field corrections for the tail are more appropriate[147]. For the case of spherical macroions one typically encloses the macrosphere and surrounding electrolyte by a concentric, impenetrable, uncharged sphere; if the annular region is wide enough one will have bulk electrolyte in the system and so mimic an isolated spherical macroion. Obviously for large radius macroions the situation is problematic, since the number of electrolyte ions required grows in proportion to the square of the radius; to date no periodic replication of an annular cell has been used. Some authors use this annular geometry to model interacting macroions, the so-called cell model; they invoke the electrolyte concentration at the outer boundary as the osmotic pressure of the dispersion[131]. The Monte Carlo tests of the cell model against isotropic solution results by Linse and Jönsson[282] show it to be inaccurate for the osmotic pressure except at low concentrations.

The double layer around a spherical macroion has been simulated within the cell model and in isotropic solution[131,171,242,282,283]. Degréve et al.[284] simulated the restricted primitive model double layer about small spherical macroions. Sloth and Sørenson[285] studied a primitive model electrolyte confined to a charged spherical pore using grand canonical Monte Carlo. Svensson and Jönsson[286] simulated the interaction of a spherical macroion with a similarly charged planar wall in the presence of counterions, and showed that the force could be of attractive. Vlachy and co-workers[118,119,123] have simulated the electric double layer inside a cylindrical pore. Cylindrical aggregates in the cell model have also been studied[121,287–289].

IV. NUMERICAL RESULTS

A. Effective surface charge

The various properties of an isolated planar double layer have been extensively reviewed[2,3]. In particular, and amongst other things, Carnie and Torrie[2] cover the modified Poisson-Boltzmann approximation and singlet hypernetted chain approximations in some detail, and Blum[3] compares a number of theories for the ion profiles in 1M monovalent electrolyte at a high surface charge density. However since the asymptotic results for electrolytes and the electric double layer discussed in §§I and II have begun to be emphasised only in recent times, it seems appropriate to begin with some numerical examples of these for an isolated wall. Perhaps the key result is that the ion density profiles behave as predicted by the Poisson-Boltzmann approximation, but with effective parameters. The screening length of the bulk electrolyte κ^{-1} is relatively close to the Debye length κ_D^{-1}, and the dielectric factor ν is almost unity, at least for electrolytes in the monotonic regime. Hence the most important effective parameter is the surface charge density $\tilde{\sigma}$, which is given by Eq. (127). This effective surface charge density may also be called the fitted charge density because it is what one would obtain if one were to fit experimental measurements with the linear Poisson-Boltzmann approximation, at least in the asymptotic regime. As mentioned at the end of §IIB2, either one may use a sophisticated theory to describe the double layer, or one may use the simplest Poisson-Boltzmann approximation and correct this fitted surface charge to obtain the actual surface charge. The following data is presented with the latter procedure in mind. Note that the bulk electrolytes explored here are all in the monotonic regime, since this is the case where the effective surface charge can be given a physical interpretation.

Several methods will be used to obtain the effective surface charge. The most sophisticated use the singlet hypernetted chain approximation in conjunction with Eq. (127). This approximation is at least qualitatively reliable for the isolated planar double layer, and may be described as quantitatively accurate at not too high concentrations or surface charges[2,3]. The accuracy of the singlet hypernetted chain approximation is improved by the inclusion of the first bridge diagram[143], and results for the effective surface charge with and without the bridge diagram are given. (In the data below the bridge function was recalculated to self-consistency, up to ten times in the case of the divalent

electrolyte at the highest surface charge density, in order to obtain a reliable value for the effective surface charge.) An analytic approximation will also be used, namely the extended Poisson-Boltzmann theory of Attard et al.[194]. This is essentially the solution of the mean spherical closure to the inhomogeneous Ornstein-Zernike equation for ions of zero size; it thus includes the effects of ion correlations but not those of excluded volume. Attard et al.[194] gave a formula for converting surface charge fitted on the basis of the non-linear Poisson-Boltzmann approximation to actual surface charge, but it is straightforward to re-express this in terms of a fit to the linear Poisson-Boltzmann approximation. Assuming that to a good enough approximation $\kappa \approx \kappa_D$, $\nu \approx 1$, the result is

$$\tilde{\sigma} = \sigma \frac{A}{2s} \left[1 + \frac{\beta q^2 \kappa_D}{4\epsilon} \{2I + \ln 2\} \right]^{1/2}, \tag{277}$$

where $A \equiv 16(-1 + \sqrt{1 + s^2/4})/s$, the dimensionless surface charge is $s \equiv 4\pi\beta q\sigma/\epsilon\kappa_D$, and I is given by Eq. (3.23) of Ref.[194],

$$\begin{aligned} I \;=\; & \frac{1}{2}\left(1 + \frac{2z^2-3}{(2z^2-1)^3}\right)\ln 2 + \frac{2-2z^3+z}{2z(2z^2-1)^2} - \frac{1}{2}\left(1 - \frac{2z^2-3}{(2z^2-1)^3}\right)\ln(z+z^2) \\ & - \frac{\sqrt{z^2-1}}{z}\left(1 + \frac{2z^2+1}{(2z^2-1)^3}\right)\tan^{-1}\sqrt{\frac{z-1}{z+1}}, \end{aligned} \tag{278}$$

where $z \equiv \sqrt{1 + s^2/4}$.

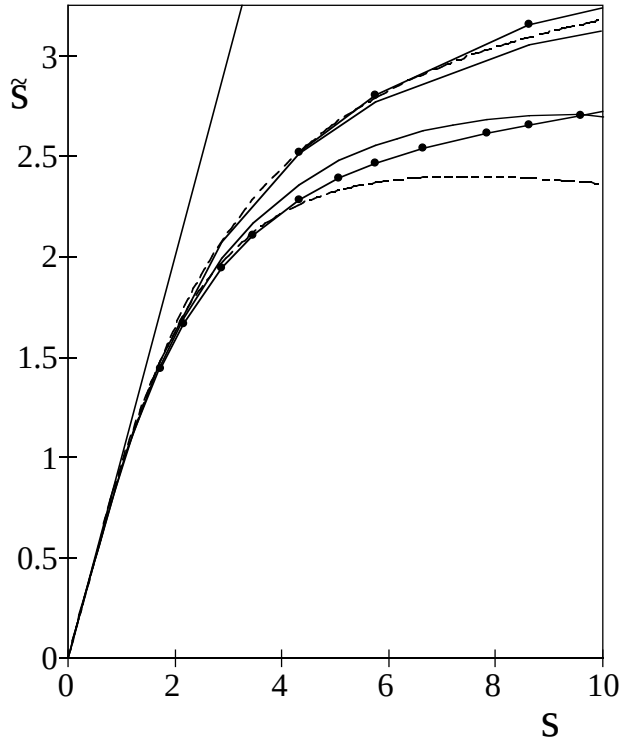

FIG. 5: The effective or fitted surface charge density, $\tilde{s} = 4\pi\beta q\tilde{\sigma}/\epsilon\kappa_D$, as a function of the actual surface charge density, $s \equiv 4\pi\beta q\sigma/\epsilon\kappa_D$, for the restricted primitive model at a concentration of 10^{-3}M, ($\epsilon_r = 78.358$, $T = 298.15$K, $d = 4.25$Å). The upper triplet of curves is for monovalent ions, the lower triplet is for divalent ions, and the straight line is a guide to the eye. The solid curves with and without symbols are the hypernetted chain approximations, Eq. (127), with and without the first bridge diagram, and the dashed curve is the analytic result of the extended Poisson-Boltzmann approximation[194], Eq. (IV A).

Figure 5 shows the effective surface charge, (i.e. that which would be fitted on the basis of the linear Poisson-Boltzmann approximation), for monovalent and divalent 1mM electrolyte. The extended Poisson-Boltzmann approximation, Eq. (IV A), is compared to the hypernetted chain approximation with and without the first bridge diagram using Eq. (127). In general the fitted surface charge is noticeably less than the actual surface charge, and the departure is larger for high surface charge densities and in divalent electrolyte. If the two were equal, (i. e. the linear Poisson-Boltzmann approximation were exact), one would get the straight line. At low surface charge this is indeed the case.

As the surface charge is increased one finds a departure from linearity which is the same in all three approximations. Evidently the analytic extended Poisson-Boltzmann approximation provides the primary correction to the mean-field approximation. One therefore concludes that this departure is dominated by electrostatic correlations, and that excluded volume effects make a minor contribution in this regime, (the extended Poisson-Boltzmann approximation includes the former but not the latter[194]). That the monovalent and divalent curves coincide here supports the use of the parameter $s \equiv 4\pi\beta q\sigma/\epsilon\kappa_D$ as a dimensionless measure of surface charge. At higher surface charge densities the three approximations begin to disagree, particularly in the case of the divalent electrolyte, although qualitatively they behave similarly. The hypernetted chain approximation with the first bridge diagram is expected to be the most accurate of the three approximations, and the fitted surface charge calculated with it should be taken as definitive.

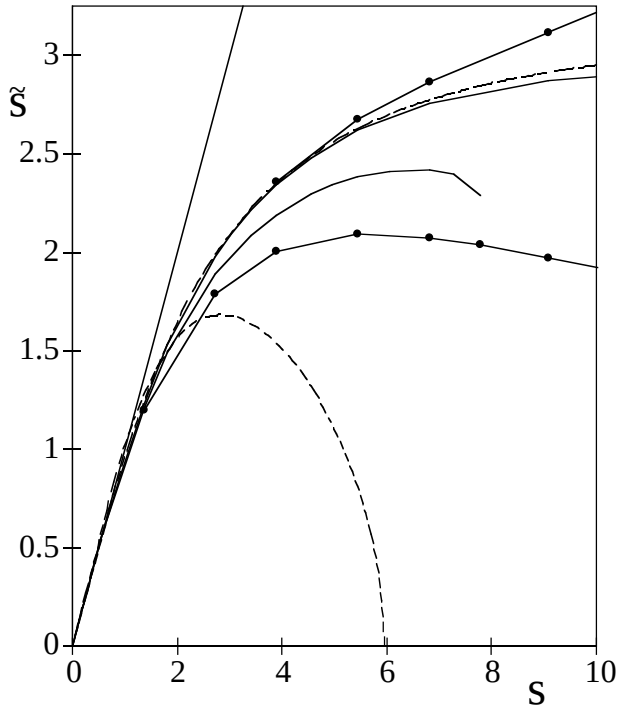

FIG. 6: As in the preceding figure at a concentration of 10^{-2}M.

In the divalent data one sees that the curve actually has a maximum in the bare hypernetted chain and in the extended Poisson-Boltzmann approximations (these approximations also predict that a maximum occurs in the monovalent electrolyte at higher surface charges than those shown). This effect is clearer in the data for the higher concentration of 0.01M shown in Fig. 6. Here again all the curves coincide at low surface charge densities, and they would also coincide in this regime with the low concentration data in Fig. 5, which lends further support to s as the appropriate dimensionless surface charge density. The divalent extended Poisson-Boltzmann data has a maximum at about $s = 2.85$, (it actually predicts an unphysical asymptotic attraction beyond $s = 5.9$), the bare hypernetted chain approximation has a maximum at about $s = 6.8$, (it did not converge beyond $s = 8$), and including the first bridge diagram shifts the maximum to about $s = 5.5$, (and extends the regime of convergence). The non-monotonic behaviour of the fitted surface charge density is even more noticeable at the higher electrolyte concentration of 0.1M, (Fig. 7), and can also be seen in the monovalent data in the figure. The experimental consequence of this behaviour is that for a given electrolyte the surface charge density will appear to saturate. Alternatively there will be an ambiguity in its value that can only be resolved by additional information, such as data fitting in the non-asymptotic regime. This non-monotonic behaviour is both unusual and counterintuitive, but it is perhaps consistent with other hypernetted chain predictions for the double layer. In the case of the 0.1M monovalent electrolyte, the maximum fitted charge occurs at an actual area per unit charge of 100–125Å^2. Shortly it will be shown that the hypernetted chain approximation predicts that the electric double layer interaction between two charged walls at small separations changes from repulsive to attractive at an area per unit surface charge of about 200Å^2. Finally, the potential drop across the isolated double layer is predicted by the hypernetted chain approximation to begin to *decrease* with *increasing* surface charge; the diffuse part at an area per unit surface charge of 50Å^2, and the total at about 10Å^2.

The rate of change of the electrostatic potential with surface charge density is called the differential capacitance, and the fact that the hypernetted chain approximation predicted it to be negative was at one time seen as a serious failing

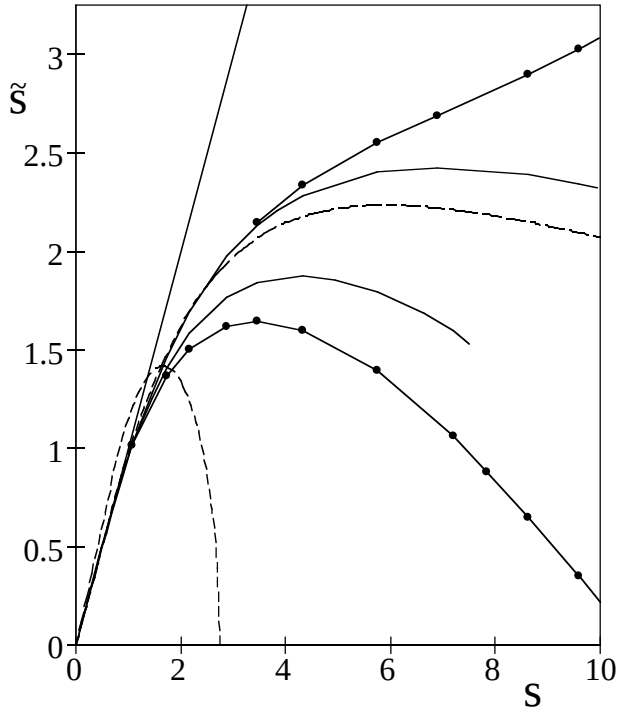

FIG. 7: As in the preceding figure at a concentration of 10^{-1}M.

of that approximation. In fact however there appears no fundamental proscription against a negative differential capacitance, and there is certainly no proof that it must be positive[290]. It has been shown that a negative differential capacitance could occur if the derivative of the charge density profile with respect to surface charge was anywhere positive, which appears to be what happens in the hypernetted chain calculations at high surface charge densities. Simulations of the restricted primitive model show a flattening of the potential–surface charge curve, (without it actually turning over), but the diffuse part of the potential drop does turn over in simulations of the restricted primitive model, as does the total potential drop in simulations of an asymmetric electrolyte[291]. Hence the fact that the hypernetted chain approximation predicts a negative differential capacitance for areas per unit charge less than 10Å^2, whereas simulations only show a small positive one in this case, is only a quantitative failing of that approximation, not a qualitative one. Similarly, the turn-over in the effective surface charge shown in Figs 5–7 is likely qualitatively correct, and the surface charge at which is occurs is probably accurately given by the hypernetted chain approximation that includes the first bridge diagram.

At high surface charge densities the effective surface charge continues to decrease, and for the 0.1M divalent electrolyte it goes through zero and changes sign at $s \approx 11$. A layer of counterions forms at the wall with essentially close-packed density, excluding the coions, and at the same time over-neutralising the surface charge. Charge reversal occurs due to a combination of ion size and valence, and it also depends upon the bulk electrolyte concentration and surface charge density, which determine the concentration in the layer. The mechanism is clear in Fig. 8, where it can be seen that there is a dense layer of counterions next to the wall and that there are almost no coions in this region. Slightly beyond one diameter ($d = 4.25$Å) from the wall an inversion occurs and the co-ion density exceeds the counterion density. It is emphasised that this is a local charge oscillation induced by the high surface charge on the wall. The bulk electrolyte is in the monotonic regime, (with decay length $\kappa^{-1} = 5.4$Å), and the density profiles and potential will decay monotonically beyond this surface region. In particular, although the surface is positively charged, the electrostatic potential turns negative at about 3Å from the wall and remains negative. Measuring techniques that sample the double layer some distance from the surface will ascribe to the particle a charge with the wrong sign. For example, electrophoresis, in which the motion of a particle in an applied electric field depends upon the electrostatic potential at the zeta plane away from the surface, may show a highly charged particle stop and reverse direction as the concentration is varied, even though its actual surface charge remains unchanged. The point of zero charge and the subsequent reversed effective charge are not due to physical binding of counterions to the surface, or to chemical association or dissociation, but rather to the electrostatic attraction and layering of the counterions and exclusion of the coions due to packing in the diffuse part of the double layer adjacent to the surface.

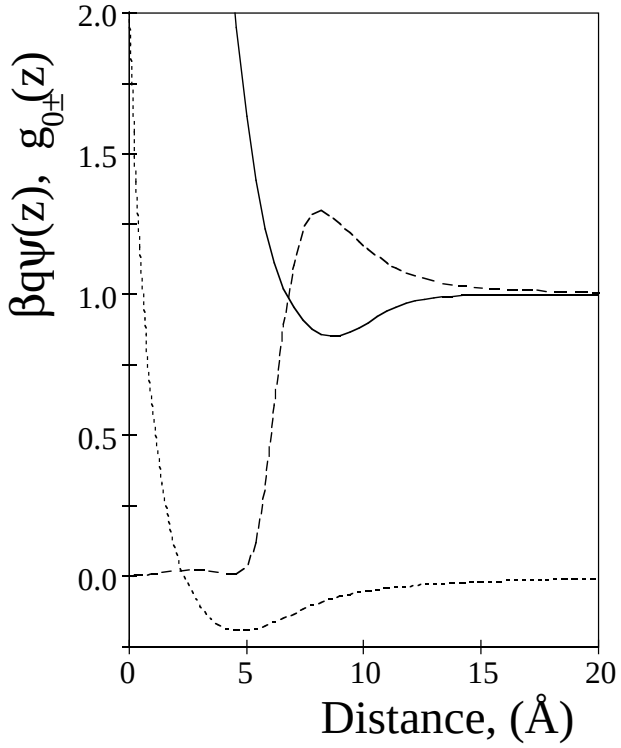

FIG. 8: The mean electrostatic potential $\beta q\psi(z)$, dotted curve, and the counter- and co-ion distributions $g_{0\pm}(z)$, solid and dashed curves, respectively, for the 0.1M divalent electrolyte with $e/\sigma = 75\text{Å}^2$.

The modified Poisson-Boltzmann theory was perhaps the first to predict charge reversal, where it was seen in a primitive model electrolyte, (monovalent coions, divalent counterions), at 0.15M[292]. (The authors were careful to distinguish this surface-induced inversion of the ion profiles in the bulk monotonic regime from asymptotic oscillations present at higher concentrations.) The charge reversal, as evidenced by the inversion and the change in sign of the potential, were confirmed by simulations[246]. Similar behaviour was also seen in a 0.5M 2:2 electrolyte, which is very near the bulk monotonic-oscillatory transition, in Monte Carlo simulations by Torrie and Valleau[246], in the singlet mean spherical approximation by Feller and McQuarrie[146], and in density functional approaches by Mier-y-Teran et al.[233] and by Patra and Gosh[154]. Ennis[293] has carried out an extensive study of the effective surface charge by fitting the asymptote to inhomogeneous hypernetted chain data, (in contrast to the singlet approach implemented here), and has systematically explored the reversal of the surface charge. That approximation has also shown charge reversal in a 2:1 primitive model electrolyte[294]. It appears that charge reversal occurs more readily in mixed valence (divalent counterions) than in symmetric electrolytes. Finally, charge reversal has also been seen in singlet hypernetted chain calculations for a *molecular* aqueous double layer[5,295]. The solvent-induced fast screening and over-compensation of the surface charge in the 1M monovalent electrolyte appears sensitive to the relative sizes of the solvent, counterions, and coions. The disparate ion diameters and consequent differential solvation doubtless quantitatively affect the point of zero charge. More generally, the values of the effective surface charge given above for the primitive model will be altered by a molecular solvent because they are a surface-sensitive property, although the asymptotic functional form will remain the same.

The agreement between the various approximations in Figs 5-7 suggests that the effective surface charge data are fundamentally correct and even quantitatively accurate for the primitive model. That the extended Poisson-Boltzmann approximation agrees with the hypernetted chain based theories shows it to be soundly based. Furthermore, since the former neglects ion-size, one concludes that the dominant contribution to the departure from the Poisson-Boltzmann approximation comes from the electrostatic correlations of the ions. In the context of the interactions between charged surfaces due to overlapping electric double layers, ion correlations add an attractive screened van der Waals component to the mean-field Poisson-Boltzmann repulsion[193,194]. Hence in order to describe double layer force measurements with Poisson-Boltzmann theory, one needs to fit a smaller than actual surface charge, which gives a lower repulsion and effectively accounts for the otherwise neglected electrostatic fluctuations. This is precisely what is shown in the figures, where the effective surface charge density lies below the actual surface charge density.

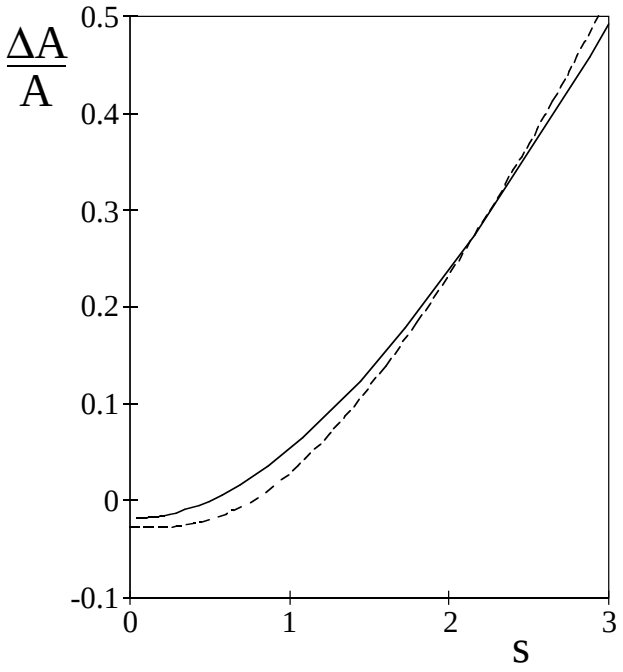

FIG. 9: The relative change in the area per unit surface charge, $\sigma/\tilde{\sigma} - 1$, at low surface charge densities in the 0.1M electrolyte.

Paradoxically, the hypernetted chain data in Fig. 9 appear to confirm the prediction made some time ago by Attard et al.[194] that at very low surface charge densities the fitted surface charge actually becomes greater than the actual surface charge. Those authors rationalised this behaviour by arguing that ions are effectively repelled from an inert wall due to attractive correlations with ions in the bulk electrolyte (the Onsager-Samaris effect). At low surface charge densities this depletion of the electrolyte near the surface becomes important, and results in less screening of the surface charge by the double layer than is predicted by Poisson-Boltzmann theory, which gives rise to an effective surface charge that is greater than the actual surface charge. This effect was seen in every one of the six electrolytes analysed in Figs 5–7. In practice this effect may be difficult to measure since it is relatively small and it occurs at extremely low surface charge densities.

An alternative analytic approximation for the effective surface charge may be developed on the basis of the self-consistent Debye-Hückel approach of §IC1, as applied to the double layer. Using the formally exact asymptote for the ion profiles, Eq. (68), for all distances from the wall, and using the electroneutrality condition, one obtains for ions all with the same diameter d

$$\tilde{\sigma} = \sigma \frac{\kappa^2}{\kappa_D^2}(1 + \kappa d)e^{-\kappa d}, \tag{279}$$

from which the linear nature of the approximation is evident. At low concentrations the effective surface charge is less than the actual surface charge. A non-linear version can be derived by applying the asymptote to the potential of mean force for all distances. For the restricted primitive model the effective surface charge satisfies

$$\frac{4\pi\beta q\sigma}{\epsilon\kappa_D} = \kappa_D \int_0^\infty \sinh\left[\frac{4\pi\beta q\tilde{\sigma}e^{\kappa d}}{\epsilon\kappa(1+\kappa d)}e^{-\kappa z}\right]\, dz. \tag{280}$$

This predicts that the effective surface charge will appear to saturate at high surface charge densities, (more precisely it will increase logarithmically), but it doesn't turn over as is predicted by the hypernetted chain data. The linear result gives the tangent as $\sigma \to 0$. This analytic result is compared to the hypernetted chain data in Figs 10. For the monovalent data it appears to give the primary departure correctly, but as the surface charge increases it underestimates difference between the actual surface charge density and the effective surface charge density. This is a consequence of the hypernetted chain data beginning to attain its maximum. In the divalent case the analytic approximation performs poorly, and does not appear to have even the correct limiting tangent.

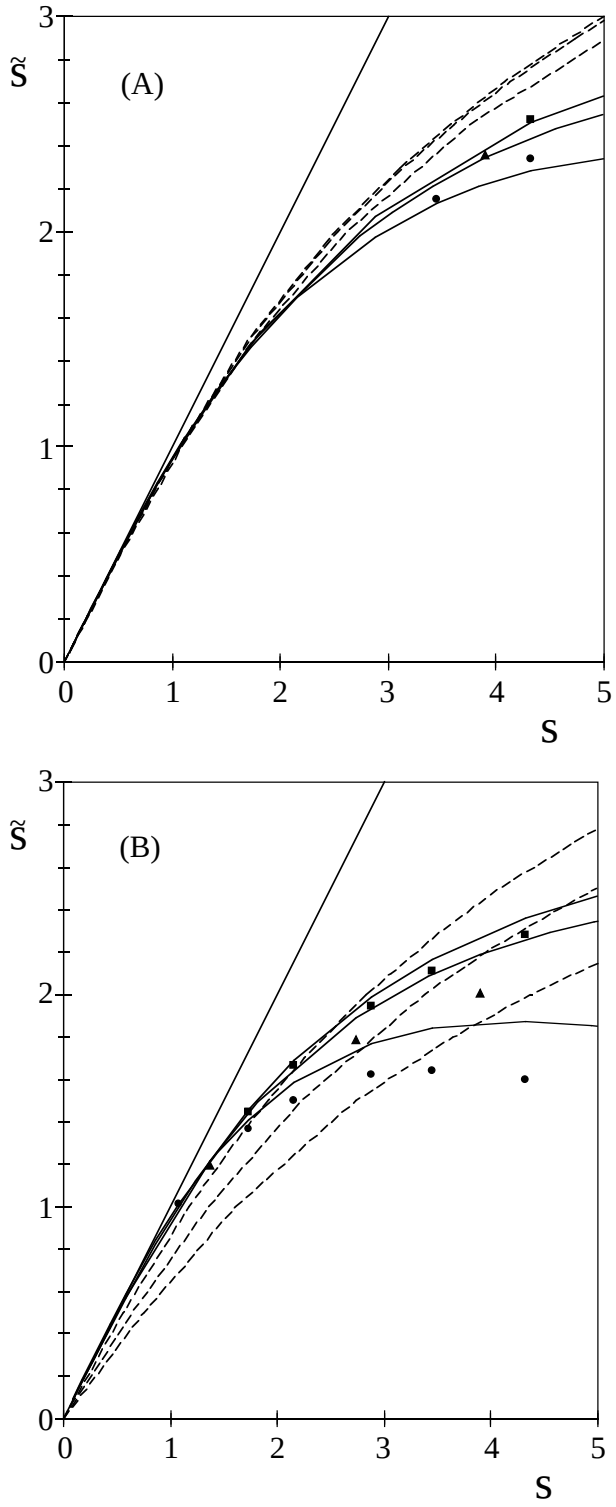

FIG. 10: The effective surface charge density for, from bottom to top, 0.1, 0.01, and 0.001M electrolyte, (other parameters as in Fig. 5). The data represents the singlet hypernetted chain approximation with (symbols) and without (solid lines) the first bridge diagram, the dashed lines are the non-linear self-consistent Debye-Hückel approximation, Eq. (280), and the straight line is a guide to the eye. **A.** Monovalent electrolyte. **B.** Divalent electrolyte.

B. Interacting double layers

This section presents results for the double layer interaction of two planar walls. The primary quantity of interest is the net pressure, since this, in balance with the van der Waals attraction, determines whether charged particles in electrolyte flocculate or remain dispersed, and in addition it may be directly measured with molecular resolution. The net pressure is a rather sensitive property of overlapping double layers, and it provides a good test of the various approximations. Density functional theories for the pressure between planar walls have already been favourably compared to the simulation results for divalent electrolyte[235,241]. Here the two singlet hypernetted chain methods, the dumb-bell and the wall-wall, will be compared with inhomogeneous hypernetted chain and simulation data. Computational methods for the last three approximations have been given in the literature[84,189,260], and an algorithm for the planar dumb-bell results presented here is now described.

The singlet Ornstein-Zernike equation for a planar dumb-bell, §IID3, was solved with the hypernetted chain closure without bridge diagrams. As usual the solute-ion total correlation functions were iterated using a simple Picard method with mixing. The Ornstein-Zernike convolution integral was evaluated by fast Fourier transform, using the transform of the bulk hypernetted chain short-ranged direct correlation function. The wall contributions to this integral were evaluated at the start of the program and stored. (The walls were of infinite thickness, and the limits discussed in §IID3 were utilised.) The hypernetted chain closure requires the mean electrostatic potential, and the current iterate of this was evaluated by the robust algorithm of Badiali et al.[143,144], modified for the present geometry, and with a few other changes. First, and probably of minor importance, the basic quantity $\psi''(z;t) - \kappa_D^2\psi(z;t)$ was replaced by $\psi''(z;t) - \kappa^2\psi(z;t)$, with the actual decay length obtained from the bulk electrolyte, and Eq. (68) being used. Second, the integration constant needed by the algorithm was the mid-plane potential, $\psi_0(t)$, (since the integrals began at the mid-plane). The mid-plane potential cannot arbitrarily be set to zero, and its actual value was determined from negative feedback on the electroneutrality condition,

$$\psi_0^{(n+1)}(t) = \psi_0^{(n)}(t) + \frac{\sigma - \sigma^{(n)}}{q\Gamma^{(n)}}, \tag{281}$$

where $\sigma^{(n)}$ is the charge density and $\Gamma^{(n)}$ is the total number density in the double layer on the n-th iteration. This particular choice for the gain ensures that electroneutrality will be satisfied by the next iterate of the density profiles to linear order in the closure. Mixing (≈ 0.1) of old and new iterates was performed on the density profiles, but not on the potential except at large separations. Experience showed this procedure in combination with the algorithm of Badiali et al.[143,144] to be quite robust, and it was confirmed that $\psi(0;t) \to 0, \;\; t \to \infty$. In the present calculations some 2^{13} grid points were used at a spacing of between 0.01 and 0.1Å, depending upon the concentration. Once electroneutrality was satisfied to 1 part in 10^7, the dumb-bell–ion short-ranged direct correlation functions were evaluated, Eq. (206), and used in conjunction with the results for the isolated wall to evaluate the interaction free energy, Eq. (249). The net pressure was obtained by first order finite difference of this, and also from the contact theorem, Eq. (213). Whereas the former went smoothly to zero at large separations, the cancellation of various terms required in the latter gave rise to numerical errors at large separations. This appears to be related to the fact that the contact values in the singlet hypernetted chain approximation are related to the compressibility of the bulk electrolyte, and hence one should really subtract this quantity rather than the osmotic pressure. In the results shown below, the net pressure from the contact pathway equals the calculated pressure less the pressure calculated at a separation beyond those shown.

1. *Monovalent electrolyte*

Figure 11 shows the pressure between two walls with one charge every 250Å^2 in a 0.1M monovalent restricted primitive model electrolyte. The inhomogeneous hypernetted chain results are from Ref.[212] and are the benchmarks against which the simpler singlet results are to be judged. The inhomogeneous approach has been compared against simulations for the counterions only double layer[207], and for symmetric electrolytes[157,214,260]. In all cases the agreement has been very good, and in the absence of simulation data one may take the results of the inhomogeneous calculations to be exact. (The exception is the large separation regime, where both simulations and inhomogeneous integral equations become problematic because one requires the precise cancellation of several terms in order to obtain the net pressure.)

In this particular example the non-linear Poisson-Boltzmann theory remains relatively close to the accurate results, but it does overestimate the repulsion. This is due to the neglect of correlations in that approximation, and is consistent with the data in Fig 7, where in this regime the fitted surface charge is larger than the actual surface charge, (see also figs 3 and 4 above). The singlet wall-wall hypernetted chain approximations bracket the inhomogeneous

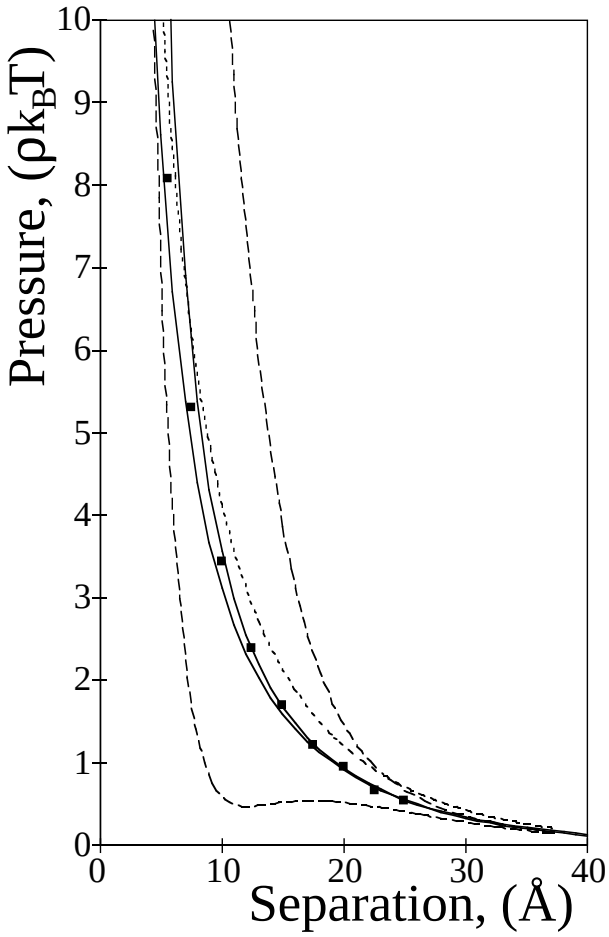

FIG. 11: The net pressure between planar walls with an area per unit charge of 250Å^2 in 0.1M monovalent binary symmetric electrolyte (T = 298K, ϵ = 78.5, d = 4.25Å). The symbols represent inhomogeneous hypernetted chain results[213], and the dotted curve is the non-linear Poisson-Boltzmann prediction. The pair of dashed curves are the singlet wall-wall hypernetted chain approximation[84] (the lower curve is the bare hypernetted chain approximation, and the upper curve includes the first bridge diagram). The pair of solid curves is the dumb-bell hypernetted chain approximation, (the lower curve utilises the contact theorem, and the upper curve comes from differentiating the interaction free energy). The separation here and in the remaining figures is the width of the region available to the centers of the ions; the walls may be taken to be an ion diameter further apart. The pressure is normalised by the kinetic pressure of the bulk electrolyte.

results. The bare hypernetted chain approximation overestimates the attractive component due to ion correlations; this deficiency occurs quite regularly, and will be seen in a number of the figures below. (The extended Poisson-Boltzmann approximation predicts an even greater attractive contribution, and again this is a general failing of that approximation[194].) The addition of the first bridge diagram over-corrects the hypernetted chain, and it predicts too high a repulsion at small separations. At large separations both wall-wall approximations appear accurate. The dumb-bell hypernetted chain approximation is clearly the best of those compared in the figure; the contact route and the free energy route are in good agreement with each other and with the inhomogeneous hypernetted chain calculations.

The reason for the superior performance of the dumb-bell compared to the wall-wall hypernetted chain approximation most likely lies in the fact that the two walls are treated as individual solutes in the latter, but as a single solute in the former. The diagrams with $n+1$ field points in the wall-wall approach roughly correspond to diagrams with only n field points in the dumb-bell approach because both root points are solutes in the former, whereas one is a solute and one is an ion in the latter. Similarly, the inhomogeneous approach outperforms the singlet approaches because both root points represent ions, and hence the equivalent diagrams only require $n-1$ field points. Further, since the solute-ion potential is more problematic than the ion-ion potential, it is an advantage to treat it via the formally exact equations for the density profiles, as in the inhomogeneous approach, rather than via the approximate

closure as in the singlet approaches.

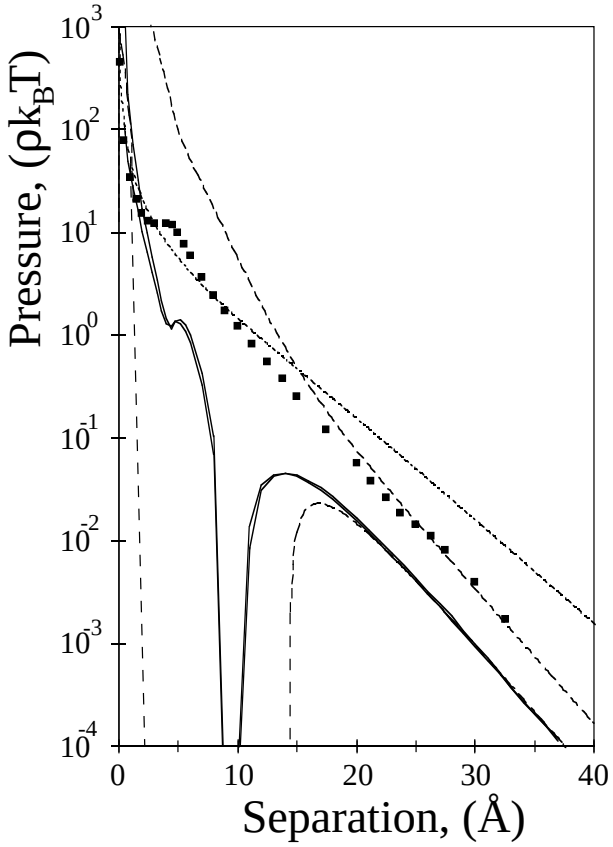

FIG. 12: The net pressure for $|e/\sigma| = 60\text{Å}^2$ in a 0.5M monovalent electrolyte with $d = 4.6$Å. The remaining parameters are as in Fig. 11, and so are the various curves, except that the inhomogeneous hypernetted chain data is taken from Ref.[212].

Figure 12 shows the pressure at a higher concentration (0.5M) and surface charge density ($|e/\sigma| = 60\text{Å}^2$). Again the bare wall-wall hypernetted chain approximation predicts an attractive regime that is not present in the inhomogeneous data[212], but which in this case also appears in the dumb-bell approach. (The two dumb-bell routes to the pressure are almost coincident.) When the first bridge diagram is added to the wall-wall hypernetted chain approximation the attraction disappears, but at small separations the bridge diagram once again over-corrects the bare hypernetted chain approximation and gives too large a repulsion. The bridge diagrams fail to give the hump shown by the inhomogeneous calculations at a separation of one diameter ($h \approx d = 4.6$Å), but this is certainly present in the dumb-bell calculations, even if the magnitude is underestimated. This peak is related to the (structural) free energy minimum that occurs when two integral layers of ions are confined between the surfaces. At large separations it is evident that the non-linear Poisson-Boltzmann approximation does not have the correct decay length. The Debye length is here $\kappa_D^{-1} = 4.2$Å, whereas the actual decay length is $\kappa^{-1} = 3.3$Å. Evidently all the approximations based upon the hypernetted chain closure have the same decay rate, but it requires the inclusion of the first bridge diagram to obtain quantitative agreement with the inhomogeneous approach in the asymptotic regime. That is, the amplitude of the decay, which depends upon the effective surface charge, is only given accurately when the first bridge diagram is included in the wall-wall approach. The bare hypernetted chain approximation for the effective surface charge would likely be inaccurate at this concentration; it is approximately 10% higher than is predicted by including the first bridge diagram at this actual surface charge density in the 0.1M monovalent electrolyte of Fig. 7.

As the separation goes to zero, the pressure becomes increasingly repulsive, as is evident in Figs 11 and 12. In fact the exact limiting result is[84]

$$p(h) \sim \frac{-2\sigma k_B T}{q_c h} + \mathcal{O}(h^0), \quad h \to 0, \tag{282}$$

where q_c is the charge on the counterions (assuming a single species), and h is the width of the region accessible to the ion centers. This result arises from the electroneutrality condition and the contact theorem. At small separations

only the counterions necessary to balance the surface charge remain in the double layer, (or at least the contribution from those beyond these is bounded, see below). One may take the density profile of the counterions to be constant, (equivalent to doing a Taylor expansion and keeping only the zeroth term because the separation and hence the distance is going to zero), and hence the contact density is $\rho(0;h) \sim -2\sigma/q_c h + \mathcal{O}(h^0), \quad h \to 0$. Both remaining contributions to the net pressure, the wall-wall electrostatic interaction and the bulk osmotic pressure, are independent of separation, which gives the above result. All the numerical approaches except for the wall-wall hypernetted chain approximation appear to obey the limiting result; one can show analytically that the Poisson-Boltzmann approximation satisfies this limit for the counterions-only double layer.

This limiting result for the double layer is an extension of the corresponding result for uncharged walls[264,296,297]. For the restricted primitive model it is

$$\frac{p(h)}{\rho k_B T} \sim \gamma_\pm - \phi + \mathcal{O}(h), \quad h \to 0, \tag{283}$$

where ϕ and $\gamma_\pm$ are the osmotic coefficient and the activity of the bulk electrolyte, respectively, and $\rho = \rho_+ + \rho_-$ is its total number density. This result derives from the fact that the chemical potential, which is fixed, is comprised of an ideal part and an excess part. At small separations the excess part is just that of a two-dimensional fluid (plus terms of order h), and vanishes as the two-dimensional number density vanishes, (because the three-dimensional number density remains finite). Hence the contact density equals the fugacity, (plus terms of order h) and the net pressure is simply this less that of the bulk electrolyte. Hence the only difference between this result and that of the double layer is the two-dimensional number density, which in the latter case is fixed by the surface charge on the walls.

The divergence of the pressure at small separations, Eq. (282), is shown in the inset of Fig. 13 for the case of 1M electrolyte at an area per unit surface charge of 85Å^2. The non-linear Poisson-Boltzmann approximation, the inhomogeneous hypernetted chain approximation, and the dumb-bell hypernetted chain approximation for the contact pressure all quantitatively satisfy this result. (The neglected constant term in Eq. (282) becomes irrelevant on the logarithmic plot at small separations.) In contrast, the wall-wall hypernetted chain approximation does not diverge as $h \to 0$, but appears to have a finite contact value, and when the first bridge diagram is added this value actually decreases. The pressure via the free energy route in the dumb-bell hypernetted chain approximation does diverge, but apparently somewhat faster than the limiting law.

More broadly, in Fig. 13 one sees once again that the wall-wall hypernetted chain approximation shows attractive double layer forces over much of the regime, and in this case the attractions persists over a limited range even when the first bridge diagram is included. (The attractive regime is signified on the logarithmic plot by a break in the curve, which is cut nearly perpendicularly by the abscissa.) The inhomogeneous data[212] does not show this small-separation attraction, but it does hint at a plateau at about a diameter separation, presumably due to the packing of two layers of ions. The dumb-bell hypernetted chain approximation also shows this broad plateau, but underestimates its magnitude, as in Fig. 12. The two thermodynamic pathways to the pressure in the dumbell hypernetted chain approximation are mutually consistent.

At larger separations once more it is apparent that the non-linear Poisson-Boltzmann approximation has the wrong decay length, but what is interesting in this case is that the pressure is actually oscillatory in the asymptotic regime. This is manifest by the turn down in the wall-wall hypernetted chain data that include bridge diagrams, and as discussed in §II, the oscillations mimic those in the ion distribution functions of the bulk electrolyte. The bridge approximation is here quite accurate, and it gives 33Å for the period of the oscillations, and 1.8Å for the decay length. The dumb-bell hypernetted chain approximation shows an attraction beyond about 10Å, presumably due to asymptotic oscillations. On balance this approximation probably has the wrong phase, and the first asymptotic attraction likely begins at about 15Å. There is perhaps a hint of this in the extreme inhomogeneous hypernetted chain data, but realistically it is not possible to extend that method into the asymptotic regime. At large separations one has problems in accurately calculating the net pressure because numerical errors mask the exact cancellation that is required. The situation is even worse for simulations, and at large separations the best approaches are the wall-wall hypernetted chain approximation with the first bridge diagram, or equivalently the asymptotic expressions using parameters calculated for the bulk electrolyte and for the isolated wall, again by the hypernetted chain approximation with the first bridge diagram.

In summary, the net double layer pressure for monovalent aqueous electrolytes shows a repulsion that increases as h^{-1} as the separation goes to zero, and a plateau at about one diameter separation due to the layering of ions. Attractions of the van der Waals type at small and intermediate separations are not present in the inhomogeneous data, but they are predicted by the singlet approaches. It is likely that such correlation attractions really do occur in monovalent aqueous electrolytes, but at higher surface charges than is indicated by the singlet approaches. At larger separations the double layer force is either monotonically repulsive or oscillatory, depending upon the concentration of the bulk electrolyte. Of the approximate schemes tested, the non-linear Poisson-Boltzmann approximation performs well at small separations, but has the wrong magnitude at intermediate concentrations, and the wrong decay length

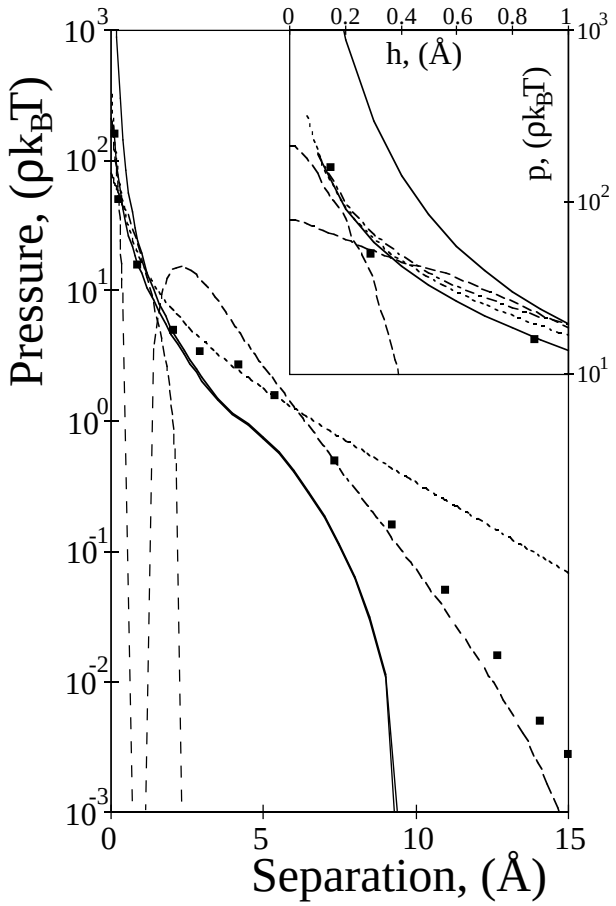

FIG. 13: The net pressure for $|e/\sigma| = 85\text{Å}^2$ in a 1M monovalent electrolyte. The remaining parameters and curves are as in Fig. 11, and the symbols are inhomogeneous data from Ref.[212]. **Inset**. The dot-dashed curve shows the divergence of the pressure at small separations, Eq. (282), and almost coincident is the non-linear Poisson-Boltzmann approximation (dotted curve). The wall-wall hypernetted chain approximations (dashed curves) appear to have finite values at contact, (the lower of the two at contact is the one with the first bridge diagram), whereas the dumbell approximations (solid curves) appear to diverge, (the contact route is almost coincident with the limiting equation).

at high concentrations. The wall-wall hypernetted chain approximation is certainly the best in the asymptotic regime, particularly when the first bridge diagram is included, but it does not show the correct divergence at small separations, and it predicts attractions rather too readily. The dumb-bell hypernetted chain approximation is remarkably self-consistent, it is the only approximate singlet theory to show the correct structure in the pressure at high concentrations, and it is quantitatively accurate at concentrations of 0.1M.

2. Divalent electrolyte

In general divalent aqueous electrolytes show attractive double layer forces at lower surface charge densities than do monovalent aqueous electrolytes. This may be seen in Fig. 14, which is for a 0.1655M divalent electrolyte with one surface charge every 176Å^2. The Monte Carlo data[260] at small separations have just begun to turn repulsive and one sees the limiting law, Eq. (282), begin to have an affect on the various approximations. The simulations show an attractive regime for separations between 5–15Å. The dumb-bell hypernetted chain approximation, does not agree with the simulation data, and instead of an attraction both pathways predict a positive plateau in the pressure. The singlet wall-wall hypernetted chain data show an attractive regime for separations less than about 10Å. As in the case of monovalents, including the first bridge diagram decreases the attraction predicted by the wall-wall hypernetted chain approximation, and in this case brings that theory into almost quantitative agreement with the simulation data. This bulk concentration corresponds to the monotonic regime, ($\kappa^{-1} = 3.85\text{Å}$, compared to $\kappa_D^{-1} = 3.74\text{Å}$), and hence

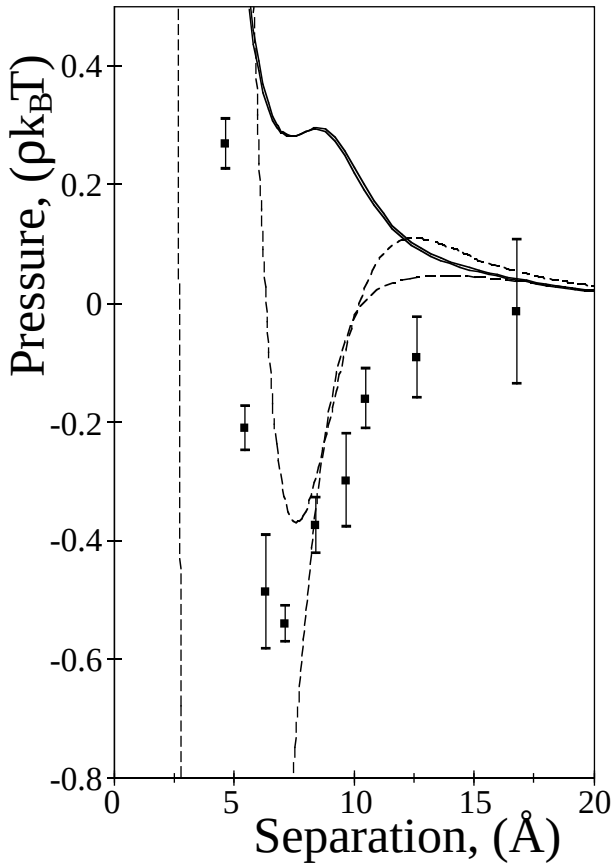

FIG. 14: The net pressure for $|e/\sigma| = 176\text{Å}^2$ in a 0.1655M divalent electrolyte, ($T = 298$K, $\epsilon = 78.5$, $d = 4.2$Å). The symbols represent Monte Carlo data[260], the dashed lines are wall-wall hypernetted chain results[84], (The bare approximation shows more of an attraction than does the one that includes the first bridge diagram), and the nearly coincident solid curves result from the two pathways to the pressure in the dumb-bell hypernetted chain approximation.

one knows that the attraction shown in Fig. 14 must be finite in extent, and that the pressure at large separations must be monotonic repulsive, as is predicted by all of the hypernetted chain based theories. (The simulations evidently have difficulties in the large separation regime.) The attraction shown in the figure must therefore be of the van der Waals type, due to the fluctuations of the electrolyte confined between the walls.

The earliest prediction that the double layer force between identically charged surfaces could be attractive was made by Oosawa[298,299]. He made an approximate estimate of the influence of ion correlations and concluded that at high enough couplings, which in practice meant divalent aqueous electrolytes, the electrostatic fluctuations could give an attractive component that dominated the mean-field double layer repulsion. Oosawa clearly recognized that these attractions were properly considered as part of the van der Waals force. Patey[165] found attractions between highly charged macroions using the singlet hypernetted chain approximation, and they were also found for divalent counterions between charged planar walls by Guldbrand et al.[256] using Monte Carlo simulation, and by Kjellander and Marčelja[207] using the inhomogeneous hypernetted chain approximation. These numerical results were all rather sophisticated, but what became obscured was the physical interpretation that related the attraction to the van der Waals force. Although Guldbrand et al.[256] made connections to the work of Oosawa[298,299], it was probably not until Attard et al.[193,194] and Podgornik and Žekš[195] extended the Poisson-Boltzmann approximation to analyse the effects of correlations between ions in the double layer that the van der Waals origin of the attractions was once more explicit. Seen in this light attractive double layer forces between similarly charged surfaces can no longer be regarded as mysterious; it has always been known that the van der Waals attraction dominates the double layer repulsion at small separations. The strength of the attraction increases with ion coupling, principally characterised by valence and concentration, but also dependent in the general case upon the dielectric constant and the temperature. Correlation effects are also important at higher surface charge densities because more ions are confined between the surfaces.

The case of zero surface charge, Fig. 15, is interesting because here there is no mean field interaction, and the pressure is due solely to the correlated electrostatic fluctuations of the ions. In this case the pressure is monotonic

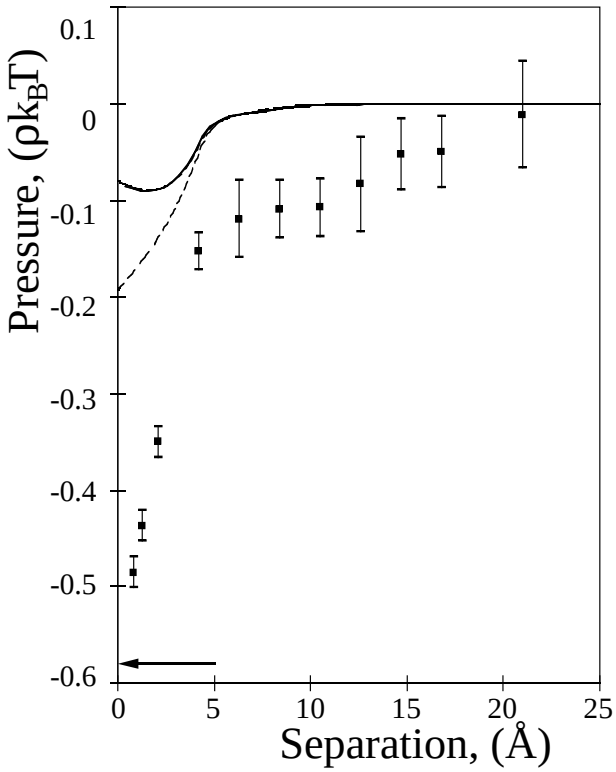

FIG. 15: The net pressure between uncharged walls in a 0.971M divalent electrolyte. The remaining parameters and curves are as in Fig. 14. The bare wall-wall hypernetted chain approximation is coincident with the dumb-bell results, and including the first bridge diagram makes the pressure more attractive at contact. The arrow denotes the limiting result, Eq.(283).

attractive and its van der Waals origin is unmistakable. Because there is no net charge on the surfaces in Fig. 15, one expects that the net pressure will go like[194,300–302]

$$p^{\rm net} \sim -\alpha^2 e^{-2\kappa h}, \quad h \to \infty. \tag{284}$$

Such a fast decay is not evident in the simulation data, which is somewhat surprising because the separations are already greater than several decay lengths (the bulk electrolyte has a decay length of 2.28Å, and a period of oscillation equal to 10.4Å). The simulations by Bratko and Henderson[265] are in good agreement with the data of Valleau et al.[260] shown in the figure, and exhibit a similar range. In Fig. 15 the simulation data is tending to the limiting law, Eq. (283), but none of the hypernetted chain based singlet approximations are particularly accurate here. The closest is the wall-wall approximation with bridge diagrams, and considerably less attractive at contact are the dumb-bell and the bare wall-wall, which are coincident. Note that the wall-wall hypernetted chain results for this divalent 0.971M electrolyte here and in the remaining figures are more accurate than those given in Ref.[84]. Also, the cycle of calculating wall-ion total correlation functions and bridge functions was repeated up to five times in order to obtain self-consistency.

Fig. 16 shows the pressure in the 0.971M divalent electrolyte at the comparatively low surface charge density of 1 charge every 1780Å^2. The minimum in the simulation data at about 2.5Å separation is present in all the singlet hypernetted chain approximations, albeit underestimated in magnitude. Including the first bridge diagram certainly improves the wall-wall approach in estimating the value of this maximal attraction. The simulation data has just begun to turn repulsive at small separations, in accord with the limiting divergence, Eq. (282). As in Fig. (13), the wall-wall hypernetted chain results appear to have a finite contact value, whereas the dumb-bell approximation shows the correct divergence. Once again the two routes to the pressure in the dumb-bell approximation are in good agreement. As in Fig. 15 for neutral walls, the simulated attraction appears strangely long ranged, particularly in comparison to the hypernetted chain approximations, which on this scale are indistinguishable from zero by about 10Å separation.

At the higher surface charge density of 176Å^2, Fig. 17, the small separation repulsion is more evident, and the position of the greatest attraction is shifted to a larger separation of about 5Å. The wall-wall hypernetted chain approximations are in quite good agreement with each other and with the dumb-bell approximation, where the two thermodynamic pathways are coincident. The approximations may be described as quantitatively reliable here,

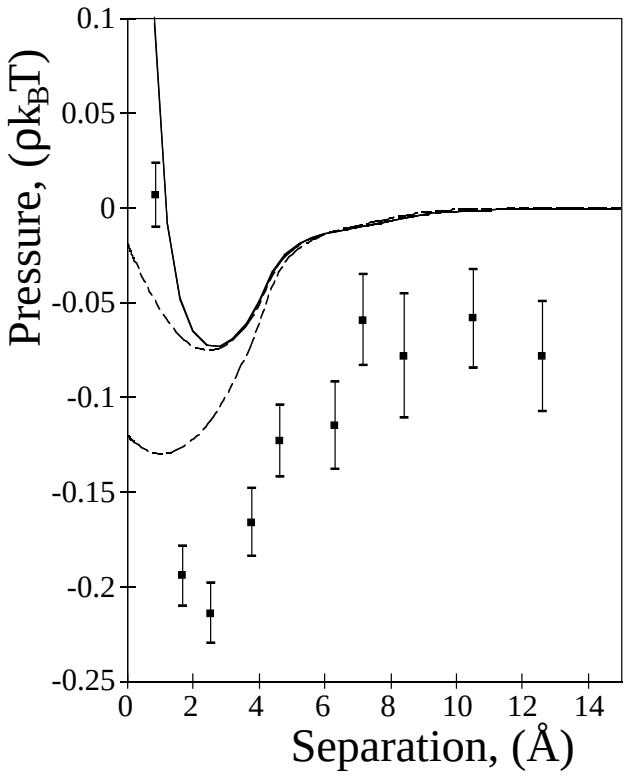

FIG. 16: The net pressure for $|e/\sigma| = 1780\text{Å}^2$, other parameters and curves as in Fig. 14. The wall-wall hypernetted chain approximation is made more attractive at small separations by the inclusion of the first bridge diagram.

and they are certainly relatively more accurate in this case than in the same electrolyte at a lower surface charge density, Fig. 16. Compared to Fig. 14, which has the same surface charge density but lower concentration, (giving a dimensionless surface charge 2.4 times larger), in the present case the approximations are much more accurate. Indeed in Fig. 17 the dumbell approximation almost passes through all of the simulation data, but in Fig. 14 it fails to predict any attractions. What is also evident in all the approximations in Fig. 17 is the secondary maximum at about 8Å separation, and which may just be made out in the simulation data. It is possible that this represents the first discernible peak of the oscillations in the pressure that are predicted to dominate asymptotically because the bulk electrolyte is here in the oscillatory regime, (with a period of 10.4Å).

In the case of the highest surface charge density for which simulation data is available, (Fig. 18, $|e/\sigma| = 58.9\text{Å}^2$), it was not possible to obtain solutions to the dumb-bell hypernetted chain equations. The highest surface charge density at this concentration for which convergence could be obtained was 100Å^2, which suggests that it may be worthwhile to include the first dumb-bell–ion bridge diagram. It was however possible to solve the wall-wall hypernetted chain approximation with and without the bridge function, and the results are shown in the figure. (The bridge function and wall-ion total correlation functions were in this case iterated to self-consistency five times.) The inclusion of the first bridge diagram certainly improves the bare hypernetted chain approximation, and it may be seen that the depth of the attraction is quite well estimated by that theory. Also evident is the small separation repulsion, and the secondary maximum at about 7Å separation, which is relatively accurately given by both wall-wall hypernetted chain approximations.

In Fig. 19 the pressure given by density functional theories is compared to simulations[260] and to the wall-wall hypernetted chain approximation with the first bridge diagram[84]. The non-local density functional theory of Tang et al.[235] uses the Carnahan-Starling hard-sphere free energy, evaluated at an effective density using a weighting due to Tarazona[232], and the mean spherical approximation for a residual ion-ion direct correlation function of the bulk electrolyte. Patra and Ghosh[241] use the mean spherical approximation for the hard-sphere and residual electrostatic ion-ion direct correlation function evaluated at an effective bulk density, obtained using a weighting due to Denton and Ashcroft[237]. The two approaches are similar in spirit, and it can be seen that they are of similar accuracy for the net double layer pressure. The approach of Tang et al.[235] possibly exaggerates the amplitude of the oscillations, but there is little to choose between the two recipes. The accuracy of the density functional theories is comparable to

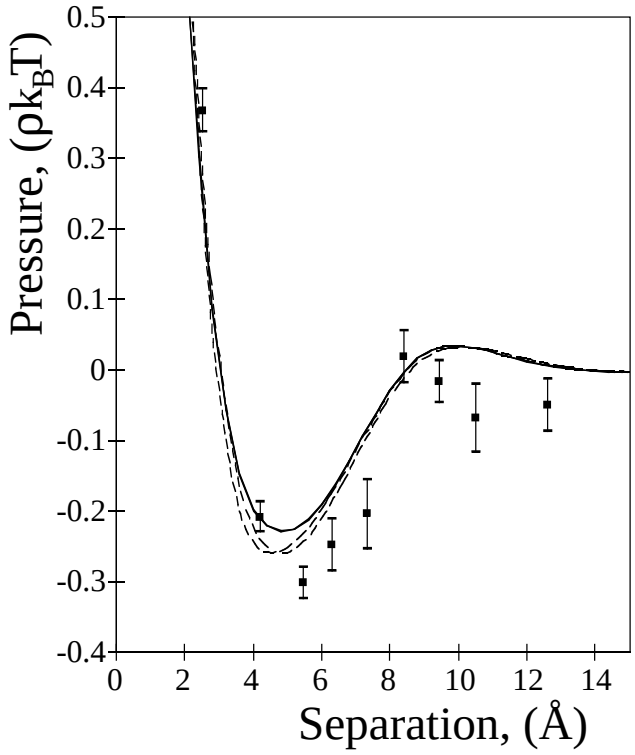

FIG. 17: The net pressure for $|e/\sigma| = 176\text{Å}^2$, other parameters and curves as in Fig. 14.

the wall-wall hypernetted chain approximation with the first bridge diagram. For the highest surface charge density (Fig. 19b), the singlet approach predicts a repulsion that increases too rapidly at the smallest separations, whereas the density functional theories pass through the simulation datum.

In summary, the electric double layer force in divalent aqueous electrolyte shows small separation attractions due to ion fluctuations of the van der Waals type. At still smaller separations the pressure between charged surfaces becomes large and repulsive, whereas neutral surfaces shows a finite adhesion in contact. The singlet hypernetted chain approximations appear relatively more accurate at higher surface charge densities and higher electrolyte concentrations, which is perhaps surprising. When structure is present in the double layer, the approximate theories appear capable of a quantitative description. At zero or low surface charge densities, the simulation data[260,265] appear to have a much longer range than one would have believed possible on the basis of the usual asymptotic notions.

V. BEYOND THE MINIMAL MODEL

This review has been concerned with the behaviour of electrolytes and the electric double layer, with particular emphasis on recent advances in theory that predict phenomena beyond the classical mean field notions. The treatment was deliberately fundamental in an attempt to elucidate the general principles that apply to the various occurrences of the double layer, and it avoided as much as possible the specific details that make each system unique. It seems appropriate in this section to restore the balance by discussing some of the elaborations of the basic model, and the modifications that they necessitate. Specifically, concentrated dispersions, more realistic models for the charged surface, dielectric images, and molecular solvents will be mentioned.

A. Concentrated dispersions

A large part of this review has been concerned with the interaction between particles due to the overlap of their double layers. This is an important topic because it is these forces that determine whether particles may approach, adhere, and fuse, and also the behaviour of colloidal dispersions (flocculation and sedimentation or flotation, rheology). Are results obtained for the double layer interaction between particles at infinite dilution applicable to dispersions of

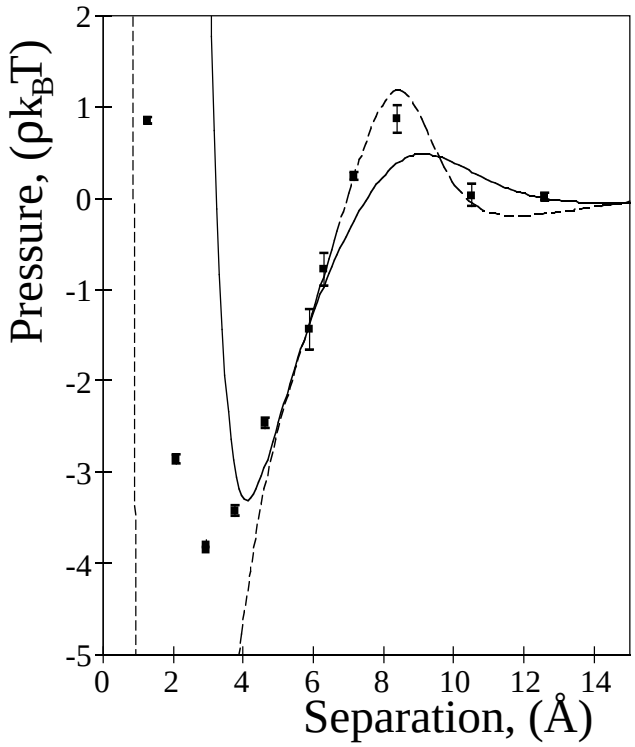

FIG. 18: The net pressure for $|e/\sigma| = 58.9\text{Å}^2$, other parameters as in Fig. 13. The symbols represent Monte Carlo data[260], the dashed curve is wall-wall hypernetted chain data, and the solid curve includes the first bridge diagram. In this case the dumb-bell hypernetted chain approximation did not converge.

particles at finite volume fractions? One might guess that when the size of the particles is large compared to their separation and the decay length, the results given above for the pair-wise double layer interaction will quantitatively hold. In the other extreme, the interactions between concentrated colloids small compared to the decay length is not pair-wise additive at larger separations, and one cannot apply the interactions calculated at infinite colloid dilution except in some qualitative sense. In these cases one needs to treat the multicomponent mixture explicitly.

There have been two approaches to this problem. In the cell model one imagines space to be tiled with an infinite number of cells that have the same shape as the colloidal particle, and one calculates the properties of the double layer within a cell, subject to appropriate boundary conditions. The concentration of the dispersion is set by the size of the cell, and the interaction between particles is determined from the electrolyte concentration at the cell boundary[131]. The cell model has been used for spherical macroions[131,171,242,282,283] and for cylinders[121,287,288]. The cell model is probably of limited reliability; there are obvious questions about the physical realisation of the tiling, and it appears to be inaccurate for the osmotic pressure of concentrated dispersions[282]. Probably preferable to the cell model are the integral equation methods for multicomponent mixtures. Here the colloid particle is just one of the components of the mixture, and it is treated on the same footing as the electrolyte ions. This is essentially the singlet approach, and the hypernetted chain approximation and variants have been used to study concentrated dispersions of charged spherical colloids[168–173].

One long running question that can be addressed in the context of the asymptotic analysis of this review concerns the decay length of the concentrated dispersion. Should one include the macroions and their counterions in addition to the electrolyte in the Debye length? On the basis of the results detailed above, one can say in the first place that the highly asymmetric electrolyte will have a unique decay length, but it will not be the Debye length. The macroions will appear in the formal expression for the decay length with an effective charge that depends upon the direct correlation functions of the dispersion. This effective charge is likely much reduced from the bare macroionic charge, which reduction may be interpreted as counterion binding, (which interpretation would be of limited value in the likely event of oscillatory correlations). For relatively dilute dispersions with low concentrations of added electrolyte, such that the correlations remain monotonic, the approximate formulae of §IVA for the effective surface charge may be useful in giving the amount of bound and free counterions. The latter, the macroions with reduced charge, and the electrolyte may then be used to calculate the decay length of the dispersion, Eq. (68).

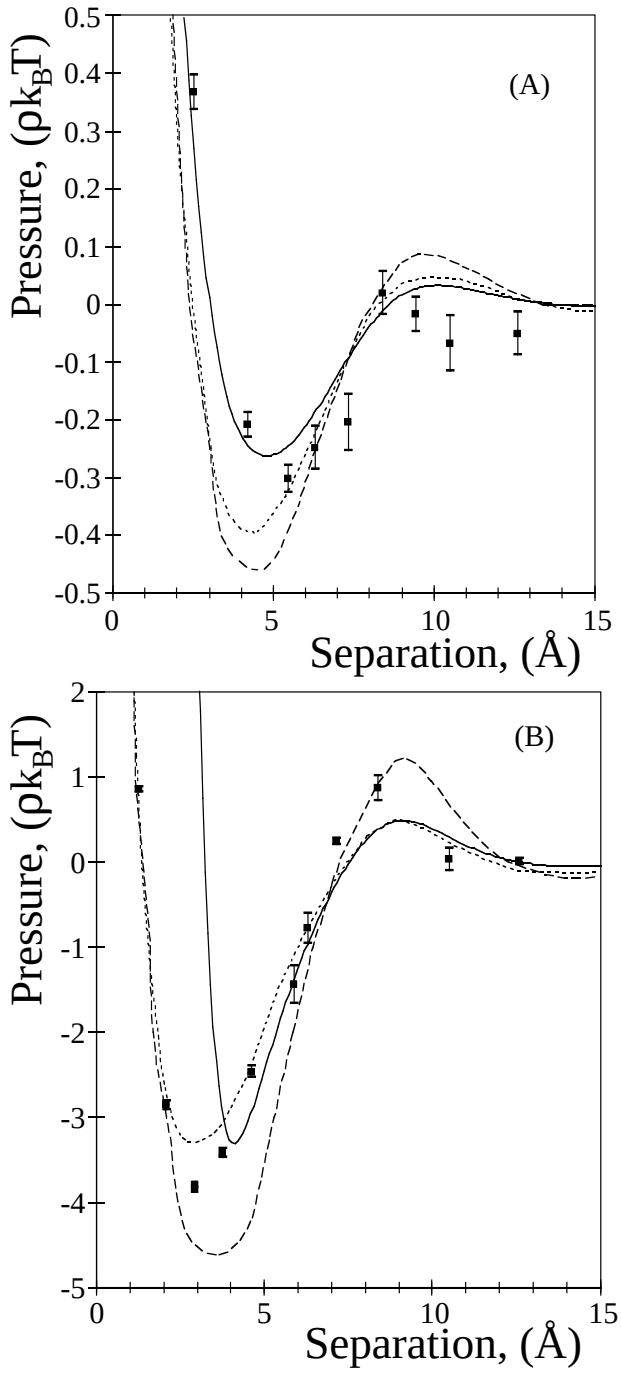

FIG. 19: The net pressure as a function of separation for the 0.971M divalent electrolyte. The symbols represent simulations[260], the solid curve is the wall-wall hypernetted chain approximation with the first bridge diagram[84], and the dashed and the dotted curves are density functional results of Tang et al.[235] and of Patra and Ghosh[241], respectively. **A.** $|e/\sigma| = 176\text{Å}^2$. **B.** $|e/\sigma| = 58.9\text{Å}^2$.

B. Discrete and regulated surface charges

The surface charge that gives rise to the electric double layer when a particle is immersed in an electrolyte arises either from dissociation of ionisable groups on the surface or from preferential adsorption of ions from the electrolyte. In both cases the charges are discrete, although for utilitarian reasons the double layer is almost always modelled with a uniform surface charge. For the case of fixed charges, one expects that the charges will not be seen as individuals at

distances large compared to their separation, so that discrete effects must decay at a rate at least in inverse proportion to their separation. In fact it is competition between the separation and the screening length that determines the rate of decay of discrete charge effects. For a periodic array of surface charges, the discrete contribution to the mean electrostatic potential goes like $\exp[-(G^2+\kappa^2)^{1/2}z]$, where the smallest reciprocal lattice vector is related to the mean spacing between the surface charges by $G = 2\pi/a$. (The uniform or smeared out contribution corresponds to $G = 0$, and will only vanish if the surfaces with discrete charges are overall electroneutral.) The decay length for discrete charge effects is determined by the smaller of the bulk electrolyte screening length and the separation between the surface charge groups, and hence discrete charge effects may be expected to be important at low electrolyte concentrations. The discrete contribution to the interaction between two surfaces can be attractive or repulsive depending upon their juxtaposition, and any disorder in the discrete charge lattice or distribution of charge about the lattice sites diminishes the effects of discreteness.

Richmond[303] analysed the interaction between net neutral surfaces with a periodic distribution of discrete charges on the basis of the linear Poisson-Boltzmann approximations, and found that the attraction due to perfectly misaligned lattices could be comparable to the van der Waals attraction for realistic parameters. Nelson and McQuarrie[304] also used the linear Poisson-Boltzmann approximation and explored the influence of discrete charges on the electrostatic potential near a membrane. Miklavic and co-workers[305] used both the linear and non-linear Poisson-Boltzmann approximations to discuss the interaction between surfaces, and pointed out that thermal averaging in the lateral direction favours misalignment and consequently gives an attractive contribution similar to that found by Richmond[303], and to that found between dipolar lattices with[306] and without[307] electrolyte. (As mentioned above discrete charge effects are minimised if the lattices are not perfect or if there is any smearing of charge in the unit cell.) The simulations of a wall embedded with a periodic array of fixed charges reported by van Megan and Snook[244,245] are vitiated by programming errors[2]. Zara et al.[258] performed simulations for counterions only confined between two planes bearing periodic distributions of discrete charges.

Kjellander and Marčelja[211] have used the inhomogeneous hypernetted chain approximation to obtain the double layer force between walls bearing *mobile* surface charges. Although the charges are discrete, the fact that they form a two-dimensional ionic fluid on the surface means that *on average* they have a uniform charge distribution, which probably accounts for the rather small discrete charge effect found in this model[211]. The model however is of interest in its own right, and has been elaborated upon by Marčelja[213] to include specific adsorption of ions from the electrolyte by means of a short-ranged adsorption potential. The density of adsorbed ions changes as the separation is changed, and the model represents a realistic development of the two extreme boundary conditions commonly used in double layer theory —constant surface charge or constant surface potential. The non-linear Poisson-Boltzmann equation can be solved in planar geometry in terms of elliptic functions for constant charge[308] and for charge regulation by ionisable surface groups[309], and it has been linearised and solved in cylindrical geometry in terms of Bessel functions for the case of charge regulation[104]. In this review attention has been focussed on the constant charge condition because it is the easiest to treat both analytically and numerically. However singlet hypernetted chain results have been presented for the constant surface potential case[4,161,162], and Spalla and Belloni[170] have used that approximation to treat macroions with short-ranged adsorption potentials, which is similar to the model later used by Marčelja[213] to mimic charge regulation.

The surface charge may not only be non-uniform and non-constant, but the surface itself may have variable curvature. Surface roughness becomes particularly important for self-assembled systems such as micelles, membranes, and lamellae, where the energetics of undulation, protrusion, and curvature can be a crucial consideration. For small curvatures, where the departure from planarity may be treated as a perturbation, the Poisson-Boltzmann approximation has been used to analyse the double layer contribution to the bending constants and curvature free energy of surfaces and membranes[310–315]. Goldstein et al.[316] found the electrostatic potential and free energy of isolated and interacting rough planar double layers in linearised Poisson-Boltzmann approximation using perturbative and iterative techniques. Blum[3] has generalised the contact theorem for the pressure to a rough electrode. The double layer interaction of a charged macrosphere and a *deformable* planar surface has been calculated self-consistently in linear Poisson-Boltzmann approximation[317].

Related to the possibility of surface roughness is the fact that even for a smooth surface not all ions may approach to within the same distance, due to their differing sizes or to their specific degree of hydration. In this review a single plane of closest approach was assumed since the additional complication does not appear to lead to any new principles. Nevertheless a realistic model for the double layer in the region close to the surface may need to account not only for the ion exclusion region, but also the location of adsorbed surface charges and changes in the solvent dielectric constant (see below). In colloid science the simple division into the diffuse layer and the Stern layer, (from which all ions are excluded), has been augmented with inner and outer Helmholtz planes, triple layers and other embellishments for the compact inner layer. (See Ref.[318] for a review of the traditional approaches to this region in the context of discrete surface charges.) A distribution of surface charge over a region of finite thickness that is available to the electrolyte ions is important in modelling biological membranes[319,320]. Surfaces with tethered

polyelectrolytes are perhaps the extreme example; these may constitute the surface charge, or they may neutralise it, and their conformation is influenced by any inter-penetrating electrolyte ions. The extent of the surface region about an isolated particle, and their interaction due to the combined effects of overlapping double layers and steric hindrance is of some practical importance[277–281,321,322].

In the context of the analysis of this review, any discreteness in the surface charge will not be evident at asymptotic separations, and the equations are formally unchanged. Obviously however, the effective surface charge depends upon the electrolyte in the vicinity of the surface and its quantitative value will change in the case of discrete charges, (where it will likely *decrease*), charge thickness, and surface roughness. Asymptotically the double layer properties remain formally unchanged; in particular charge regulation becomes a second order effect at large separations. The van der Waals attraction at short separations ought be enhanced by mobile surface charges, (because of the extra correlations), and also in the case of fixed discrete charges, (because of the additional ions near the surface due to the more intense fields associated with each surface charge).

C. Dielectric images

One of the major complications that was ignored in the minimal model of the electric double layer was that in general the charged particles have a different dielectric constant to the solvent, and at the continuum level this gives rise to image charges. These fictitious image charges represent the polarisation responses of the media, and they ensure the continuity of the displacement electric field across the dielectric discontinuity at the boundary. When the dielectric constant of the particle is lower than that of the ions, which is the usual case for particles in aqueous electrolytes, the ions are repelled from the interface, and the coupling between them is increased. On the other hand an image charge of opposite sign is induced in a metallic electrode, which attracts ions to the interface and reduces their correlations.

The image potential between two ions depends upon their mutual separation and upon their distances from the particle. That is, the pair potential of the ions is non-central and depends upon the position of the particle. This poses no difficulties for simulations, where they have been included in simulations of a single wall[247], nor for inhomogeneous integral equations, because the image potential has the same symmetry as the pair correlation functions[189,199]. An infinite sum of dielectric images arises from two walls, which represent a challenge for simulations that has to date been solved only approximately[257]. The sum can be expressed in closed form in Fourier space, which is suited to the inhomogeneous integral equation method[189]. Similarly a Legendre transform renders the image potential tractable in spherical geometry.

Dielectric images are problematic for singlet integral equation approaches because they represent a three-body interaction. They have been approximately treated in the singlet method by including the self-image potential with a screening factor[247,323]. Although seemingly ad hoc, the procedure is based upon the Onsager-Samaras analysis of an uncharged dielectric interface[324], and it avoids the spurious power law decay that would result from treating only part of the image interactions. (For example, it would be erroneous to attempt to modify Gouy-Chapman theory by including the one-body self-image interaction in the Boltzmann factor.) For simple liquids that interact with three-body potentials it is possible to formulate a type of hypernetted chain approximation that invokes an effective pair potential[325–330]. A linearised version of this effective pair potential has been used for a multipolar solvent without ions against a polarisable wall[331]. However for the case of electrolyte, where in an exact treatment the density profile remains exponentially screened due to the cancellation of various diagrams, the hypernetted chain effective pair potential for the image interaction produces power law contributions to the profile because it only partially includes certain families of diagrams. A resummation to secure the correct screened form has not yet been carried out, and the double layer with dielectric images remains to be satisfactorily treated with singlet methods.

The effects of dielectric images are strongest at low surface charge densities and low electrolyte concentrations, and also in divalent electrolyte. Compared to no images, the ion densities near a wall are depleted when the wall has a lower dielectric constant than the solvent (repulsive self-image interaction) and enhanced in the opposite extreme of a metallic electrode[247]. An adsorption decrement occurs in the electrolyte at an uncharged surface of low dielectric constant that is believed to give a positive contribution to the surface tension of the air-electrolyte interface[199,323,324]. The modified Poisson-Boltzmann theory[199] has been shown to describe image charge effects at an isolated wall with high accuracy[247]. Vertenstein and Ronis[332] developed a cluster perturbation approximation for the planar double layer that included images, size, and correlations, and obtained good agreement with the simulation data[247] at low surface charge densities and low electrolyte concentrations; at higher couplings the theory overestimated the correlation effects. Spatial variation of the dielectric constant in non-planar geometries frequently occur in modelling biological systems, and numerical algorithms have been given to solve the Poisson-Boltzmann equation[333–335].

For two interacting planar walls, dielectric images have been included using the inhomogeneous hypernetted chain approximation for counterions only[207], and for a symmetric electrolyte[209,211], and approximately in simulations of

the counterions-only double layer[257]. In calculating the net pressure between the walls in the presence of images, it is essential to include the zero frequency van der Waals force in Lifshitz approximation between the dielectric half-spaces, otherwise a spurious power law repulsion results[93,94,302]. For the usual case when the walls have a lower dielectric constant than the solvent, there is a depletion of the ion densities near the surfaces. At low surface charge densities the images make the pressure even more repulsive than predicted by the Poisson-Boltzmann theory, (see the discussion of Fig. 9 above), and at higher surface charges the images enhance the correlations between the ions leading to a larger attractive component. (For neutral surfaces, which have no mean field repulsion, the van der Waals attraction is increased, c.f. Fig. 15 above, and Refs[194,209,260,300–302].)

Qualitatively, dielectric images have little effect on the non-classical behaviour of the double layer described in this review. Any van der Waals fluctuation attraction at small separations is enhanced by the increased coupling between the ions due to the induced images. The asymptotic behaviour of the profile and the interaction is still determined by the bulk electrolyte. Quantitatively, however, the effective surface charge will change, since images due to walls with a low dielectric constant are expected to decrease the effective surface charge at higher surface charge densities, and to increase it as the surface charge goes to zero. The converse will occur for metallic walls. In general, however, the effects of dielectric discontinuities appear to be small, and ignoring image charges is probably less serious than the other physical simplifications or theoretical approximations that are made in describing the electric double layer.

D. Molecular solvents

The dielectric constant represents the continuum contribution of the solvent, and in the primitive model for electrolytes and the electric double layer it appears in Coulomb's law for the interaction between charges *in media*. The solvent contributions have been integrated out of the problem, (McMillan-Mayer representation), being subsumed into a linear polarisation response. That Coulomb's law *in media* is really a solvent mediated interaction free energy can be seen from the fact that it is temperature dependent (via the dielectric constant). One expects the continuum approach to be exact in some asymptotic sense, where the potentials are weak and the response is averaged over many solvent molecules, but it can hardly be expected to hold in the close vicinity of a charged particle. The issue is to establish the regime of validity of the primitive model and the nature of its breakdown.

In a field with as many applications as the electric double layer there have been many efforts to incorporate non-continuum contributions that account for various physical effects. The simplest such notion is to use a spatially varying dielectric constant, for example one that is lower in an inner layer adjacent to the surface than it is in the bulk solvent. While no doubt the polarisation response of the solvent is altered by the presence of a particle, the magnitude of the change and even the sign is difficult to estimate. Another development of the primitive model notes that the usual dielectric constant gives the polarisation response to a uniform electric field, and attempts to account for the structure of the solvent by using a wave vector dependent dielectric tensor, $\underline{\underline{\epsilon}}(\mathbf{k})$. Again the problem is that one has to postulate the functional form for such a dielectric function, and to guess the values of the adjustable parameters that occur. An example of the difficulties with this approach is the Yukawa form for the non-local dielectric function that was used by Kornyshev and co-workers for polar fluids[336]. This was later shown to violate certain formally exact requirements[337], and it is qualitatively inconsistent with accurate numerical results for polar fluids[337–340]. Both these examples –spatially varying and wave vector dependent dielectric functions– raise serious questions about the value of this type of elaboration of the continuum model. The postulated functions, although no doubt intuitively appealing, tend to be simplistic and to depend upon unknown parameters, and it is essential that they be tested against more sophisticated calculations if they are to be relied upon. Ultimately progress beyond the continuum has to be at the level of a molecular model for the solvent, and it is these approaches that are now discussed.

Early results for the civilised model electric double layer were mostly for dipolar hard-sphere solvents at charged walls, and were obtained with the singlet mean spherical approximation[341,342], with the linear[343], quadratic[344], and full[345,346] singlet hypernetted chain approximation, and with density functional theory[347]. Sweeney et al.[348] used a gradient density functional approximation and the Clausius-Massoti formula to calculate the dielectric profile in a double layer at a hydrocarbon-water interface and to find the electrolyte dependence of the surface tension. Exact asymptotes for the dipole density and orientation profile are also known[349,350]. Perhaps the most determined efforts to characterise solvent effects in the double layer has been the molecular hypernetted chain calculations of Torrie, Kusalik, and Patey[5,295,351,352], and it is these results that will be summarised here. These authors have concentrated on aqueous electrolytes and have developed a relatively realistic model for the water molecule, namely a hard-sphere (diameter 2.8Å) embedded with electrostatic multipoles, (mostly in the symmetric tetrahedral quadrupole approximation, but also with the full C_{2v} water molecule that includes octapole moments and that preferentially solvates anions[353]), and with an enhanced permanent dipole moment determined self-consistently to account for the molecule's polarizability[354]. The solution of the molecular Ornstein-Zernike equation and hypernetted chain closure is accomplished by expanding the orientation-dependent pair distribution functions in rotational invariants, which are

just generalised spherical harmonics. The reference bridge function approximates that of a pure hard-sphere fluid. The integral equation approximation has been shown to be accurate by testing against molecular dynamics simulations for the solvent-solvent and ion-solvent correlation functions for a bulk electrolyte[355]. The tetrahedral model appears to provide an acceptable description of water, giving a dielectric constant of $\epsilon_r = 93.5$.

Calculations with this multipolar aqueous model of the bulk electrolyte yield information on ion solvation and other properties that have implications for the electric double layer. For the bulk electrolyte, Kusalik and Patey[46,353] find that at the density of bulk water the ion-solvent distribution functions oscillate with period around the solvent diameter, and they have large peak at contact. The primitive model seeks to account for this strong solvation shell of water about each ion by using a larger diameter than in the ionic crystal, (for example the bare diameter of Sodium is 2.4Å, whereas a typical diameter used in the primitive model is 4.2Å). In consequence of the behaviour of the solvent, the ion-ion potentials of mean force at infinite dilution oscillate at separations of several solvent diameters, but are dominated by Coulomb's law *in media* asymptotically. The potential is either a maximum or a minimum at contact, depending upon the relative signs of the two ions, and small unlike ions have a maximum at about half a solvent diameter from bare ion contact, whereas small like-charged ions have a primary minimum at this position. (This attractive well for similar ions has also been seen in reference interaction site calculations[356] and in simulations[357–359], which show it to be sensitive to the potentials and the boundary conditions.) Ions larger than the water molecule are less affected by solvation effects, and show smaller departures from Coulomb's law. Evidently using an hydrated ion diameter that is about half a solvent diameter larger than the bare diameter roughly accounts for this solvation effect in the primitive model. At finite electrolyte concentrations the short-range structure in the ion-ion potentials is largely unchanged, but the screening length is observed to depart from the Debye length as the concentration is increased. In the context of the primitive model results of §IC1, where for monovalent electrolyte the screening length was mostly less than the Debye length in the monotonic regime, and where at a given concentration the departure increased as the ion diameter increased, Kusalik and Patey[46] find in the multipolar aqueous solvent that small ions such as NaCl indeed have a shorter screening length than the Debye length, but they also find that the departure *decreases* for larger sized ions such as KCl, and for CsI ions, which are larger than the water molecule, the screening length is actually longer than the Debye length. Also found in the calculations is the decrease in dielectric constant with electrolyte concentration[46], which is observed experimentally, but which is not allowed for in the primitive model and which may contribute to the departure from the Debye length, (which is calculated using the dielectric constant of pure water).

The multipolar model for water has been applied to the isolated electric double layer at the singlet hypernetted chain level of approximation by treating charged macrospheres at infinite dilution[5,295,351,352]. (Results have also been obtained for dipolar fluids at planar walls[331,360,361].) Macroions with diameters up to 30 times that of the solvent, and with surface charge densities up to one charge per 91Å^2 have been studied. At the surface of the macrosphere the water shows an ice-like structure, similar to ice I with the *c*-axis normal to the surface[351]. This gives one hydrogen bond per molecule dangling toward the surface, but maximises the hydrogen bonds in the double plane of molecules adjacent to the surface. The structure is more developed for larger macroions, and the hypernetted chain results for the largest diameter are in good agreement with simulations for water at a planar wall[362–364]. The water near the surface remains mobile, but the average ice-like arrangement is rather stable and is hardly perturbed by the electric fields associated with a uniform surface charge[351,364].

The induced structure and polarisation of the water affect the distribution of ions in the double layer in a fashion that is sensitive to the relative size of the ions. Ions which are smaller than the water molecule experience a deep potential well out to about a solvent diameter from contact, whereas larger ions show a broad potential maximum out to about one and a half solvent diameters. This induced adsorption or desorption due to solvent structure is insensitive to the surface charge density on the macroion, (but the solvent structure does depend upon surface curvature), and holds for both counterions and coions; to a good approximation it may simply be added to Coulomb's law *in media* to obtain the total ion-macroion potential of mean force[5,352]. Finite electrolyte concentrations have little effect on the structure of the solvent in the vicinity of the surface; at 4M KCl there is a relatively minor enhancement of the peak in the macroion-solvent distribution function[5,295].

The solvent structure has a very great influence on the rate of neutralisation of the macroion charge, and Torrie et al.[295] found that there is a fast screening regime induced very close to the surface. The rapid screening of the macroionic charge means that the solvent polarisation oscillations induced at high surface charge densities in the pure solvent are not evident at finite electrolyte concentrations. In 0.1M KCl at the highest surface charge density, about 80% of the macroion charge is neutralised within about a solvent diameter of the surface. In part no doubt this is due to the fact that ions see the truly bare surface charge that is screened by neither salt nor solvent. In addition, in this case the solvent-induced counterion adsorption may be enhanced by the fact that the Potassium counterion (3.0Å) is slightly smaller than the Chlorine coion (3.2Å); KCl is the only salt that has been studied at finite concentrations, and the effect of a larger counterion and/or a smaller coion is unclear. At 1M the preferential induced adsorption in KCl is so marked that about 20% over-neutralisation occurs so that beyond one solvent diameter from the macroion

its charge appears to have the *opposite* sign. This is the charge reversal discussed in §IVA. These results of Torrie et al.[5,295] clearly indicate that surface-induced solvent structure has a major influence on the ion distribution in the double layer in the immediate vicinity of the surface, and that this can be quite dependent on the size of the specific ions. One expects that the asymptotic analysis of the primitive model described in detail in this review to hold in a formal sense, with the actual value of the effective surface charge being different from the numerical results given above.

The interaction between spherical macroions in the model multipolar aqueous solvent without added electrolyte has been characterised with the singlet hypernetted chain approximation[10]. (Dipolar fluids between planar walls and their interaction have been treated by density functional theory[347,365,366], and by the singlet wall-wall hypernetted chain approximation[77].) For small neutral macrospheres there is a short-ranged hydrophobic attraction, and for large macrospheres (30 times the diameter of the solvent) there is an oscillatory force that is due to the ice-like structure induced at an isolated surface discussed above. What is remarkable about these oscillations is that they have period equal to almost twice the solvent diameter. This unusual phenomenon, which does not occur for a hard-sphere or for a dipolar fluid, appears to be due to the fact that in the ice I structure the water molecules lie in pairs of planes perpendicular to the c-axis, and it is energetically favourable for an integral number of these doubled planes to be between the surfaces. For charged macrospheres these oscillations at small separations persist, and in addition there is an r^{-4} cavity repulsion at intermediate separations and the continuum Coulomb asymptote at large[10]. Unpublished results by the authors of Ref.[10] show that the addition of 0.1M KCl hardly changes the short-ranged structural interaction, and that the effective surface charge due to solvent-induced rapid neutralisation at an isolated macroion is the quantity that characterises their asymptotic interaction, which is of course exponentially screened.

This discussion of solvent effects in the double layer has been based on the singlet hypernetted chain studies of the multipolar aqueous solvent by Torrie, Kusalik, and Patey[5,295,351,352]. As mentioned above comparison with simulations and other approaches suggest that the model and approximation are reliable, particularly for the structure of the water at a wall[272,362–364]. Oscillatory water density profiles have also been reported in simulations of slit pores with molecular structure with[266–271] and without[273–275] mobile counterions. In agreement with the hypernetted chain calculations, the former show that specific ion solvation has a strong influence on the location of the counterions. The solvent-induced rapid screening of the surface charge seen by Torrie et al.[352] does not disagree with the concept of effective surface charge discussed here on the basis of the asymptotics of the primitive model, although quantitative calculations remain to be made.

Conclusion

In concluding this review of current theories for electrolytes and the electric double layer, it is appropriate to discuss the relevance and application to experiment, and the consequences of these recent advances in understanding for the measurement and interpretation of double layer phenomena. There are two issues in applying theory to the real world: the model and the approximation used to treat it. Most of the review has been concerned with the minimal model of the double layer, which consists of the primitive model of electrolytes, and infinitely dilute particles with uniformly charged and curved surfaces. As discussed in the preceding section, in the real world one expects discrete surface charges, charge regulation, surface undulations and roughness, surface charge layers of finite and perhaps variable thickness, ion-specific surface contact distances, and of course dielectric image effects. Doubtless the most serious simplification is the neglect of the solvent molecules; although the continuum picture is valid in some asymptotic sense, it must break down for close approach of the ions to each other and to the surface.

So much has been left out of the minimal model that the relevance of results such as those reviewed here needs to be addressed. There are several arguments to support the basic philosophy of the present approach. The simplest model captures the essence of double layer phenomena and as such it has a certain aesthetic appeal. It is prefered because it trims complications and other hirsute possibilities from consideration while accounting for most of the data. This allows a detailed analysis at the heart of the matter, and an understanding of the double layer at its most fundamental level. One avoids the mere empirical collection of data in favour of a unified description that rationalises the data within a broad context; exceptional behaviour can then be recognised and treated as such. The simplest model is also the most general. It ignores specifics and particulars, which may be quantitatively important in each system, but which limit interest to a specialised audience. By focussing on the common denominator, the minimal model remains relevant across a spectrum of fields and technologies.

The minimal model yields to sophisticated mathematical and computational analyses in ways that are not possible in more complicated models of the double layer. A number of limiting and benchmark results have been established that are suitable for well-defined and unambiguous tests of more tractable or more approximate theories, which themselves can be applied to experimental data or to more realistic models. Furthermore, the predictions of the sophisticated theories for the minimal model may be relied upon, and there is no doubt that the non-classical phenomena described

herein (effective surface charges, non-Debye lengths, attractions, oscillations) really do occur in this model. And if they occur in the simplest model than they can also be expected in more elaborate models and in reality.

The dichotomy in theory between the model and the approximation is reflected in the two possible avenues for improving the Gouy-Chapman approach to the double layer. The alternative to the more advanced treatment of the minimal model that is advocated here is to apply the Poisson-Boltzmann theory to more developed models. While the motivation for such a program is firmly based on experimental pragmatism, the concern is that divergence of theory and experiment is as likely due to an artifact of the approximation as it is to a physical detail neglected in the model. A better fit obtained by embellishing the model may owe more to cancelling the errors of the approximation than to accounting for some real physical effect; the model may be more realistic, but it is not described any more accurately than the original. The advantage of using sophisticated theories to treat the simplest model is that one can remove the uncertainty associated with the approximation itself. Any disagreement between theory and experiment can be reliably ascribed to the model, and it may be possible to anticipate which particular aspect requires elaboration. It is this ambiguity that prevents one testing an approximation scheme against experiment, and which has motivated the benchmarks being established for the simplest model. These benchmarks have enabled approximations such as the singlet integral equations that were discussed in some detail herein to be characterised, their reliability and regime of applicability has been established, and their feasibility for the analysis of experimental data remarked upon.

These then are the reasons for concentrating on the simplest possible model: its simplicity captures the essence of the double layer, which can then be treated in a sophisticated and reliable fashion, and any discrepancy between theory and experiment can then be unambiguously ascribed to a breakdown of the model.

Although it is feasible to go beyond the Poisson-Boltzmann theory, most experiments continue to be described within that context, and a substantial amount of theoretical development follows the alternate path, namely developing and using that approximation for more realistic models. The mean field theory has been manifestly successful in describing the double layer for the better part of this century, and reports of its demise are perhaps premature. Why has it apparently succeeded, when the approximations inherent in the approach —the neglect of electrostatic and excluded volume correlations— can have such serious consequences, as detailed herein? Of course the Poisson-Boltzmann theory is expected to be valid at low electrolyte concentrations and surface charge densities where the correlations are relatively small. However it is often applied at surprisingly high concentrations without obvious contradictions. Part of the reason for this is that the Poisson-Boltzmann theory gives a formally exact description of an ideal gas in an external field, (which happens to be the mean field). As such it is an internally consistent theory, which partially explains its ability to account for a variety of data without discrepancies appearing. The asymptotic analysis detailed in this review also provides part of the answer. The electrostatic potential and ion profiles due to a charged particle have linear Poisson-Boltzmann form far from the surface, as does the interaction between surfaces. Measurements that sample this regime will appear to confirm the applicability of that approximation, and the fitted surface charge will be taken as the actual surface charge. Hence a certain amount of ion binding or dissociation will be said to have been measured, and an independent measurement of surface charge may be difficult if not impossible to obtain. In other words the Poisson-Boltzmann theory apparently describes the data, although in fact its error has been quantitatively incorporated into the fit.

Of course it is not always possible to reconcile the Poisson-Boltzmann theory of the minimal model with measured data, even with effective parameters. In these cases it is tempting to conclude that the model has broken down, and to incorporate some extra physical effect or other. However, this article has stressed that the advanced treatments of recent years show that even the minimal model can display behaviour beyond the classical Poisson-Boltzmann prediction. For the case of an isolated planar double layer, the effective surface charge increases less rapidly than the actual surface charge, until it reaches a maximum. Thus the surface charge that can be supported by a given electrolyte appears to saturate. As the surface charge is further increased the effective charge begins to decrease. It would be difficult to account for this effect with a Poisson-Boltzmann theory for an embellished counterion binding model. At even higher charge densities the effective surface charge passes through zero and changes sign, due to the packing of the finite-sized ions against the surface. This over-screening in the vicinity of the surface would appear as charge reversal in any measurement that sampled the double layer potential beyond about one diameter from the surface. (Of course the force between identical particles would still be asymptotically repulsive if both their effective charges are reversed and the bulk electrolyte is in the monotonic regime.)

Another non-classical effect appears in the bulk electrolyte, namely the departure of the screening length from the Debye length. However this effect is relatively small, and it would take a rather precise measurement to quantify it. The departure does increase as the electrolyte increases, but the double layer shrinks even faster, which may again preclude measurement. One case where one may possibly see the effect is for ions with a large size at moderate decay lengths, since the departure depends upon $\kappa_D d$.

For even higher electrolyte concentrations the bulk ion correlation functions become oscillatory, and consequently so do the double layer ion profiles, potential, and interaction. This certainly contradicts the Poisson-Boltzmann picture, but the decay length is so short that it would be difficult to measure directly. However there are likely measurable

indirect consequences, particularly for the flocculation and coagulation of colloids, or for the interaction between charged surfaces. The traditional picture of colloid stability, due to Derjaguin, Landau, Verwey, and Overbeek[1], relies upon the barrier to the primary minimum that arises from the balance of the van der Waals attraction and the Poisson-Boltzmann repulsion. In contrast, the modern theories predict that at high concentrations of the bulk electrolyte multiple oscillations in the double layer occur, which considerably complicates the calculation of the most likely particle separation and the behaviour of the colloid.

Double layer interactions do provide one of the most direct tests of theory, since the forces between charged surfaces can be directly measured. The net force is of course a surface phenomenon; it has the bulk electrolyte contribution automatically subtracted and hence the entire signal yields information about the double layer. Even at moderate electrolyte concentrations non-classical behaviour has been predicted. Modern theories —simulation, singlet and inhomogeneous integral equation, density functional— all show that at intermediate to small separations the double layer interaction between *like*-charged surfaces can be *attractive*. This is the van der Waals regime, and it occurs at high ion couplings, which in practice means divalent aqueous electrolytes. (It can also be induced by high surface surface charge densities.) As contact is approached there is a repulsive pressure that diverges as the reciprocal of the separation, (at least for fixed surface charge), and at large separation the force between like-charged surfaces must be repulsive, (in the bulk monotonic regime). But there is also this intermediate regime where the double layer force can be attractive due to the electrostatic fluctuations of the ions, (part of the zero-frequency van der Waals force), which can dominate the osmotic repulsion that is calculated in the mean-field Poisson-Boltzmann approximation.

Double layer attractions are now well established in theory, and there is some experimental support for the idea. As one qualitative example, the correlation between divalent ions and double layer attractions may provide new insight into the rôle of Calcium and Magnesium in colloid and soil science, and in cell biology. Thus irreversible adhesion and coagulation in the presence of these particular cations need not be ion bridging in a literal sense, but may in large part be due to a deep van der Waals minimum arising from the mechanism discussed above. More quantitatively, inhomogeneous hypernetted chain calculations have been compared with the attractive double layer interactions measured between charged mica surfaces[294,367,368] and between clay platelets[369] in divalent electrolyte. The attractive regime predicted by the theory agrees relatively well with that inferred from the measurements, and the experiments clearly show non-classical behaviour.

The prediction of double layer attractions is one of the high points of recent double layer theory, and its apparent confirmation is a tribute to the sophistication of the experiments. At the same time the limitations of the continuum picture are becoming increasingly evident. The same experiments that support the above interpretation[294,367–369] show oscillations with period several Ångstöms in the measured forces. The primitive model double layer calculations don't exhibit oscillations, (they mostly correspond to the monotonic regime of the bulk electrolyte), and the experimental data therefore provides relatively direct evidence of molecular solvent effects. This is a case where the sophisticated treatment of the minimal model has heralded reliable experimental evidence for its breakdown. It is the precision of these and other contemporary measurements that provides strong motivation for theory to include the solvent as a distinct molecular species and to go beyond the continuum model of electrolytes and the electric double layer.

Acknowledgements

I thank Emma Chorley and Clem Colman for assistance with the dumbell hypernetted chain and the effective surface charge calculations, respectively. I thank Stan Miklavic and Stjepan Marčelja for critical comments on the manuscript.

---

[1] E. J. W. Verwey and J. Th. G. Overbeek, *Theory of the Stability of Lyophobic Colloids*, (Elsevier, Amsterdam, 1948).
[2] S. L. Carnie and G. M. Torrie, *Adv. Chem. Phys.* **56**, 141 (1984).
[3] L. Blum, *Adv. Chem. Phys.* **78**, 171 (1990).
[4] M. Lozada-Cassou, Chapter 8 in *Fundamentals of Inhomogeneous Fluids* edited by D. Henderson, (Marcel Dekker, New York, 1992)
[5] G. N. Patey and G. M. Torrie, *Chemica Scripta* **29A**, 39 (1989).
[6] Ph. A. Martin, *Rev. Mod. Phys.* **60**, 1075 (1988).
[7] A. Alastuey, in *Strongly Coupled Plasma Physics*, edited by F. J. Rogers and H. E. Dewitt, NATO Advanced Science Institute Series, No B 154, p. 331 (Plenum, New York, 1987).
[8] M. Parrinello, and M. P. Tosi, *Riv. Nuovo Cim.* **2**, No. 6 (1979).
[9] J. A. Barker, R. A. Fisher, and R. O. Watts, *Mol. Phys.* **21**, 657 (1971).
[10] P. Attard, D. Wei, G. N. Patey, and G. M. Torrie, *J. Chem. Phys.* **93**, 7360 (1990).

[11] A. E. Sherwood, A. G. de Rocco, and E. A. Mason, *J. Chem. Phys.* **44**, 2984 (1966).
[12] D. C. Brydges, *Commun. math. Phys.* **58**, 313 (1978).
[13] D. C. Brydges and P. Federbush, *Commun. math. Phys.* **73**, 197 (1980).
[14] T. Kennedy, *Commun. math. Phys.* **92**, 269 (1983).
[15] J. Z. Imbrie, *Commun. math. Phys.* **87**, 515 (1983).
[16] P. Federbush and T. Kennedy, *Commun. math. Phys.* **102**, 361 (1985).
[17] J. P. Hansen and I. R. McDonald, *Theory of Simple Liquids* (Academic, New York, 1976).
[18] P. Attard, *Phys. Rev. E* **48**, 3604 (1993).
[19] H. L. Friedman and P. S. Ramanathan *J. Phys. Chem.* **74**, 3756 (1970).
[20] P. V. Giaquinta, M. Parrinello, and M. P. Tosi, *Phys. Chem. Liq.* **5**, 305 (1976).
[21] M. Rovere, M. Parrinello, M. P. Tosi, and P. V. Giaquinta, *Phil. Mag. B* **39**, 167 (1979).
[22] P. Vieillefosse, *J. de Phys. Lettres* **38**, L43 (1977).
[23] C. N. Likos and N. W. Ashcroft, *J. Chem. Phys.* **97**, 9303 (1992).
[24] L. G. Suttorp and A. J. van Wonderen, *Physica* **145A**, 533 (1987).
[25] A. J. van Wonderen and L. G. Suttorp, *Physica* **145A**, 557 (1987).
[26] J. G. Kirkwood and F. P. Buff, *J. Chem. Phys.* **19**, 774 (1951).
[27] F. H. Stillinger and R. Lovett, *J. Chem. Phys.* **48**, 3858 (1968).
[28] F.H. Stillinger and R. Lovett, *J. Chem. Phys.* **49**, 1991 (1968).
[29] D. J. Mitchell, D. A. McQuarrie, A. Szebo, and J. Groenevold, *J. Stat. Phys.* **17**, 15 (1977).
[30] C. W. Outhwaite, *Chem. Phys. Lett.* **24**, 73 (1974).
[31] S. L. Carnie and D. Y. C. Chan, *Chem. Phys. Lett.* **77**, 437 (1981).
[32] D. Pines and Ph. Noziéres, *The Theory of Quantum Liquids* (Benjamin, New York, 1966).
[33] P. C. Martin, *Phys. Rev.* **161**, 143 (1967).
[34] P. Vieillefosse and J. P. Hansen, *Phys. Rev. A* **12**, 1106 (1975).
[35] M. Baus, *J. Phys. A* **11**, 2451 (1978).
[36] G. Stell and J. L. Lebowitz, *J. Chem. Phys.* **48**, 3706 (1968).
[37] R. Kjellander and D. J. Mitchell, *J. Chem. Phys.* **101**, 603 (1994).
[38] G. Stell, in *Statistical Mechanics Part A: Equilibium Techniques*, B.J. Berne (ed.), p. 47, (Plenum, New York, 1977).
[39] P. Attard, *J. Chem. Phys.* **93**, 7301 (1990); *ibid* **94** , 6936 (1991).
[40] G. Stell, *Phys. Rev. B* **1**, 2265 (1970).
[41] J. E. Enderby, T. Gaskell, and N. H. March, *Proc. Phys. Soc.* **85**, 217 (1965).
[42] G. Nienhuis and J. M. Deutch, *J. Chem. Phys.* **56**, 1819 (1972).
[43] J. S. Høye and G. Stell, *J. Chem. Phys.* **61**, 562 (1974).
[44] J. S. Høye and G. Stell, *J. Chem. Phys.* **68**, 4145 (1978).
[45] G. Stell, G. N. Patey, and J. S. Høye, *Adv. Chem. Phys.* **38**, 183 (1981).
[46] P. G. Kusalik and G. N. Patey, *J. Chem. Phys.* **88**, 7715 (1988).
[47] C. Gruber, J. L. Lebowitz, P. A. Martin, *J. Chem. Phys.* **75**, 944 (1981)
[48] L. Blum, C. Gruber, J. L. Lebowitz, P. A. Martin, *Phys. Rev. Lett.* **48**, 1769 (1982).
[49] P. Debye and E. Hückel, *Zeit. für Phys.* **24**, 185 and 305 (1923).
[50] S. Marčelja, D. J. Mitchell, B. W. Ninham, and M. J. Sculley, *J. Chem. Soc. Faraday Trans. II* **73**, 630 (1977).
[51] A. B. Glendinning and W.B. Russel, *J.Colloid Interface Sci.* **93**, 95 (1983).
[52] S. L. Carnie and D. Y. C. Chan, *J. Colloid Interface Sci.* **155**, 297 (1993).
[53] E. Barouch and E. Matijević, *J. Chem. Soc. Faraday Trans. I* **81**, 1797 (1985).
[54] J. E. Sánchez-Sánchez and M. Lozada-Cassou, *Chem. Phys. Lett.* **190**, 202 (1992).
[55] S. L. Carnie, D. Y. C. Chan, and J. Stankovich, *J. Colloid Interface Sci.* **165**, 116 (1994).
[56] J. Ennis, R. Kjellander, and D. J. Mitchell, *J. Chem. Phys.* **102**, 975 (1995).
[57] D. J. Mitchell and B. W. Ninham, *Phys. Rev.* **174**, 280, (1968).
[58] D. J. Mitchell and B. W. Ninham, *Chem. Phys. Lett.* **53**, 397, (1978).
[59] R. Kjellander and D. J. Mitchell, *Chem. Phys. Lett.* **200**, 76 (1992).
[60] C. W. Outhwaite, *Statistical Mechanics: A Specialist Periodical Report.* **2**, 188 (1975).
[61] R. Lovett and F. H. Stillinger, *J. Chem. Phys.* **48**, 3869 (1968).
[62] E. Waisman and J. L. Lebowitz, *J. Chem. Phys.* **56**, 3086 and 3093 (1972).
[63] L. Blum, *Mol. Phys.* **30**, 1529 (1975).
[64] L. Blum and J. S. Høye, *J. Phys. Chem.* **81**, 1311 (1977).
[65] F. H. Stillinger and J. G. Kirkwood, *J. Chem. Phys.* **33**, 1282 (1960).
[66] J. G. Kirkwood, *Chem. Rev.* **19**, 275 (1936).
[67] J. G. Kirkwood and J. C. Poirier, *J. Phys. Chem.* **58**, 591 (1954).
[68] M. E. Fisher and B. Widom, *J. Chem. Phys.* **50**, 3756 (1969).
[69] G. A. Martynov, *Fundamental Theory of Liquids: Method of Distribution Functions* (Hilger, Bristol, 1992).
[70] J. R. Henderson and Z. A. Sabeur, *J. Chem. Phys.* **97**, 6750 (1992).
[71] R. Evans, J. R. Henderson, D. C. Hoyle, A. O. Parry, and Z. A. Sabeur, *Mol. Phys.* **80**, 755 (1993).
[72] R. Evans, R. J. F. Leote de Carvalho, J. R. Henderson, and D. C. Hoyle, *J. Chem. Phys.* **100**, 591 (1994).
[73] R. J. F. Leote de Carvalho and R. Evans, *Mol. Phys.* **83**, 619 (1994).
[74] R. H. Fowler, *Statistical Mechanics* Chapter XIII, (Cambridge University Press, New York, 1929).

[75] L. Onsager, *Chem. Revs.* **13**, 73 (1933).
[76] J. G. Kirkwood, *J. Chem. Phys.* **2**, 767 (1934).
[77] P. Attard, D. R. Bérard, C. P. Ursenbach, and G. N. Patey, *Phys. Rev. A* **44**, 8224 (1991).
[78] P. Attard, C. P. Ursenbach, and G. N. Patey, *Phys. Rev. A* **45**, 7621 (1992).
[79] C. W. Outhwaite, *J. Chem. Soc. Faraday Trans. 2* **74**, 1214, 1670 (1978).
[80] C. W. Outhwaite, L. B. Bhuiyan, and S. Levine, *J. Chem. Soc. Faraday Trans. 2* **76**, 1388 (1980).
[81] D. Henderson, F. F. Abraham, and J. A. Barker, *Mol. Phys.* **31**, 1291 (1976).
[82] D. Henderson and L. Blum, *J. Chem. Phys.* **69**, 5441 (1978).
[83] S. L. Carnie, D. Y. C. Chan, D. J. Mitchell, and B. W. Ninham, *J. Chem. Phys.* **74**, 1472 (1981).
[84] P. Attard and S. J. Miklavic, *J. Chem. Phys.* **99**, 6078 (1993).
[85] B. Jancovici, *J. Stat. Phys.* **28**, 43 (1982).
[86] B. Jancovici, *J. Stat. Phys.* **29**, 263 (1982).
[87] M. Baus, *Mol. Phys.* **48**, 347 (1983).
[88] S. L. Carnie and D. Y. C. Chan, *Mol. Phys.* **51**, 1047 (1984).
[89] B. Jancovici, J. L. Lebowitz, and Ph. A. Martin, *J. Stat. Phys.* **41**, 941 (1985).
[90] F. Stern and W. E. Howard, *Phys. Rev.* **163** 816 (1967).
[91] A. L. Fetter, *Phys. Rev. B* **10** 3739 (1974).
[92] V. M. Muller, and B. V. Derjaguin, *J. Colloid Interface Sci.* **61** 361 (1977).
[93] P. Attard, R. Kjellander, and D. J. Mitchell, *Chem. Phys. Lett.* **139** 219 (1987).
[94] P. Attard, R. Kjellander, D. J. Mitchell, and Bo Jönsson, *J. Chem. Phys.* **89** 1664 (1988).
[95] W. J. Ellis, *Mol. Phys.* **82**, 973 (1994).
[96] B. Jancovici and X. Artru, *Mol. Phys.* **49**, 487 (1983).
[97] L. Blum, D. Henderson, J. L. Lebowitz, Ch. Gruber, and Ph. A. Martin, *J. Chem. Phys.* **75**, 5974 (1981).
[98] S. L. Carnie, *J. Chem. Phys.* **78**, 2742 (1983).
[99] B. V. Derjaguin, *Kolloid Z.* **69**, 155 (1934).
[100] L. R. White, *J. Colloid Interface Sci.* **95**, 286 (1983).
[101] P. Attard and J. L. Parker, *J. Phys. Chem.* **96**, 5086 (1992).
[102] D. Henderson, *J. Chem. Phys.* **97**, 1266 (1992).
[103] P. Attard and G. N. Patey, *J. Chem. Phys.* **92**, 4970 (1990).
[104] S. L. Brenner and D. A. McQuarrie, *J. theor. Biol.* **39**, 343 (1973).
[105] G. S. Manning, *J. Chem. Phys.* **51**, 924, 3249 (1969).
[106] G. S. Manning, *Biophys. Chem.* **7**, 95 (1977).
[107] R. M. Fuoss, A. Katchalsky, and S. Lifson, *Proc. Natl Acad. Sci. USA* **37**, 579 (1951).
[108] T. Alfrey, P. W. Borg, and H. Morawitz, *J. Polmer Sci.* **7**, 543 (1951).
[109] H. P. Gregor and J. M. Gregor, *J. Chem. Phys.* **66**, 1934 (1977).
[110] F. Booth, *J. Chem. Phys.* **19**, 821 (1951).
[111] T. L. Hill, *Arch. Biochem. Biophys.* **57**, 229 (1955).
[112] C. P. Woodbury, *J. Chem. Phys.* **82**, 1482 (1985).
[113] C. F. Anderson and M. T. Record, *Ann. Rev. Phys. Chem.* **33**, 191 (1982).
[114] M. Lozada-Cassou, *J. Phys. Chem.* **87**, 3729 (1983).
[115] E. González-Tovar, M. Lozada-Cassou, and D. Henderson, *J. Chem. Phys.* **83**, 361 (1985).
[116] R. Bacquet and P. J. Rossky, *J. Phys. Chem.* **88**, 2660 (1984).
[117] V. Vlachy and D. A. McQuarrie, *J. Phys. Chem.* **90**, 3248 (1986).
[118] V. Vlachy and A. D. J. Haymet *J. Am. Chem. Soc.* **111**, 477 (1989).
[119] V. Vlachy and A. D. J. Haymet *J. Electroanal. Chem.* **283**, 77 (1990).
[120] L. Yeomans, S. E. Feller, E. Sánchez, and M. Lozada-Cassou, *J. Chem. Phys.* **98**, 1436 (1993).
[121] T. Das, D. Bratko, L. B. Bhuiyan and C. W. Outhwaite, *J. Phys. Chem.* **99**, 410 (1995).
[122] L. B. Bhuiyan and C. W. Outhwaite, *Philos. Mag. B* **69**, 1051 (1994).
[123] V. Vlachy and A. D. J. Haymet *Aust. J. Chem.* **43**, 1961 (1990).
[124] C. E. Woodward, Bo. Jönsson, and T. Åkesson, *J. Chem. Phys.* **89**, 5145 (1988).
[125] A. Luzar and D. Bratko, *J. Chem. Phys.* **92**, 642 (1990).
[126] M. Lozada-Cassou, *J. Chem. Phys.* **80**, 3344 (1984).
[127] D. Henderson and L. Blum, *J. Chem. Phys.* **69**, 5441 (1978).
[128] D. Henderson, L. Blum, and J. L. Lebowitz, *J. Electroanal. Chem.* **102**, 315 (1979).
[129] S. L. Carnie and D. Y. C. Chan, *J. Chem. Phys.* **74**, 1293 (1981).
[130] S. L. Carnie and D. Y. C. Chan, *J. Chem. Phys.* **78**, 3348 (1983).
[131] H. Wennerström, B. Jönsson, and P. Linse, *J. Chem. Phys.* **76**, 4665 (1982).
[132] J. F. Springer, M. A. Pokrant, and F. A. Stevens, *J. Chem. Phys.* **58**, 4863 (1973).
[133] P. J. Rossky, J. B. Dudowicz, B. L. Tembe, and H. L. Friedman, *J. Chem. Phys.* **73**, 3372 (1980)
[134] R. Bacquet and P. J. Rossky, *J. Chem. Phys.* **79**, 1419 (1982).
[135] H. Iyetomi and S. Ichimaru, *Phys. Rev. A* **27**, 1241 (1983).
[136] P. Ballone, G. Pastore, M. P. Tosi, *J. Chem. Phys.* **81**, 3174 (1984).
[137] J. Wiechen, *J. Chem. Phys.* **85**, 7364 (1986).
[138] P. Attard and G. N. Patey, *J. Chem. Phys.* **92**, 4970 (1990).

[139] J. A. Barker and J. J. Monaghan *J. Chem. Phys.* **36**, 2564 (1962).
[140] A. D. J. Haymet, S. A. Rice, and W. G. Madden, *J. Chem. Phys.* **74**, 3033 (1981).
[141] P. Attard, *J. Chem. Phys.* **91**, 3072 (1989); **92** 3248 (1990).
[142] Y. Zhou and G. Stell, *J. Chem. Phys.* **92**, 5533 (1990).
[143] P. Ballone, G. Pastore, M. P. Tosi, *J. Chem. Phys.* **85**, 2943 (1986).
[144] J. P. Badiali, M. L. Rosinberg, D. Levesque, and J. J. Weis, *J. Phys. C* **16**, 2183 (1983).
[145] A. Alastuey and D. Levesque, *Mol. Phys.* **47**, 1349 (1982).
[146] S. E. Feller and D. A. McQuarrie, *J. Phys. Chem.* **96**, 3454 (1992).
[147] G. M. Torrie and J. P. Valleau, *J. Chem. Phys.* **73**, 5807 (1980).
[148] J. M. Caillol and D. Levesque, *J. Chem. Phys.* **94**, 597 (1991).
[149] P. Nielaba and F. Forstmann, *Chem. Phys. Lett.* **117**, 46 (1985).
[150] B. D'Aguanno, P. Nielaba, T. Alts, and F. Forstmann, *J. Chem. Phys.* **85**, 3476 (1986).
[151] R. D. Groot, *Phys. Rev. A* **37**, 3456 (1988).
[152] Z. Tang, L. Mier-y-Teran, H. T. Davis, L. E. Scriven, and H. S. White, *Mol. Phys.* **71**, 369 (1990).
[153] E. Kierlik and M. L. Rosinberg, *Phys. Rev. A* **44**, 5025 (1991).
[154] C. N. Patra and S. K. Gosh, *J. Chem. Phys.* **100**, 5219 (1994).
[155] C. Caccamo, G. Pizzimenti, and L. Blum, *J. Chem. Phys.* **84**, 3327 (1986).
[156] E. Bruno, C. Caccamo, and G. Pizzimenti, *J. Chem. Phys.* **86**, 5101 (1987).
[157] R. Kjellander and S. Marčelja, *Chem. Phys. Lett.* **127**, 402 (1986).
[158] M. Plischke and D. Henderson, *J. Chem. Phys.* **88**, 2712 (1988).
[159] D. Bratko, *Chem. Phys. Lett.* **169**, 555 (1990).
[160] M. Lozada-Cassou and D. Henderson, *Chem. Phys. Lett.* **127**, 392 (1986).
[161] M. Lozada-Cassou and E. Díaz-Herrera, *J. Chem. Phys.* **92**, 1194 (1990).
[162] M. Lozada-Cassou and E. Díaz-Herrera, *J. Chem. Phys.* **93**, 1386 (1990).
[163] S. E. Feller and D. A. McQuarrie, *J. Phys. Chem.* **97**, 12083 (1993).
[164] S. E. Feller and D. A. McQuarrie, *J. Colloid Interface Sci.* **162**, 208 (1994).
[165] G. N. Patey, *J. Chem. Phys.* **72**, 5763 (1980).
[166] M. Teubner, *J. Chem. Phys.* **75**, 1907 (1981).
[167] G. M. Bell and S. Levine, *Trans. Faraday Soc.* **54**, 785 (1958).
[168] L. Belloni, *Chem. Phys.* **99**, 43 (1985).
[169] L. Belloni, *J. Chem. Phys.* **88**, 5143 (1988).
[170] O. Spalla and L. Belloni, *J. Chem. Phys.* **95**, 7689 (1991).
[171] P. Linse, *J. Chem. Phys.* **93**, 1376 (1990).
[172] P. Linse, *J. Chem. Phys.* **94**, 3817 (1991).
[173] D. Forciniti and C. K. Hall, *J. Chem. Phys.* **100**, 7553 (1994).
[174] S. J. Miklavic and P. Attard, *J. Phys. Chem.* **98**, 4320 (1994).
[175] S. E. Feller and D. A. McQuarrie, *Mol. Phys.* **80**, 721 (1993).
[176] T. Morita, *Prog. Theor. Phys.* **23**, 829 (1960).
[177] L. Verlet and D. Levesque, *Physica* **28**, 1124 (1962).
[178] O. E. Kiselyov and G. A. Martynov, *J. Chem. Phys.* **93**, 1942 (1990).
[179] P. Attard, *J. Chem. Phys.* **94**, 2370 (1991).
[180] L. L. Lee, *J. Chem. Phys.* **97**, 8606 (1992).
[181] J. Yvon, " La Théorie Statistique des Fluides et l'Equation d'Etat" *Actualités Scientiques et Industrielles*, Vol. 203 (Hermann, Paris, 1935).
[182] J. G. Kirkwood, *J. Chem. Phys.* **3**, 300 (1935).
[183] N. N. Bogoliubov, *J. Phys. (Moscow)* **10**, 256 (1946).
[184] M. Born and H. S. Green, *Proc. R. Soc. London Ser. A* **188**, 10 (1946).
[185] M. S. Wertheim, *J. Chem. Phys.* **65**, 2377 (1976).
[186] R. A. Lovett, C. Y. Mou, and F. P. Buff, *J. Chem. Phys.* **58**, 1880 (1976).
[187] L. Blum, Ch. Gruber, D. Henderson, J. L. Lebowitz, and Ph. A. Martin, *J. Chem. Phys.* **78**, 3195 (1983).
[188] D. G. Triezenberg and R. Zwanzig, *Phys. Rev. Lett.* **28**, 1183 (1972).
[189] R. Kjellander and S. Marčelja, *J. Chem. Phys.* **82**, 2122 (1985).
[190] R. Kjellander and S. Sarman, *Mol. Phys.* **70**, 215 (1990).
[191] H. Greberg and R. Kjellander, *Mol. Phys.* **83**, 789 (1994).
[192] A. L. Loeb, *J. Colloid Sci.* **6**, 75 (1951).
[193] P. Attard, D. J. Mitchell, and B. W. Ninham, *J. Chem. Phys.* **88** 4987 (1988); **92** 3248 (1990).
[194] P. Attard, D. J. Mitchell, and B. W. Ninham, *J. Chem. Phys.* **89** 4358 (1988).
[195] R. Podgornik and B. Žekš, *J. Chem. Soc. Faraday Trans. II* **84**, 611 (1988).
[196] L. Blum, J. Hernando, and J. L. Lebowitz, *J. Phys. Chem.* **87** 2825 (1983).
[197] S. Levine and G. Bell, *J. Phys. Chem.* **64**, 1188 (1960).
[198] S. Levine and G. Bell, *Disc. Faraday Soc.* **42**, 69 (1966).
[199] C. W. Outhwaite and L. B. Bhuiyan, *J. Chem. Soc. Faraday Trans. II* **79**, 707 (1983).
[200] T. L. Croxton and D. A. McQuarrie, *Mol. Phys.* **42**, 141 (1981).
[201] F. Lado, *Phys. Rev. B* **17** 2827 (1978).

[202] S. Sokolowski, *J. Chem. Phys.* **73** 3507 (1980).
[203] S. Sokolowski, *Mol. Phys.* **49** 1481 (1983).
[204] R. M. Nieminen and N. W. Ashcroft, *Phys. Rev. A* **24** 560 (1981).
[205] S. M. Foiles and N. W. Ashcroft, *Phys. Rev. B* **25** 1366 (1982).
[206] K. Hillebrand and R. M. Nieminen, *Surf. Sci.* **147** 599 (1984).
[207] R. Kjellander and S. Marčelja, *Chem. Phys. Lett.* **112**, 49 (1984).
[208] R. Kjellander and S. Marčelja, *J. Phys. Chem.* **90**, 1230 (1986).
[209] R. Kjellander and S. Marčelja, *Chem. Phys. Lett.* **142**, 485 (1987).
[210] R. Kjellander, *J. Chem. Phys.* **88**, 7129 (1988).
[211] R. Kjellander and S. Marčelja, *J. Chem. Phys.* **88**, 7138 (1988).
[212] R. Kjellander and S. Marčelja, *J. de Physique* (Paris) **49**, 1009 (1988).
[213] S. Marčelja, *Biophys. J.* **61**, 1117 (1992).
[214] R. Kjellander, T. Åkesson, Bo Jönsson, and S. Marčelja, *J. Chem. Phys.* **97**, 1424 (1992).
[215] D. Henderson and M. Plischke, *J. Phys. Chem.* **92**, 7177 (1988).
[216] M. Plischke and D. Henderson, *J. Chem. Phys.* **90**, 5738 (1989).
[217] M. Fushiki, *Chem. Phys. Lett.* **154**, 77 (1989).
[218] P. Attard, *J. Chem. Phys.* **95** 4471 (1991).
[219] B. K. Alpert and V. Rokhlin, *SIAM J. Sci. Stat. Comput.* **12** 158 (1991).
[220] M. Fushiki, *Mol. Phys.* **74**, 307, (1991).
[221] C. W. Outhwaite and L. B. Bhuiyan, *Mol. Phys.* **74**, 367 (1991).
[222] P. J. Colmenares and W. Olivares, *J. Chem. Phys.* **88** 3221 (1988).
[223] W. Olivares and D. A. McQuarrie, *J. Chem. Phys.* **65**, 3604 (1976).
[224] R. Evans, *Adv. Phys.* **28** 143 (1979).
[225] R. Evans, Chapter 8 in *Fundamentals of Inhomogeneous Fluids* edited by D. Henderson, (Marcel Dekker, New York, 1992).
[226] M. J. Grimson and G. Rickayzen, *Mol. Phys.* **42** 47 (1981).
[227] J. R. Henderson, *Mol. Phys.* **52** 1467 (1984).
[228] G. Rickayzen and A. Augousti, *Mol. Phys.* **52** 1355 (1984).
[229] S. Toxvaerd, *J. Chem. Phys.* **55** 3116 (1971).
[230] S. Nordholm, M. Johnson, and B. C. Freasier, *Aust. J. Chem.* **33** 2139 (1980).
[231] P. Tarazona, *Mol. Phys.* **52**, 81 (1984).
[232] P. Tarazona, *Phys. Rev. A* **31**, 2672 (1985); *ibid* **32**, 3148 (1985).
[233] L. Mier-y-Teran, S. H. Suh, H. S. White, and H. T. Davis, *J. Chem. Phys.* **92**, 5087 (1990).
[234] Z. Tang, L. E. Scriven, and H. T. Davis, *J. Chem. Phys.* **97**, 494 (1992).
[235] Z. Tang, L. E. Scriven, and H. T. Davis, *J. Chem. Phys.* **97**, 9258 (1992).
[236] L. Zhang, H. T. Davis, and H. S. White, *J. Chem. Phys.* **98**, 5793 (1993).
[237] A. R. Denton and N. W. Ashcroft, *Phys. Rev. A* **44**, 8242 (1991).
[238] C. N. Patra and S. K. Gosh, *Phys. Rev. A* **47**, 4088 (1992).
[239] C. N. Patra and S. K. Gosh, *J. Chem. Phys.* **101**, 4143 (1994).
[240] C. N. Patra and S. K. Gosh, *J. Chem. Phys.* **102**, 2556 (1995).
[241] C. N. Patra and S. K. Gosh, *Phys. Rev. E* **49**, 2826 (1994).
[242] R. Penfold, S. Nordholm, Bo Jönsson, and C. E. Woodward, *J. Chem. Phys.* **92**, 1915 (1990).
[243] M. J. Stevens and M. O. Robins, *Europhys. Lett.* **12**, 81 (1990).
[244] W. van Megan and I. Snook, *J. Chem. Phys.* **73**, 4656 (1980).
[245] I. Snook and W. van Megan, *J. Chem. Phys.* **75**, 4104 (1981).
[246] G. M. Torrie and J. P. Valleau, *J. Phys. Chem.* **86**, 3251 (1982).
[247] G. M. Torrie, J. P. Valleau, and G. N. Patey, *J. Chem. Phys.* **76**, 4615 (1982).
[248] D. M. Heyes, M. Barber, and J. H. R. Clarke, *J. Chem. Soc. Faraday Trans. II* **73**, 1485 (1977).
[249] S. W. de Leeuw and J. W. Perram, *Mol. Phys.* **37**, 1313 (1979).
[250] H. Totsuji, *J. Phys.C* **19**, L573 (1986).
[251] J. Lekner, *Physica* **176**, 485 (1991).
[252] L. Zhang, H. S. White, and H. T. Davis, *Mol. Simul.* **9**, 247 (1992).
[253] J. Hautman and M. L. Klein, *Mol. Phys.* **75**, 379 (1992).
[254] J. Hautman, J. W. Halley, and Y.-J. Rhee, *J. Chem. Phys.* **91**, 467 (1989).
[255] Bo Jönsson, H. Wennerström, and B. Halle, *J. Phys. Chem.* **84**, 2179 (1980).
[256] L. Guldbrand, Bo Jönsson, H. Wennerström, and P. Linse *J. Chem. Phys.* **80**, 2221 (1984).
[257] D. Bratko, Bo Jönsson, and H. Wennerström, *Chem. Phys. Lett.* **128**, 449 (1986).
[258] S. J. Zara, D. Nicholson, N. G. Parsonage, J. Barker, *J. Colloid Interface Sci.* **129**, 297 (1989).
[259] B. Svensson, Bo Jönsson, and C. E. Woodward, *J. Phys. Chem.* **94**, 2105 (1990).
[260] J. P. Valleau, R. Ivkov, and G. M. Torrie, *J. Chem. Phys.* **95**, 520 (1991).
[261] T. Åkesson and Bo Jönsson, *Electrochim. Acta* **36**, 1723 (1991).
[262] P. G. Bolhuis, T. Åkesson and Bo Jönsson, *J. Chem. Phys.* **98**, 8096 (1993).
[263] D. Bratko, L. Blum, and L. B. Bhuiyan, *J. Chem. Phys.* **94**, 597 (1991).
[264] D. Bratko, D. J. Henderson, and L. Blum, *Phys. Rev. A* **44**, 8235 (1991).
[265] D. Bratko and D. Henderson, *Phys. Rev. E* **49**, 4140 (1994).

[266] N. T. Skipper, A. K. Soper, J. D. C. McConnell, and K. Refson, *Chem. Phys. Lett.* **166**, 141 (1990).
[267] N. T. Skipper, K. Refson, and J. D. C. McConnell, *J. Chem. Phys.* **94**, 7434 (1991).
[268] A. Delville, *Langmuir* **8**, 1796 (1992).
[269] A. Delville, *J. Phys. Chem.* **97**, 9703 (1993).
[270] Z. Gamba, J. Hautman, J. C. Shelley, and M. L. Klein, *Langmuir* **8**, 3155 (1992).
[271] D. A. Rose and I. Benjamin, *J. Chem. Phys.* **95**, 6856 (1991).
[272] S.-B. Zhu and G. W. Robinson, *J. Chem. Phys.* **94**, 1403 (1991).
[273] R. Kjellander and S. Marčelja, *Chemica Scripta* **25**, 73 (1985).
[274] R. Kjellander and S. Marčelja, *Chem. Phys. Lett.* **120**, 393 (1985).
[275] M. L. Berkowitz and K. Raghavan *Langmuir* **7**, 1042 (1991).
[276] S. H. Lee, J. C. Rasaiah, and J. B. Hubbard, *J. Chem. Phys. 86*, 2383 (1987).
[277] S. J. Miklavic, C. E. Woodward, Bo Jonssön, and T. Åkesson, *Macromolecules* **23**, 4149 (1990).
[278] M. K. Granfeldt, S. J. Miklavic, S. Marčelja, and C. E. Woodward, *Macromolecules* **23**, 4760 (1990).
[279] M. K. Granfeldt, Bo Jonssön, and C. E. Woodward, *J. Phys. Chem.* **95**, 4819 (1991).
[280] L. Sjöström, T. Åkesson, and Bo Jonssön, *J. Chem. Phys.* **99**, 4739 (1993).
[281] C. E. Woodward, T. Åkesson, and Bo Jonssön, *J. Chem. Phys.* **101**, 2569 (1994).
[282] P. Linse and Bo Jönsson, *J. Chem. Phys. 78*, 3167 (1983).
[283] P. Linse, G. Gunnarsson, and Bo Jönsson, *J. Phys. Chem. 86*, 413 (1982).
[284] L. Degréve, M. Lozada-Cassou, E. Sánchez, and E. González-Tovar, *J. Chem. Phys. 98*, 8905 (1993).
[285] P. Sloth and T. S. Sørenson, *J. Chem. Phys. 96*, 548 (1992).
[286] B. Svensson and Bo Jönsson, *Chem. Phys. Lett.* **108**, 580 (1984).
[287] D. Bratko and V. Vlachy, *Chem. Phys. Lett.* **90**, 434 (1982).
[288] C. S. Murthy, R. J. Bacquet, and P. J. Rossky, *J. Phys. Chem.* **89**, 701 (1985).
[289] L. Nilsson, L. Guldbrand, and L. Nordenskiöld, *Mol. Phys.* **72**, 177 (1991).
[290] P. Attard, D. Wei, and G. N. Patey, *J. Chem. Phys.* **96**, 3767 (1992).
[291] G. M. Torrie, *J. Chem. Phys.* **96**, 3772 (1992).
[292] L. B. Bhuiyan, C. W. Outhwaite, and S. Levine, *Mol. Phys.* **42**, 1271 (1981).
[293] J. Ennis, Ph.D. thesis, Australian National University (1993).
[294] P. Kékicheff, S. Marčelja, T. J. Senden, and V. E. Shubin, *J. Chem. Phys.* **99**, 6098 (1993).
[295] G. M. Torrie, P. G. Kusalik, and G. N. Patey, *J. Chem. Phys.* **90**, 4513 (1989).
[296] J. R. Henderson, *Mol. Phys.* **59**, 89 (1986).
[297] A. Luzar, D. Bratko, and L. Blum, *J. Chem. Phys.* **86**, 2955 (1987).
[298] F. Oosawa, *Biopolymers* **6**, 1633 (1968).
[299] F. Oosawa, *Polyelectrolytes* (Marcel dekker, New York, 1971).
[300] B. Davies and B. W. Ninham, *J. Chem. Phys.* **56**, 5797 (1972).
[301] V. N. Gorelkin and V. P. Smilga, *Sov. Phys. JETP* **36**, 761 (1973).
[302] D. J. Mitchell and P. Richmond, *J. Colloid Interface Sci.* **46**, 128 (1974).
[303] P. Richmond, *J. Chem. Soc. Faraday II* **70**, 1066 (1973).
[304] A. P. Nelson and D. A. Mcquarrie, *J. theor. Biol.* **55**, 13 (1975).
[305] S. J. Miklavic, D. Y. C. Chan, L. R. White, and T. W. Healy, *J. Phys. Chem.* **98**, 9022 (1994); S. J. Miklavic, *J. Chem. Phys.* (submitted).
[306] P. Attard, *J. Phys. Chem.* **93**, 6441 (1989).
[307] P. Attard and G. N. Patey, *Phys. Rev. A* **43**, 2953 (1991).
[308] D. Grahame, *Chem. Revs* **41**, 441 (1947); *J. Chem. Phys.* **21**, 1054 (1953).
[309] B. W. Ninham and V. A. Parsegian, *J. theor. Biol.* **31**, 405 (1971).
[310] P. G. Higgs and J.-F. Joanny, *J. Phys.* (France) **51**, 2307 (1990).
[311] P. Pincus, J.-F. Joanny, and D. Andelman, *Europhys. Lett.* **11**, 763 (1990).
[312] D. J. Mitchell and B. W. Ninham, *Langmuir* **5**, 1121 (1989).
[313] A. Fogden, D. J. Mitchell, and B. W. Ninham, *Langmuir* **6**, 159 (1990).
[314] A. Fogden and B. W. Ninham, *Langmuir* **7**, 590 (1991).
[315] J. Ennis, *J. Chem. Phys.* **97**, 663 (1992).
[316] R. E. Goldstein, A. I. Pesci, and V. Romero-Rochín *Phys. Rev. A* **41**, 5504 (1990).
[317] S. R. Dungan and T. A. Hatton, *J. Colloid Interface Sci.* **164**, 200 (1994).
[318] S. Levine, J. Mingins, and G. M. Bell, *J. Electroanal. Chem.* **13**, 280 (1967).
[319] H. Ohshima and S. Ohki, *Biophys. J.* **47**, 673 (1985).
[320] Y.-C. Kuo and J.-P. Hsu, *J. Chem. Phys.* **102**, 1806 (1995).
[321] S. J. Miklavic and S. Marčelja, *J. Phys. Chem.* **92**, 6718 (1988).
[322] T. Åkesson, C. E. Woodward, and Bo Jonssön, *J. Chem. Phys.* **91**, 2461 (1989).
[323] T. Croxton, D. A. McQuarrie, G. N. Patey, and J. P. Valleau, *Can. J. Chem.* **59**, 1998 (1981).
[324] L. Onsager and N. Samaras, *J. Chem. Phys.* **2**, 528 (1934).
[325] J. S. Rushbrooke and M. Silbert, *Mol. Phys.* **12**, 505 (1967).
[326] G. Casanova, R. J. Dulla, D. A. Jonah, J. S. Rushbrooke and G. Saville, *Mol. Phys.* **18**, 589 (1970).
[327] Q. N. Usmani, S. Fantoni, and V. R. Pandharipande, *Phys. Rev. B* **26**, 6123 (1982).
[328] G. C. Aers and M. W. C. Dharma-wardana, *Phys. Rev. A* **29**, 2734 (1984).

[329] L. Reatto and M. Tau, *J. Chem. Phys.* **86**, 6474 (1987).
[330] P. Attard, *Phys. Rev. A* **45**, 3659 (1992).
[331] D. R. Bérard and G. N. Patey, *J. Chem. Phys.* **97**, 4372 (1992).
[332] M. Vertenstein and D. Ronis, *J. Chem. Phys.* **87**, 4132 (1987).
[333] B. Honig, K. Sharp, and A.-S. Yang, *J. Phys. Chem.* **97**, 1101 (1993).
[334] M. K. Gilson, M. E. Davis, B. A. Luty, and J. A. McCammon, *J. Phys. Chem.* **97**, 3591 (1993).
[335] K. E. Forsten, R. E. Kozack, D. A. Lauffenburger, and S. Subramaniam, *J. Phys. Chem.* **98**, 5580 (1994).
[336] A. A. Kornyshev, *Electrochim. Acta* **26**, 1 (1981).
[337] P. Attard, D. Wei, and G. N. Patey, *Chem. Phys. Lett.* **172**, 69 (1990).
[338] A. Chandra and B. Bagchi, *J. Chem. Phys.* **90**, 1832 (1989).
[339] A. Chandra and B. Bagchi, *J. Chem. Phys.* **91**, 3056 (1989).
[340] T. Fonseca and B. M. Ladanyi, *J. Chem. Phys.* **93**, 8148 (1990).
[341] S. L. Carnie and D. Y. C. Chan, *J. Chem. Phys.* **73**, 2949 (1980).
[342] D. Henderson and L. Blum, *J. Chem. Phys.* **74**, 1902 (1981).
[343] J. M. Eggebrecht, D. J. Isbister, and J. C. Rasaiah, *J. Chem. Phys.* **73**, 3980 (1980).
[344] J. C. Rasaiah, D. J. Isbister, and G. Stell, *J. Chem. Phys.* **75**, 4707 (1981).
[345] W. Dong, M. L. Rosinberg, A. Perera, and G. N. Patey, *J. Chem. Phys.* **89**, 4994 (1988).
[346] G. M. Torrie, A. Perera, and G. N. Patey, *Mol. Phys.* **67**, 1337 (1989).
[347] C. E. Woodward and S. Nordholm, *Mol. Phys.* **60**, 415 (1987).
[348] J. B. Sweeney, L. E. Scriven, and H. T. Davis, *J. Chem. Phys.* **87**, 6120 (1987).
[349] J. P. Badiali, *J. Chem. Phys.* **90**, 4401 (1989).
[350] Q. Zhang, J. P. Badiali, and W. H. Su, *J. Chem. Phys.* **92**, 4609 (1990).
[351] G. M. Torrie, P. G. Kusalik, and G. N. Patey, *J. Chem. Phys.* **88**, 7826 (1988).
[352] G. M. Torrie, P. G. Kusalik, and G. N. Patey, *J. Chem. Phys.* **89**, 3285 (1988).
[353] P. G. Kusalik and G. N. Patey, *J. Chem. Phys.* **89**, 5843 (1988).
[354] S. L. Carnie and G. N. Patey, *Mol. Phys.* **47**, 1129 (1982).
[355] J. M. Caillol, D. Levesque, J. J. Weis, P. G. Kusalik, and G. N. Patey, *Mol. Phys.* **62** 461 (1987).
[356] B. M. Pettitt and P. J. Rossky, *J. Chem. Phys.* **84**, 5836 (1986).
[357] X. Dang and B. M. Pettitt, *J. Chem. Phys.* **86**, 6560 (1987).
[358] E. Guardia, A. Robinson, and J. A. Padro, *J. Chem. Phys.* **99**, 4229 (1993).
[359] R. A. Friedman and M. Mezei, *J. Chem. Phys.* **102**, 419 (1995).
[360] D. R. Bérard, M. Kinoshita, X. Ye, and G. N. Patey, *J. Chem. Phys.* **101**, 6271 (1994).
[361] D. R. Bérard, M. Kinoshita, X. Ye, and G. N. Patey, *J. Chem. Phys.* **102**, 1024 (1995).
[362] C.Y. Lee, J. A. McCammon, and P. J. Rossky, *J. Chem. Phys.* **80**, 4448 (1984).
[363] J. P. Valleau and A. A. Gardner, *J. Chem. Phys.* **86**, 4162 (1987).
[364] A. A. Gardner and J. P. Valleau, *J. Chem. Phys.* **86**, 4171 (1987).
[365] G. Rickayzen and M. J. Grimson, *J. Chem. Soc. Faraday Trans. II* **78**, 893 (1982).
[366] A. T. Augousti and G. Rickayzen, *J. Chem. Soc. Faraday Trans. II* **80**, 141 (1984).
[367] R. Kjellander, S. Marčelja, R. M. Pashley, and J. P. Quirk, *J. Phys. Chem.* **92**, 6489 (1988).
[368] R. Kjellander, S. Marčelja, R. M. Pashley, and J. P. Quirk, *J. Chem. Phys.* **92**, 4399 (1990).
[369] R. Kjellander, S. Marčelja, and J. P. Quirk, *J. Colloid Interface Sci.* **126**, 194 (1988).